EUROPEAN COMMISSION

Community Research

SEVENTH FRAMEWORK PROGRAMME

ARCHER

Collaborative Project (CP)

Co-funded by the European Commission under the Euratom Research and Training Programme on Nuclear Energy within the Seventh Framework Programme

Grant Agreement Number : 269892

Start date : 01/02/2011 Duration : 48 Months

www.archer-project.eu

Archer

Advanced Reactor for Cogeneration of Heat & Electricity-R&D

Report of complementary environmental test results

Authors : Jan Berka, Karin Stehlik, Jana Kalivodova (CVR)

ARCHER - Contract Number: 269892
Advanced High-Temperature Reactors for Cogeneration of Heat and Electricity R&D
EC Scientific Officer: Dr. Panagiotis Manolatos

Document title	Report of complementary environmental test results
Author(s)	Jan Berka, Karin Stehlik, Jana Kalivodova (CVR)
Number of pages	77
Document type	Deliverable
Work Package	WP 42
Document number	D42.22
Issued by	NRG
Date of completion	14/01/2015
Dissemination level	Confidential, only for members of the consortium (including the Commission Services).

Summary

This document contains the information about environmental (corrosion) tests of high temperature alloys: steels P91 and 316 and Alloy 800 H. Specimens of these alloys were exposed in helium atmosphere containing defined concentrations of selected impurities (CO, H2, CH4, CO2) and also residual moisture at 750 - 760°C for up to 1500 hours. For exposure two devices were used: High Temperature Furnace (low gas pressure and low gas flow) and High Temperature Helium Loop (high gas pressure and high gas flow). First exposure of specimens in High Temperature Helium Loop were performed during test operation of the device at unstable parameters. Exposure at defined parameters is planned after end of the test operation. After exposure the specimens were subjected to several tests: surface and subsurface layers of specimens were observed by SEM/EDX and GD-OES, changes of weight of specimens and changes of microstructure of bulk metal were investigated and also tests of hardness, micro-hardness and fracture toughness were carried out.

Approval

Date	By
14/01/2015	Derek BUCKTHORPE
14/01/2015	Derek BUCKTHORPE
14/01/2015	Steven KNOL

Distribution list

Name	Organisation	Comments
P. Manolatos	EC DG RTD	Through the EC participant portal
All beneficiaries	ARCHER	Through the private online workspace

Content

List of figures

List of tables

List of acronyms

BM	Base Metal
GD-OES	Glow Discharge Optical Emision Spectroscopy
HAZ	Head affected zone
HTF	High Temperature Helium Furnace
HTHL	High Temperature Helium Loop
SEM/EDX	Scanning Electron Microscope/Energy Dispersive X-ray spectroscopy
WM	Weld Metal

Introduction

High temperature corrosion (HTC) tests have been conducted with three types of high-temperature materials: ferritic-martensitic steel P91, austenitic steel 316, and Incoloy 800H. Properties and application of these alloys can be found in the literature, e.g. [1, 2]. The samples of high-temperature alloys at first were exposed to an atmosphere of helium containing the typical contaminates occurring in cooling agent of VHTR. Experiments were carried out in High Temperature Furnace and High Temperature Loop with duration of each test up to 1500h and temperature of 750 to 760°C. after the HTC tests samples were further analysed and also for the samples of alloy P91 and 316 the fracture toughness was evaluated.

Experimental

Tested materials

The chemical compositions of the tested high-temperature materials are shown in Table 1 to Table 4. The material specifications are taken from the data sheets of the material supplier.

Table 1: Chemical composition of steel 316 (wt. %)

Element	**C**	**Si**	**Mn**	**P**	**S**	**Cr**	**Mo**	**Ni**	**Co**	**N**	**Fe**
Min.						16.50	2.00	10.00			Bal.
Max.	0.021	0.34	1.73	0.027	0.025	16.50	2.03	10.03	0.120	0.0320	Bal.

Table 2: Chemical composition steel P91 (wt. %)

Element	**C**	**S**	**Mn**	**Si**	**P**	**Cu**	**Ni**	**Cr**	**Mo**	**V**
	0.12	0.002	0.36	0.39	0.011	0.041	0.034	10.06	0.88	0.22
Element	**Ti**	**W**	**Co**	**Nb**	**As**	**Sb**	**Sn**	**Al**	**N**	**Fe**
	0.007	<0.005	<0.003	0.052	0.003	0.001	0.002	0.005	0.065	Bal

Table 3: Chemical composition of alloy 800H (wt. %)

Element	**C**	**S**	**Cr**	**Ni**	**Mn**	**Si**	**Ti**	**Nb**	**Cu**	**Fe**
	0.06	<0.002	20.5	30.5	0.7	0.50	0.34	0.01	0.10	R46.7
Element	**P**	**Al**	**Co**							
	0.010	0.28	0.1							

Table 4: Chemical composition of Nicrofr S7020 S03 (weld metal)

Element	C	S	Cr	Ni	Mn	Si	Ti	Nb	Cu	Fe
	0.003	0.002	20.4	72.9	3.2	0.11	0.32	2.7	0.01	0.2
Element	**P**									
	0.002									

Procedure of sample preparation

Samples of steel P91 a 316

Samples from P91 and SS316 materials were prepared from the supplied bar. In case of steel P91 the bar had a diameter of 91mm, a diameter of bar SS316 the bar was 30mm. A plan for cutting was developed, the samples were cut lengthwise to the axis of the bar accordingly.

Several types of samples were prepared:

- sheets measuring 5×2×40 mm and 15X2X40 for corrosion tests,
- disks with notch called type sub-size 3PB SEN for tests of quarry tenacity and samples having size of 11X11X5 mm for testing hardness.

The surface of specimens for corrosion tests were prepared in two ways. The surface was either grounded or machined. A summary of all samples provides Table 5.

Table 5: Samples of steel P91 and 316

Sample	Steel	Labelling	Quantity	Surface
Sub-size 3PB SEN	P91	P01 – P58	58	grounded
Sub-size 3PB SEN	316	L01-L45	45	grounded
5X2X40 mm	P91	P01-P30	30	machined
5X2X40 mm	P91	P31-P60	30	grounded
5X2X40 mm	316	L01-L27	27	machined
5X2X40 mm	316	L28-L54	27	grounded
15X2X40mm	P91	PG1-PG19	19	grounded
15X2X40mm	316	LG1-LG12	12	grounded

11X11X5 mm	P91	PT1-PT26	26	grounded
11X11X5 mm	316	LT1-LT20	20	grounded

At the samples sub-size 3PB SEN was also prepared a pointed initial defect. To create this defect the method of periodic fatigue toughness was used. The length of the defect was chosen in that way, that the initial damage was approx. 50% of the bearing cross-section. For the periodic fatigue breakage method the parameters of the testing device SF-Test were selected for all cycles to be within the range of 10^5–10^6.

Samples of alloy 800H

The initial form of the material Alloy 800H was a welded plate with dimensions 150X310X10 mm, , see Figure 1. Details about the material and the applied welding technology can be found in report [3]. From the plate mentioned above various samples were prepared according to the cutting plan (Figure 2).. The aim of the investigation was to compare the HTC behaviour of base metal, weld, and heat affected zone under specific He environment.

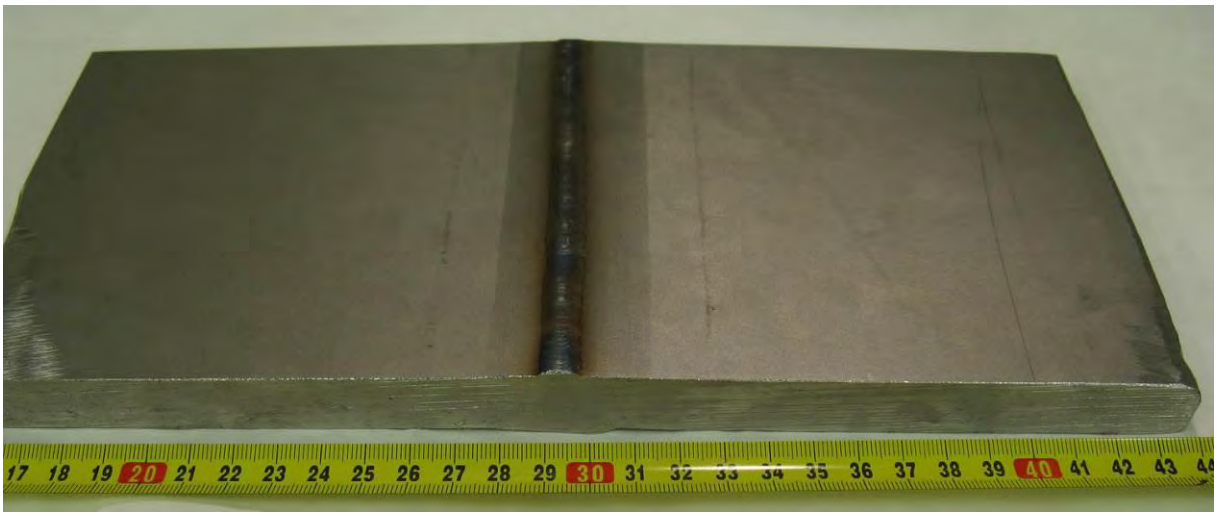

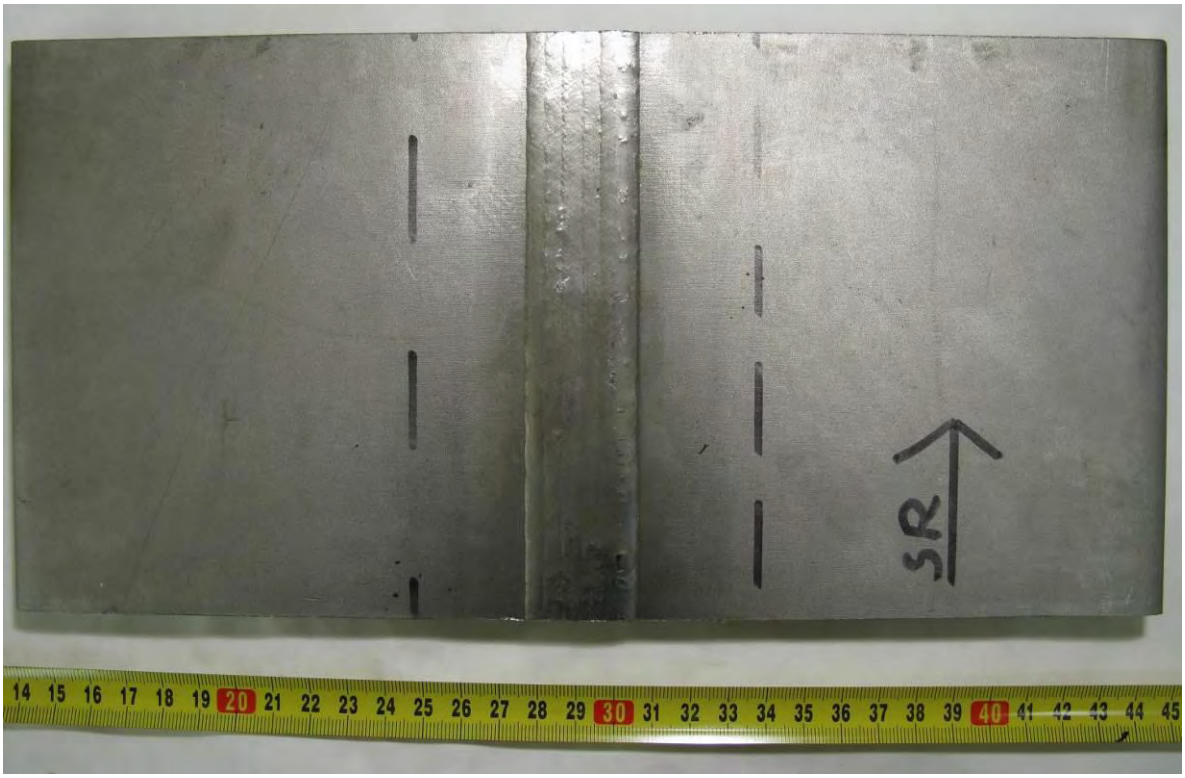

Figure 1: Sheet of alloy 800H for sample preparations

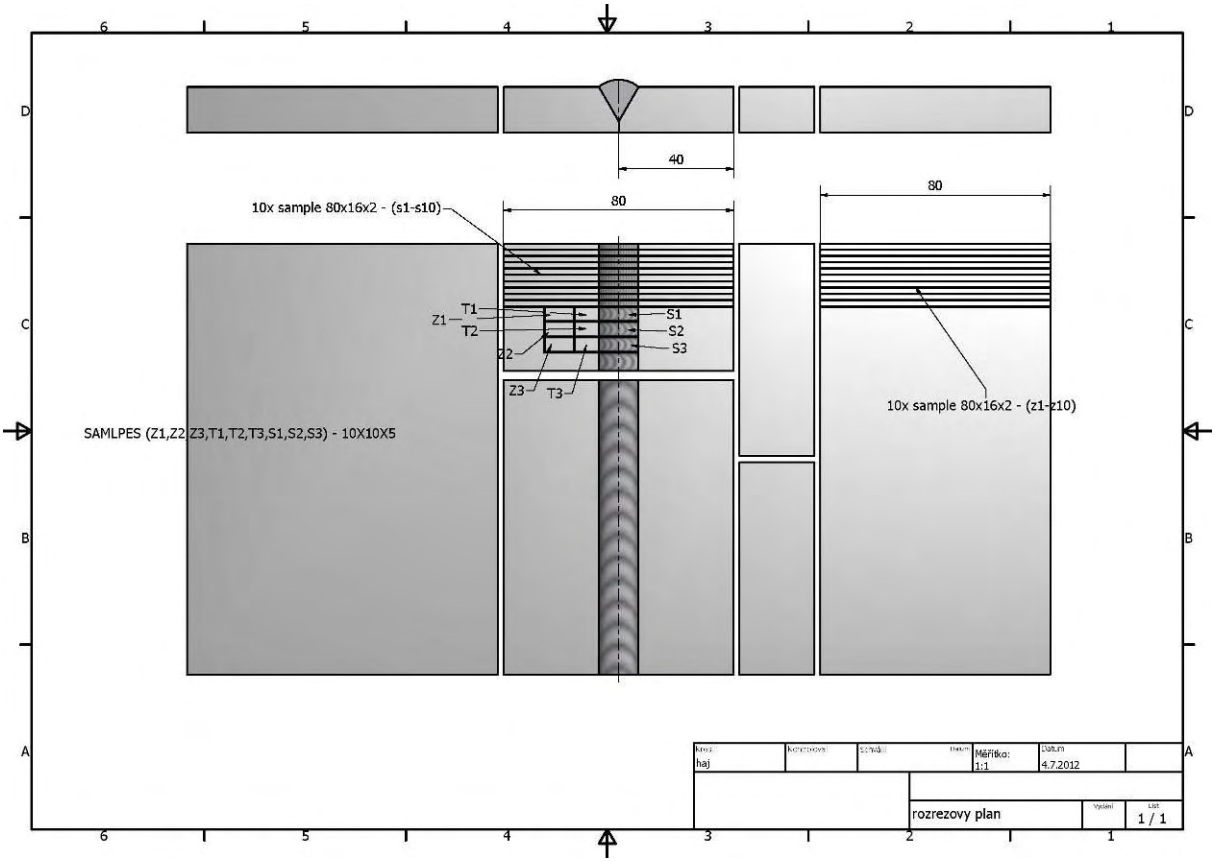

Figure 2: Cutting plan for preparation of samples from alloy 800H

Table 6: Samples from alloy 800 H

Sample	Material	Labelling	Quantity	Surface
approx. 80X16X2 mm, uneven	BM+WM+HAZ	1S – 10S	10	grounded
80X16X2 mm	BM	1Z – 10Z	10	grounded
10X40X2 mm*	BM	Z1 – Z6	6	grounded
10X40X2 mm*	BM+WM+TOZ	S1 – S6	6	grounded
10X10X5 mm	BM	Z1 – Z3	3	grounded
10X10X5 mm	WM	S1 – S3	3	grounded
10X10X5 mm	HAZ	T1 – T3	3	grounded

BM = Base Metal

WM = Weld Metal

HAZ = Heat Affected Zone

*These samples were produced from one sheet measuring 80X16X2 mm

Experimental set-up for corrosion tests

High Temperature Furnace (HTF)

HTF (Figure 3) is the horizontal furnace for HTC testing. The diameter of the inner tube is 40mm which allows for corrosion test in gaseous atmosphere at atmospheric pressure, a gas flow of up to 1l/min, and a maximum temperature of 900°C. The oven temperature can be programmed for the duration of the experiments. The space with constant temperature has a length of approx. 15cm and is arranged in the middle of the oven. The source of the gas atmosphere is a pressurized gas bottle contained a gas mixture of defined composition. The gas bottle is connected to the oven with flexible tubes. For several experiments the gas was dehumidified before entering the oven using a molecular sieves TAMIS 5A. The humidity of the entering gas was controlled with an optical hygrometer BARTEC 5673. The gas passes the retort and is then released into the environment (one – through).

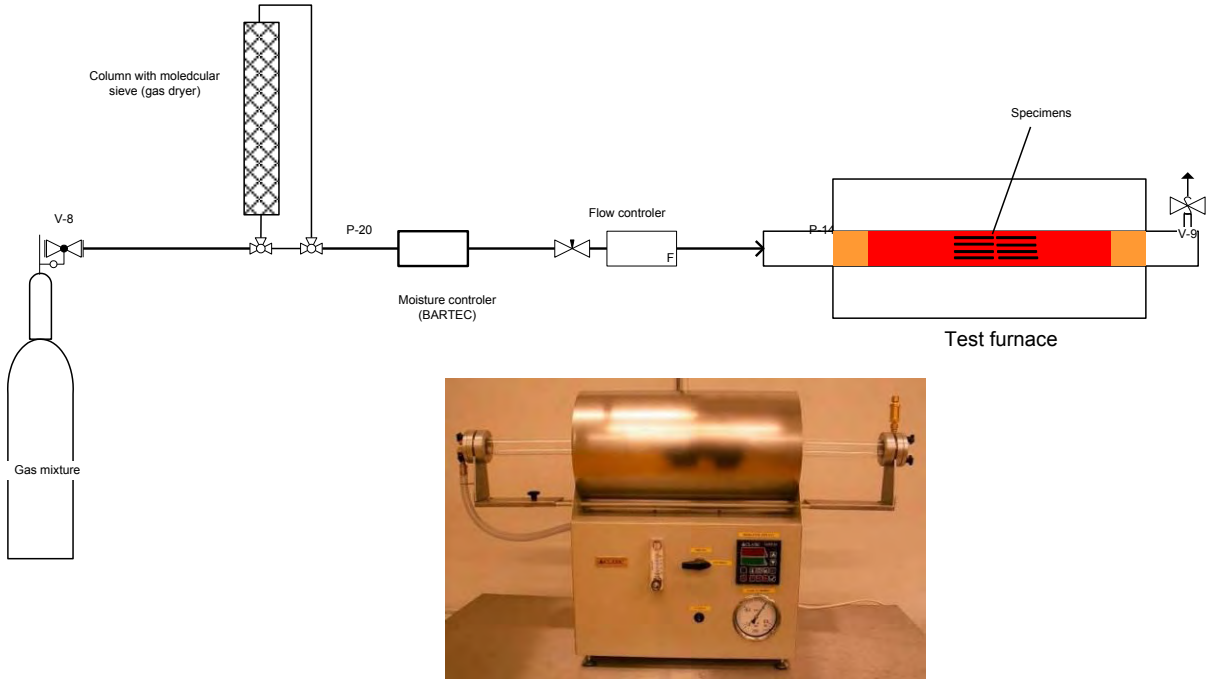

Figure 3: High temperature helium furnace used for corrosion tests

High Temperature helium loop (HTHL)

HTHL (Figure 4) is a device which cycles helium determined for corrosion tests of construction materials a research of the chemistry of gaseous cooling agents. HTHL is equipped with individual circuit for cleaning, dosage, and control of purity of helium. For control of gaseous impurity an optical hygrometer BARTEC and a gas chromatograph with HID detector (GC-HID) were used. The space of the samples had the size of approx. ϕ30 x 500 mm.

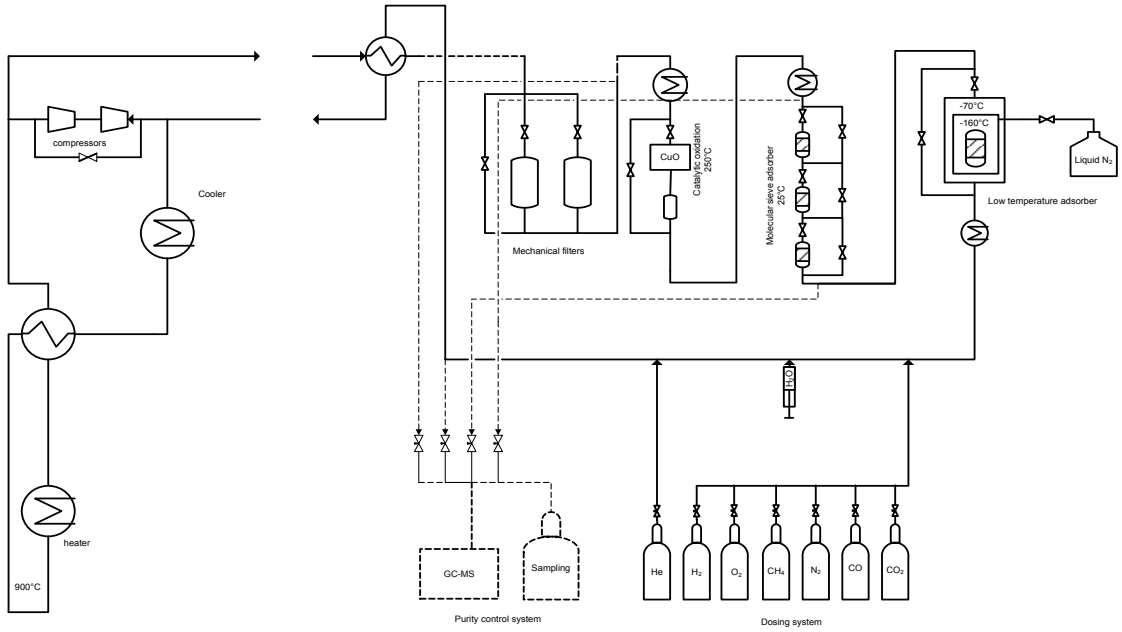

Figure 4: Scheme of High Temperature Helium Loop

Main project parameters of HTHL are:

Pressure of gaseous media:	max. 7 MPa
Max. temperature (only in the region of the sample):	900°C
Max. main gas flow in the main circuit:	38 kg h^{-1}

Further details about the HTHL can be found in [4].

Exposure of samples in corrosive environment - preparation

Exposure of samples from steel P91 and 316

Exposure in HTF

Several tests were provided, the longest lasted 1000h. Usually the samples were taken out of the oven after 500-100h for following evaluation steps. Additional to these tests a big number of tests were conducted with a shorter exposure time.

The samples were fixed at a special holder so that the gas could flow evenly around the samples, (Figure 5). Gas flow in the retort was approx. 0.1 l min^{-1}.

At the beginning of the test the temperature gradient was 3°C min^{-1} until reaching the temperature of 750°C. At this temperature the samples were exposed up to 1000h. Already until heating up the retort was flushed with gas for the corrosive atmosphere. Their composition can found in Table 7. Before taking the samples out of the oven the temperature in the oven was gradually reduced by 3°C min^{-1} until room temperature also in corrosive atmosphere.

One sample of steel P91 (labelled PG 15) was exposed together with a sample from alloy 800H for 1500h at a temperature of 760°C. The atmosphere during the experiment is given in table 7. In this case the temperature gradient for heating up and cooling down was 1°C min^{-1}. More information is provided in the following chapter.
During these tests the set-up was not yet equipped with the sensor for humidity control and the facility for removal of residual humidity for the entering gas.

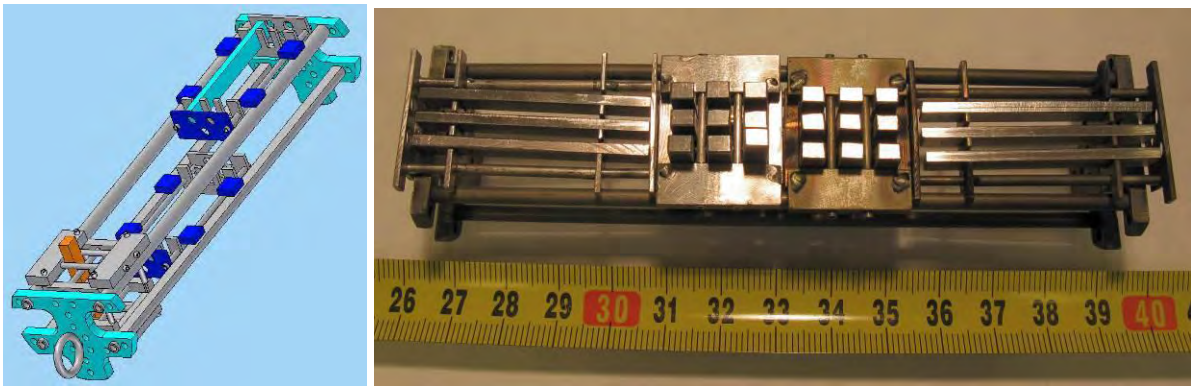

Figure 5: Design of the sample holder and picture of sample holder with sub-size samples 3PB SEN a 5X2X40 mm

Table 7: Chemical composition of gaseous atmosphere during the endurance tests of the selected steels

Component	Concentration [vppm]	Partial pressure [Pa]
CO_2	1	0.1
O_2	2	0.2
CH_4	35	3.5
CO	250	25
H_2	400	40
Helium	Bal.	Bal.

Length of exposure, used sample and testing of samples after exposure are summarized in Table 8.

Table 8: Exposed samples of steel P91 a 316 in HTF and tests after exposure

Time of exposure	Samples (quantity)	Tests after exposure
Initial state (as received, with-out exposure)	3PB SEN (2X8), , 5X2X40 mm, 15X2X40 mm, 11X11X5 mm	Quarry tenacity, metallography, hardness, micro hardness, GD-OES
0,53h	11X11X5 mm (2X1)	Hardness, micro hardness
1h	11X11X5 mm (2X1)	Hardness, micro hardness
2,02h	11X11X5 mm (2X1)	Hardness, micro hardness
2,2h	11X11X5 mm (2X2)	Hardness, micro hardness
23,65h	11X11X5 mm (2X1)	Hardness, micro hardness
24h	5X2X40 mm grounded (2X1), 15X2X40 mm (2X1), 28X49X2 mm (2X1)	GD-OES, mass change
48,4h	11X11X5 mm (2X1)	Hardness, micro hardness
74h	11X11X5 mm (2X1)	Hardness, micro hardness
75,33h	11X11X5 mm (2X1)	Hardness, micro hardness
75,4h	11X11X5 mm (2X1)	Hardness, micro hardness
77h	11X11X5 mm (2X1)	Hardness, micro hardness
120h	5X2X40 mm grounded (2X1), 15X2X40 mm (2X1), 28X49X2 mm (2X1)	GD-OES, mass change
151,6h	11X11X5 mm (2X1)	Hardness, micro hardness
312h	11X11X5 mm (2X1)	Hardness, micro hardness
500h	5X2X40 mm grounded (2X1)	Metallography, micro structure, line scan, SEM-EDX, mass change
1000h	5X2X40 mm grounded (2X1), 5X2X40 mm machined (2X1), 3PB SEN (2X9), towed (2X2+2)	Fracture toughness, metallography, hardness line scan, SEM-EDX, mass change
1500h (in He, composition see Table 7)	5X2X40 mm grounded	Metallography, micro structure, line scan, SEM-EDX, mass change

Exposure in HTHL

Within the test phase of the experimental set-up the samples PG11 and PG12 were exposed. Except the material P91, also samples of Alloy 800 H were exposed (see the chapter below). Tests with constant quality of helium and also tests with variable gas conditions (moisture content) were carried out. Helium of purity 4.6 was used in helium loop for the test runs, The humidity of the gaseous media was recorded, see below (p.22) for details.

Exposure of samples from alloy 800H

Exposure in HTF

The atmosphere for the exposure of the samples is listed in Table 9. The exposure took up to 1500h and the gas flow was approx. 0.1 $l.min^{-1}$. The oven temperature during the experiment was 760°C, the gradient for heating up and cooling down was 1°C min^{-1}.

Table 9: Chemical composition of gaseous mixture for endurance test of alloy 800 H

Component	Concentration [vppm]	Partial pressure [Pa]
CH_4	100	10
CO	500	50
H_2	100	10
Helium	Bal.	Bal.

During this test the humidity of the gases was controlled before entering the oven, the optical hygrometer and molecular sieve are installed. A picture of the holder can be seen in Figure 6.

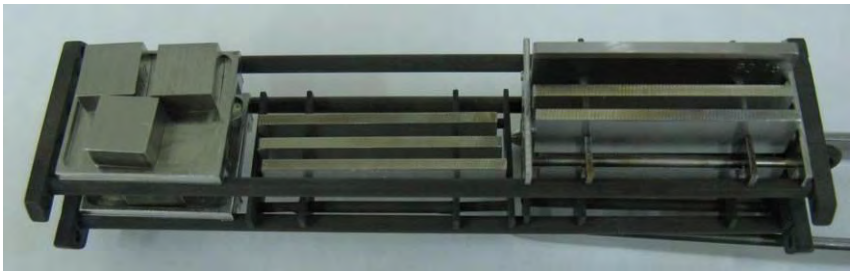

Figure 6: Samples of alloy 800 H in the holder before exposure in HTF

Table 10: Exposure of alloy 800 H in HTF and test after exposures

Time of exposure	Samples (quantity and labelling)	Test after exposure
As received (without exposure)	10X2X40 mm - BM (2 - Z1, Z2), WM+HAZ (2, S1, S2) 1X010X5 mm – BM (1, Z1), WM (1, S1), HAZ (1, T1)	metallography, SEM-EDX, hardness, micro hardness
372h	10X2X40 mm - BM (1 - Z3), WM+HAZ (1, S3) 1X010X5 mm – BM (1, Z2), WM (1, S2), HAZ (1, T2)	metallography, SEM-EDX, micro hardness, line scan, mass change
1000h	10X2X40 mm - BM (1 - Z4), WM+HAZ (1, S4)	metallography, SEM-EDX, micro hardness, line scan, mass change
1500h	10X2X40 mm - BM (2 - Z5, Z6), WM+HAZ (2, S5, S6) 1X010X5 mm – BM (1, Z3), WM (1, S3), HAZ (1, T3)	metallography, SEM-EDX, micro hardness, line scan, mass change

Exposure in HTHL

For tests in the HTHL a special holder was developed in which several samples can be placed. The schema of the holder shows Figure 7. A picture of the holder before mounting the samples to it is Figure 8a. To fix the samples on to the holder it was necessary to drill holes into them, Figure 8b.

Test operation of HTHL

During the test operation the basic parameters, the function of the set-up, and the reliability of long-term tests were identified. Another aim was the estimation and correction of potential defects. As mentioned before in the course of test run it was not possible to set all parameters of the loop and changes of the parameters occurred, which were monitored and recorded. Helium of purity 4.6 was used again. The gas contained residual water (moisture), which was monitored. Other contamination could have occurred by traces of O_2 a N_2. By that time it was not possible to determine their concentration. During the last period of the test operation of HTHL also other compounds (CO, CO2, H_2, CH_4) were present in helium gas and monitored by gas chromatography.

The physical and chemical parameters of helium gas during test operation and exposure of specimens are represented in Figure 9.

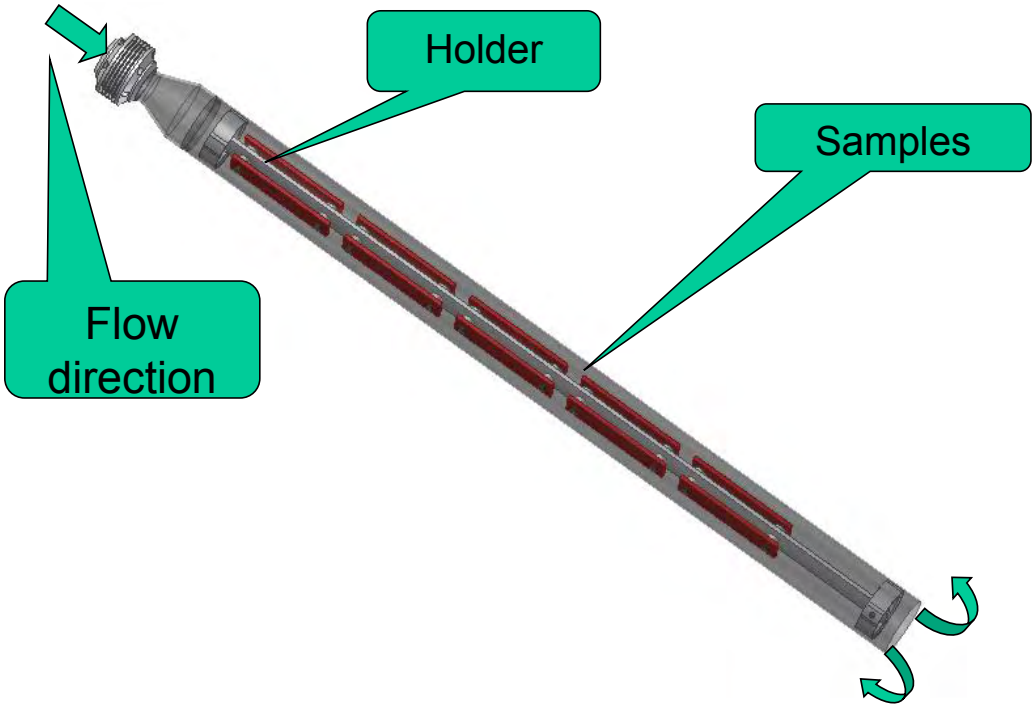

Figure 7: Scheme of samples arranged on the holder in the test zone of HTHL

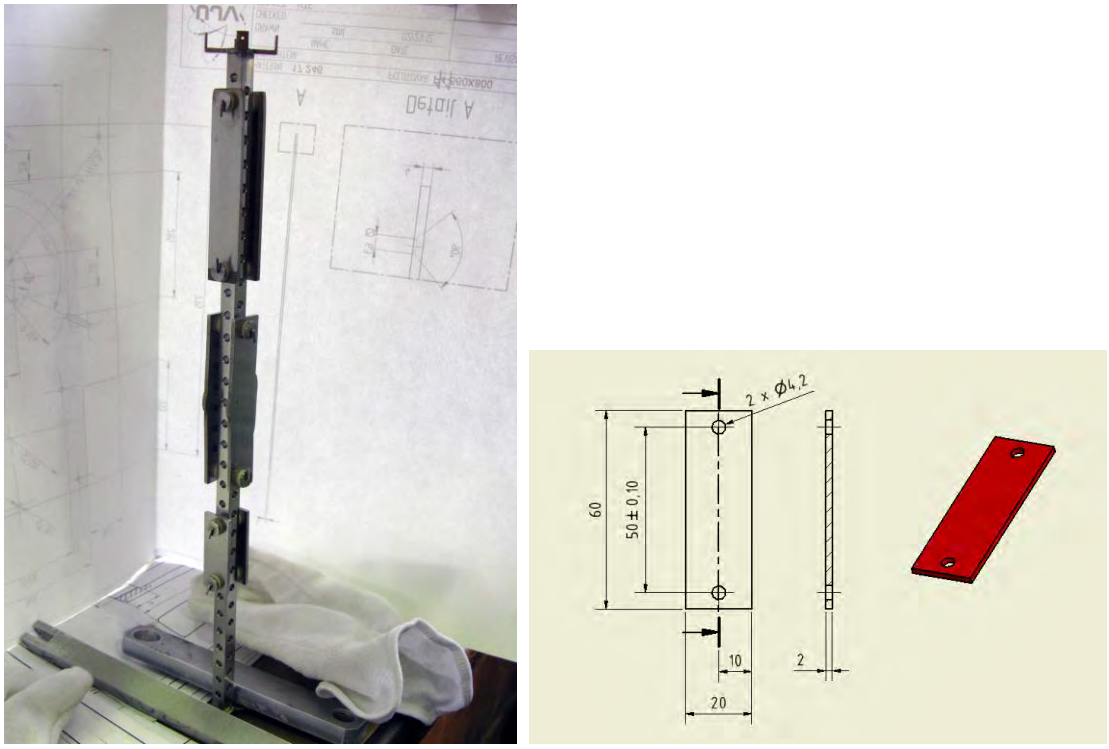

a) b)

Figure 8: a) samples on the holder before mounting it into the test zone of HTHL, b) design of samples for test in HTHL

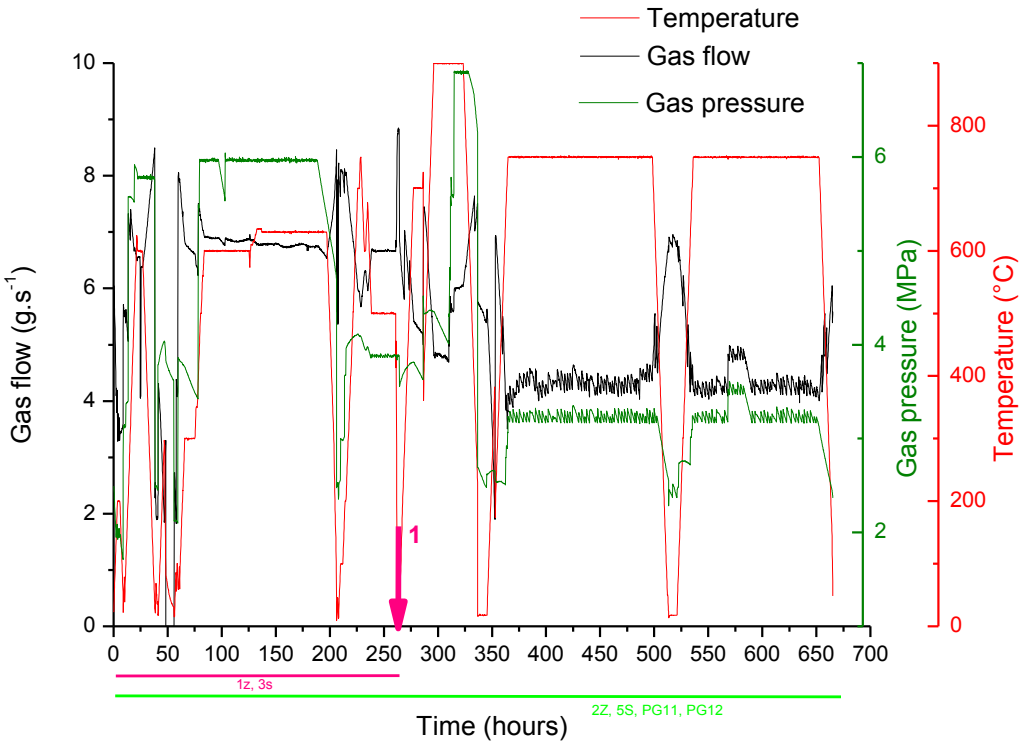

a

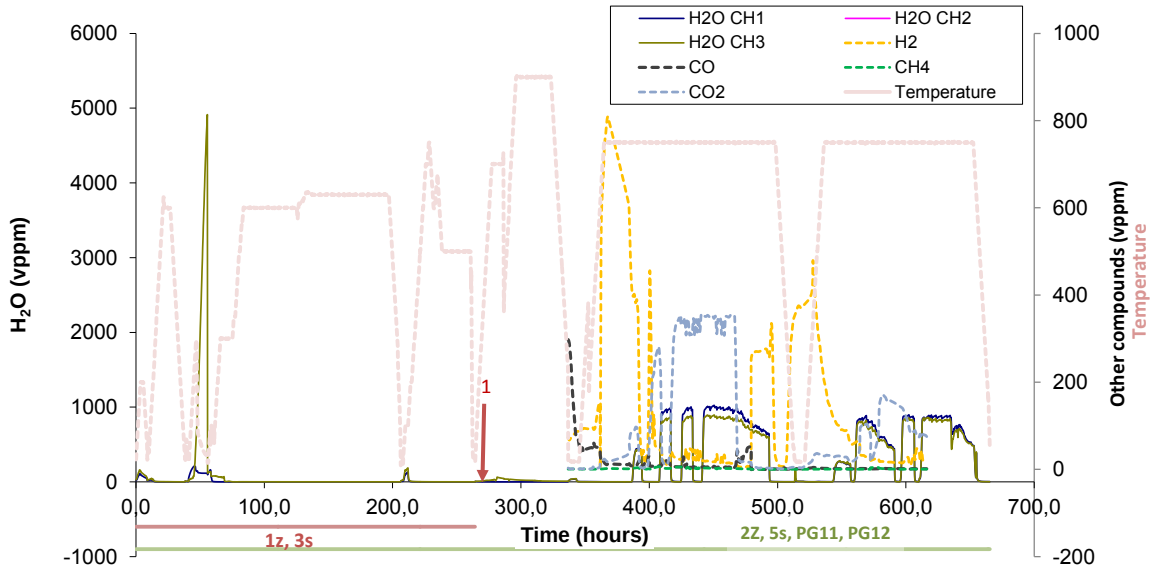

b

Figure 9: a – Physical parameters and b- chemical composition of helium gas during the test operation of HTHL. Point 1: Dismantling of active section and withdrawal of the samples 1z and 3 s

Total duration of the test operation was 665 hours (with several interruptions). Maximum temperature in the first period (First 264 hours) was 750°C, average temperature was 460°C. After this period the active part of the loop was dismantled and 2 specimens withdrawn.

Table 11: Samples exposed in HTHL during test operation

Time of exposure (hours)	Samples (labelling)	Material	Tests after exposures
264	1Z	800 H BM	metallography, SEM-EDX, micro hardness, line scan, mass change
264	3S	800 H WM, HAZ, BM	metallography, SEM-EDX, micro hardness, line scan, mass change
665	2Z	800 H BM	metallography, SEM-EDX, micro hardness, line scan, mass change
665	3S	800 H WM, HAZ, BM	metallography, SEM-EDX, micro hardness, line scan, mass change
665	PG11	P91	metallography, SEM-EDX, micro hardness, line scan, mass change
665	PG12	P91	metallography, SEM-EDX, micro hardness, line scan, mass change

Corrosion tests in HTHL

Before the start of the corrosion tests the test zone of the HTHL was dismounted. Thus it was able to insert the new samples. After that the loop was filled with a gaseous mixture according to

Table 12. Test was originally planned for 1000h at a temperature of 760°C and pressure of minimum 3 MPa. The concentration of gas contamination and other parameter are monitored during the whole period of the experiment. After 160 hours of operation of HTHL (109 hour at 760°C) serious failure of the device occurred. Therefore the test had to be interrupted and the device completely dismantled. After dismantling 2 specimens were taken out for evaluation. The rest of the specimens were retained for continuation of exposure after repair of the device (after finishing of this report)

Table 12: Chemical composition of gaseous mixtures for corrosion tests in HTHL

component	Concentration [vppm]	Partial pressure [Pa]
CH_4	10	30
CO	50	150
H_2	10	30
Helium	Bal.	Bal.

The samples used in this test are stated and described in Table 13.

Table 13: Samples exposed in HTHL during corrosion tests

Time of exposure (hours)	Samples (quantity and labelling)	Material	Tests after exposures
1000	5Z	800H base metal	SEM of surface, metallography, microstructure, mass change
160	2S	800H , WM, HAZ, BM	SEM of surface, metallography, microstructure, mass change
1000	4S	800H , WM, HAZ, BM	SEM of surface, metallography, microstructure, mass change
160	6S	800H , WM, HAZ, BM	SEM of surface, metallography, microstructure, mass change
1000	PG16	P91	SEM of surface, metallography,

			microstructure, mass change

Concentration of minor admixtures in helium gas changed (mostly decreased) during operation. The gas was continually dried during operation. The main parameters of the 160 hours operation are summarized in Figure 10. The gas flow through the test section of HTHL ranged from 3-8 $g.s^{-1}$.

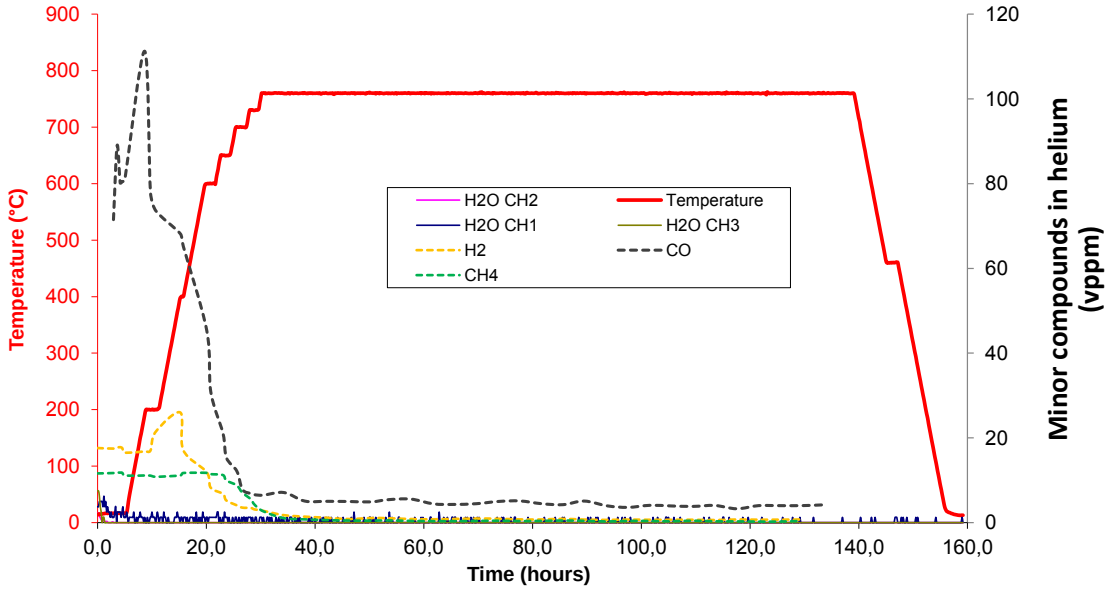

Figure 10: Concentration of minor compounds in helium gas and temperature during 160 h operation of HTHL.

Evaluation of samples after exposure

These tests are summarized in Table 8, Table 10, Table 11, and Table 13. These tests were performed mainly for determination of fracture toughness (in the case of steel 316 and P91), of hardness and micro hardness, investigation of corrosion layers using electron microscopy (SEM-EDX), metallographic evaluation and the study of changes in micro structure and chemical composition in cross section applying line scan. With some samples the surface layer was studied using the glow discharge optical emission spectroscopy (GD-OES) method [5]. Fracture toughness was tested at bodies measuring 3X4X27 mm containing the produced notch and an initial defect using the periodic fatigue toughness method.

Hardness tests were conducted using so-called Vickers indenter. Hardness was tested at a strain of 30 kgf, micro hardness was evaluated using strain of 300 gf. The parameters for each test can be found in Table 14.

Determination of thickness of corrosive surface layer:
The measuring of the corrosive layer was conducted at several samples using metallography at the cross section. Further methods for estimation of the thickness of the corrosive layer were line scan and GD-OES at the position of the intersection of the lines of Cr and Fe content in dependence of the thickness of the material.

Table 14: Parameters for measuring

Parameters	Micro hardness	Macro hardness
Type of indenter	Vickers	Vickers
strain (gf or kgf)	300 gf	30 kgf
Dwell time (s)	10	10
Number of imprints onto samples	7	3

Most of the tests for evaluation of the samples after exposure were carried out at partner organizations: ÚJV Řež a.s., VŠCHT Praha (ICT Prague), and ČVUT (Czech technical university).

Results and discussion

Tests of samples from steel P91 and 316

Tests after exposure in HTF

Appearance of samples and mass changes after exposure

The samples before exposure are shown in Figure 11 at the left side, on the right side after exposure. In the left column of each picture are the samples of steel P91. At the surface of samples after exposure is a visible, dark, greenish layer. This is an indicator of the presence of chromium oxide.

The average mass changes of the samples in dependence of time of exposure at 750°C are shown in the graph in Figure 12. From the graph it is obviously that the mass change of steel 316 during long-term exposure are lower than those of steel P91.

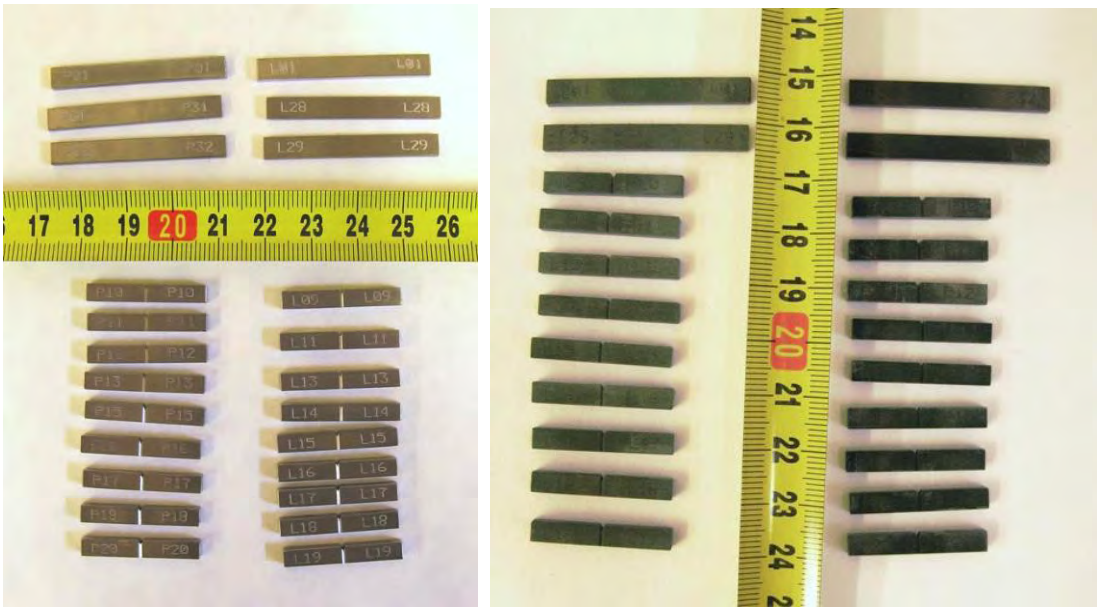

Figure 11: Samples of steel P91 a 316 before and after exposure at 750 °C for 1000 h

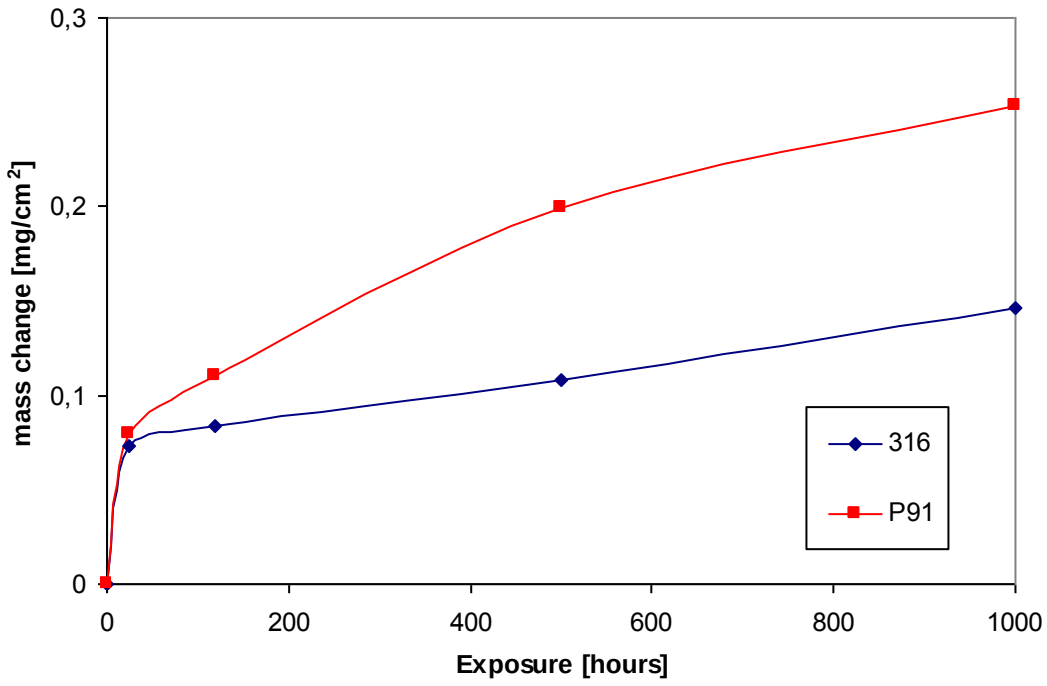

Figure 12: Mass changes of samples from steel P91 a 316 after exposure in helium containing impurity, in HTF at a temperature of 750°C

Results from tests of fracture toughness

The results of theses tests are summarized in Table 15.

Steel 316

From the results it is evident that the fracture toughness of steel 316 is significantly lower after exposure. Before exposure steel 316 shows substantially higher resistance against crack propagation, i.e. the value of fracture toughness $J_{0,2}$ (resp. $KJ_{0,2}$) is greater than for the samples of steel 316 after exposure in helium with impurity for 1000h at 750°C

The following fractographic analysis of the broken test bodies of steel 316 at initial state showed crack propagation due to ductile, transcrystalline crack mechanism during testing fracture toughness. In the case of samples after exposure for 1000h at 750°C in a gaseous atmosphere containing helium and other compounds (see Table 7) crack growth obeyed to ductile, dimpling crack micro-mechanism. Figure 13 shows a comparison of lines of force F over movement v for samples before and after exposure.

Table 15: Changes in fracture toughness at 25°C for steels 316 and P91

	steel 316					**steel P91**				
	Initial state		**After exposure (He-tab. 1-10, 750°C, 1000h.)**			**Initial state**		**After exposure (He-tab. 1-10, 750°C, 1000h)**		
Nr. of samples	8		9			8		9		
	$J_{0.2}$ [J/cm^2]	$K_{J0.2}$ [MPa.m$^{1/2}$]	$J_{0.2}$ [J/cm^2]	$K_{J0.2}$ [MPa.m$^{1/2}$]	Change $J_{0.2}$ [%]	$J_{0.2}$ [J/cm^2]	$K_{J0.2}$ [MPa.m$^{1/2}$]	$J_{0.2}$ [J/cm^2]	$K_{J0.2}$ [MPa.m$^{1/2}$]	Change $J_{0.2}$ [%]
average	62	320	20,6	212,7	67	27,3	247,6	27,3	244,9	0
variance	10,9	32,2	1,8	9	-	3,5	16,5	3,2	14	-

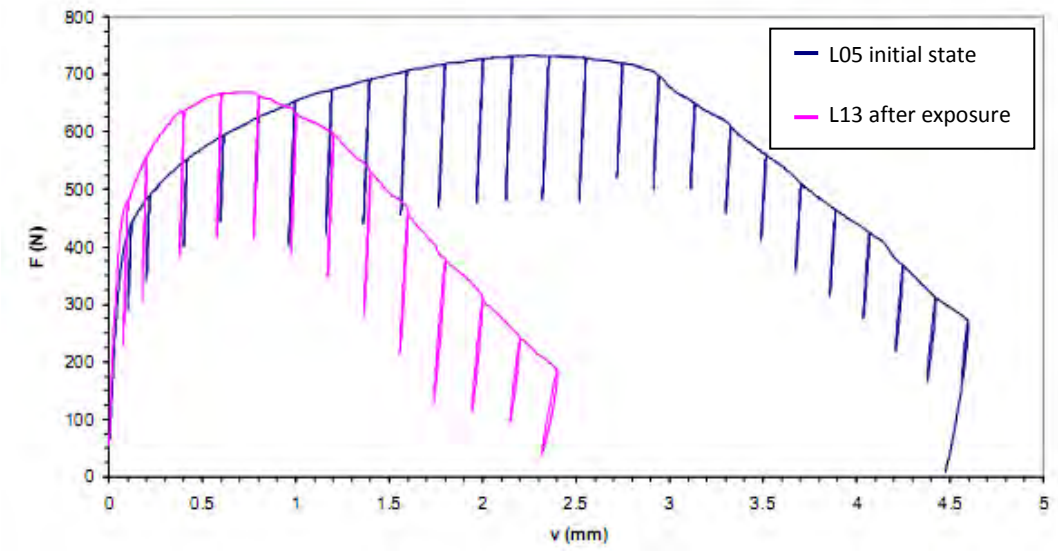

Figure 13: Comparison of graphs of force F over movement v for samples of steel 316 before (blue line) and after exposure for 1000h at 750°C in helium with impurity (red line)

Steel P91

It was found that for steel P91 the fracture toughness $J_{0,2}$ (resp. $KJ_{0,2}$) was not changed by exposure for 1000h at 750°C in helium with impurity. Fracture tests on samples from P91 without exposure showed that crack growth appeared according to ductile, transcrystalline crack mechanism. The samples from P91 after exposure (1000h, 750°C, helium with impurity) showed different crack behaviour. In some samples occurred pop-in cracks, which are clearly indicated by the curve force F over movement v as sudden decrease in force. To these hop-in cracks correspond areas of disrupted transcrystalline fission on the crack surface. It can be assumed that the change in micro structure is caused by elevated transition temperature from fragile to tough crack. The graphs of force F over movement v for the samples form steel P91 is shown in Figure 14.

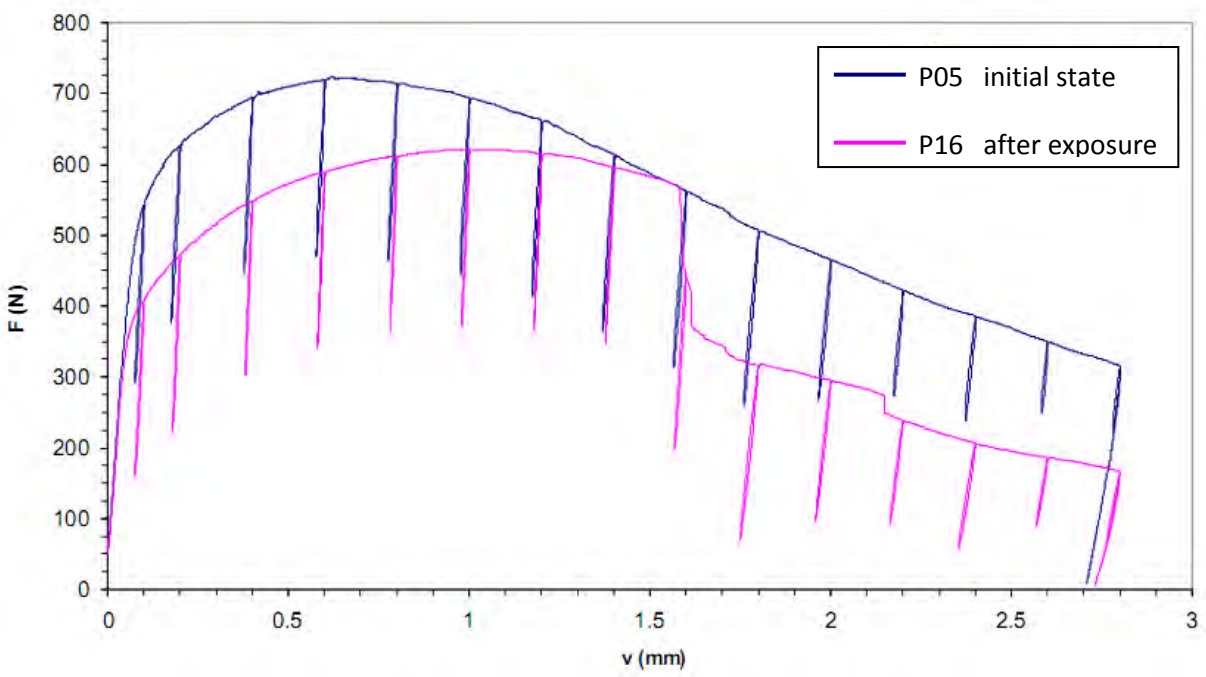

Figure 14: Comparison of graphs of force F over movement v for samples of steel P91 before (blue line) and after exposure for 1000h at 750°C in helium with impurity (red line)

Results of tests of hardness and micro hardness

Figure 15 and Figure 16 show hardness and micro hardness, respectively, of steel P91 and 361 depending on exposure time. They show that hardness and micro hardness of steel P91 starts to decrease after approx. 100min of exposure. The hardness of steel 316 shows an oscillating trend over exposure time. The reason for this behaviour cannot be clearly estimated, for clarification further and more detailed tests are necessary.

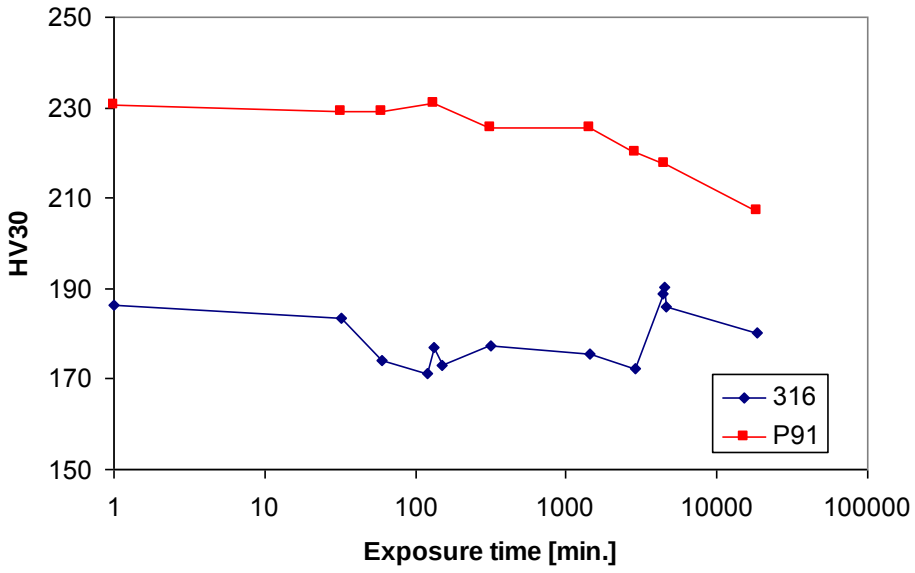

Figure 15: Dependence of hardness of steel P91 (red line) a 316 (blue line) on time of exposure in helium containing impurity at 750°C

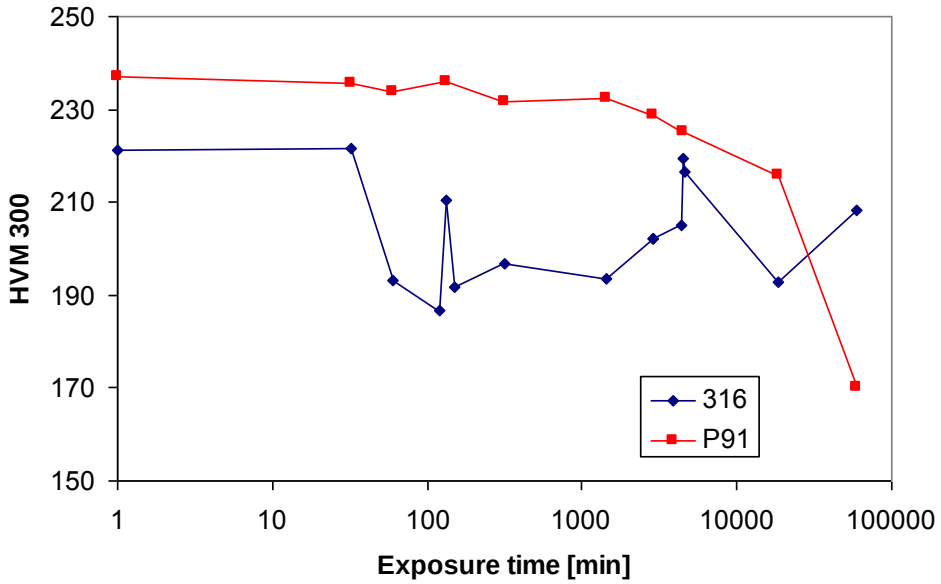

Figure 16: Dependence of micro hardness of steel P91 (red line) a 316 (blue line) on time of exposure in helium containing impurity at 750°C

Sample surface, metallography, and corrosive surface layers

Figure 17 and Figure 18 show a microscopic picture of samples of steel P91 and 316, respectively. A very non-compact layer was observed for samples with machined surface after exposure for 1000h. Therefore further tests were conducted only with samples with grounded surface.

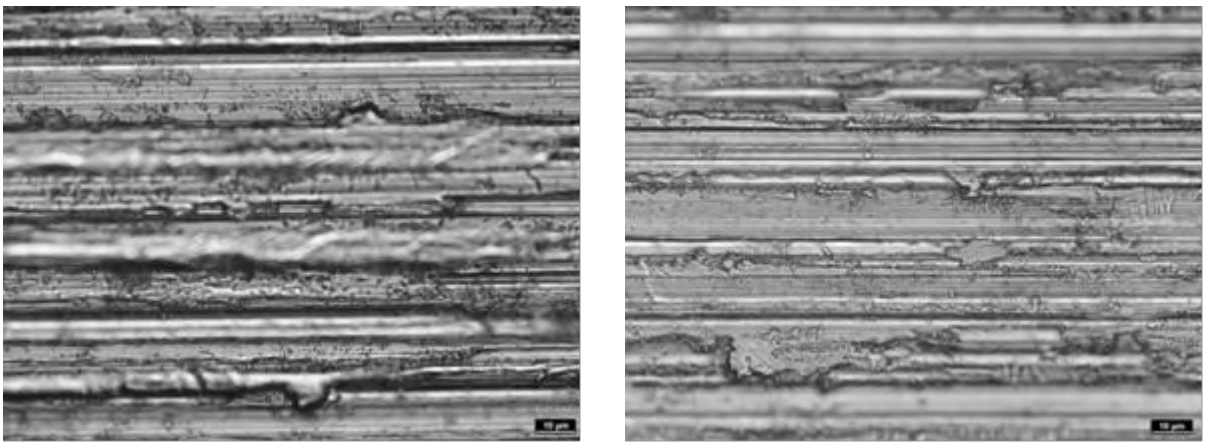

Figure 17: Surface of samples L35 (steel 316) and P45 (steel P91) in initial state (grounded surface)

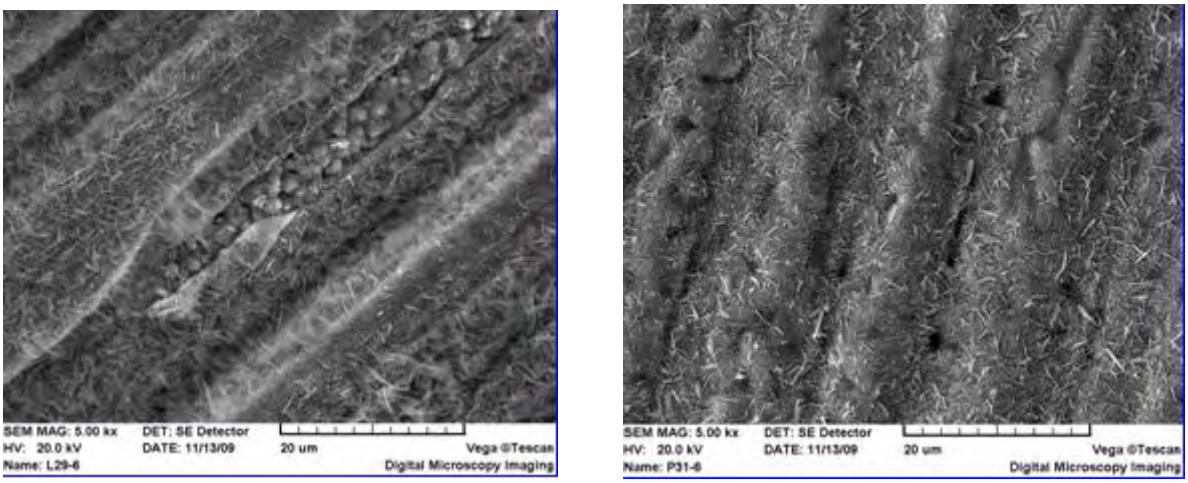

Figure 18: Surface of samples L29 (steel 316) and P32 (steel P91) after exposure for 1000h at 750°C

The **micro structure of steel 316** in the initial state is formed by almost equiaxed austenitic grain with numerous twins a high content of δ-ferrite, elongated in the direction of shaping. It was shown that within the structure can be found thin, oval, and elongated intrusions, too. After exposure at 750°C and 500h a considerably decomposition of δ-ferrite takes place at particles and secondary austenite. It was further observed a separation of rough particles, mainly at the grain borders. Roughening of particles could be found in regions of segregation, too. After 1000h of exposure a further decomposition of δ-ferrite was noticed and also a separation of rough particle mostly at the border and also in the matrix. Areas of segregation are not visible. Separated particles have several shades of grey and it can be expected that they consist of various kinds of carbides ($M_{23}C_6$, M_6C) and intermetallic phases (δ, η, χ). Figure 19 shows the changes in micro structure of steel 316.

The **micro structure of steel P91** in the initial state is typical for annealed martensitic-ferritic steel. The structure is formed by carbide-ferritic mixture, whereat carbide (most likely $M_{23}C_6$) are separated mainly at borders of martensitic material, in small amount can be found proeutectoid ferrite, too. The boundary of austenitic grains was not well-defined. The few inclusions have an oval shape. After exposure at 700°C for 500h the borderline of primary austenitic material was much more accentuated due to separation of particles (carbides). It also came to roughening of particles at the grain boundary and the material structure. Proeutectoid ferrite was not detected. Figure 20 illustrates changes in micro structure of steel P91.

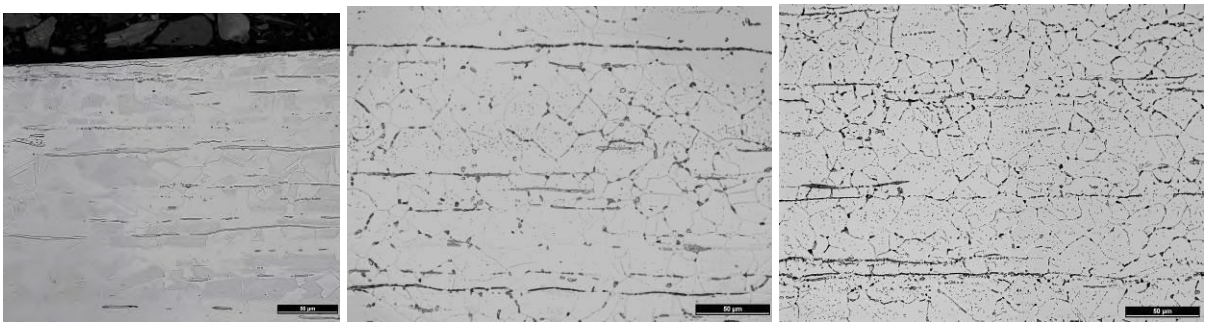

a) b) c)

Figure 19: Microstructure of steel 316 a) initial state, b) after exposure in He 750°C/500h, c) after exposure in He 750°C/1000h

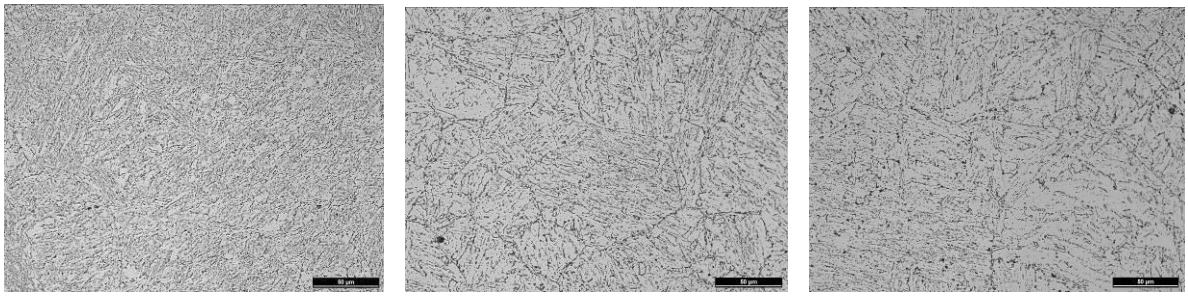

a) b) c)

Figure 20: Microstructure of steel P91 a) initial state, b) after exposure in He 750°C/500h, c) after exposure in He 750°C/1000h

After exposure of the samples the thickness of corrosive (oxidic) surface layer was determined. The thickness was measured on the one hand directly on the polished cross section of the samples, on the second hand it was estimated from line scan or GD-EOS (and the velocity of dust separation from material volume) analysis of the chemical composition of the material at the cross section. In most cases responded the thickness of this layer to the distance from the point of intersection of depth profile for Fe and Cr to surface of the samples. The layer thickness can be estimated from the width of the peak of the content of O_2 at the sample surface. The measuring of the surface thickness at several samples after exposure for 120h was carried at ICT Prague and for other samples after exposure for 500h and 1000h at ÚJV Řež. The results form direct measurements at ÚJV Řež differ from the estimation of thickness from GD-OES and line scan. The graph containing the chemical analysis from line scan and GD-OES of surface and subsurface layers can be found in the appendix of this report. The discrepancy in thickness measured and estimated can be explained with the differentness of these methods, the different sensitivity of them, and with the inhomogeneity of the corrosion layer. It is know the estimation method from the depth profile of Fe and Cr is not very precise. Examples of direct measuring of the oxidic layer show Figure 21.

It was found out that the corrosive layer after exposure is not uniform and is a two-layer. The outer layer consists mainly of Fe oxides, on basis of Fe_3O_4. The inner layer is rich in Cr (Cr_2O_3). Beneath the corrosion layer a layer impoverished in chrome was observed. For steel P91 the sub-corrosive layer contained no carbides. The data of corrosion layers, layers Cr impoverished, and layers without carbides are summed up in Table 16. The dependence of corrosion layer thickness on time of exposure at 750°C in gaseous atmosphere (according to Table 7) is shown in Figure 22. Results used for Figure 22 are taken from direct measuring of corrosive layer. Figure 22 does not contain data from GD-OES and SEM/EDX analysis.

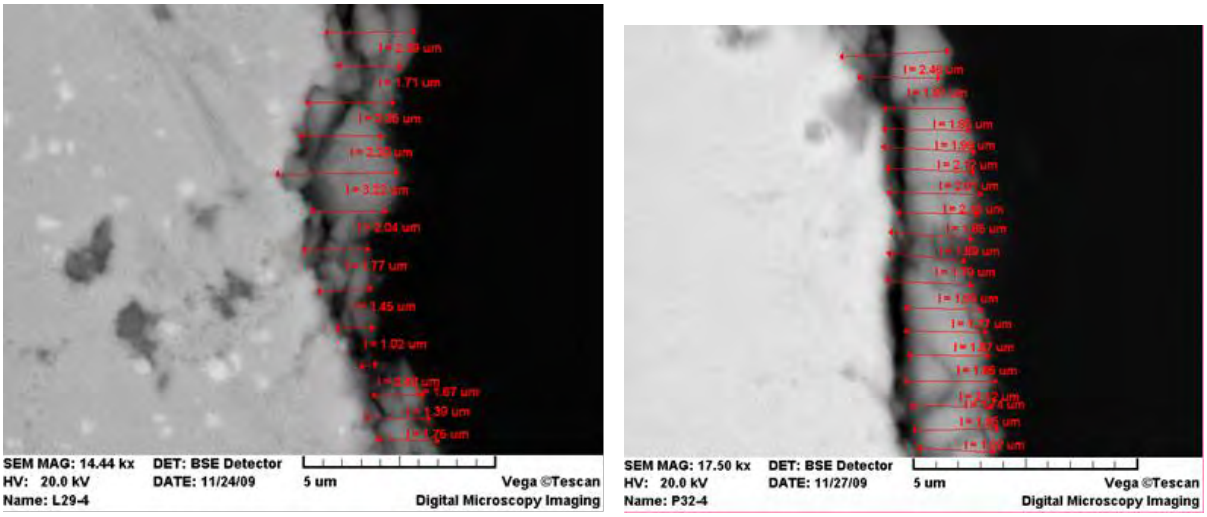

a b

Figure 21: Determination of average thickness of oxide layer: a) 1.96µm at sample L29, steel 316, after exposure 750°C, 1000h, b) 1.86µm at sample P32, steel P91, after exposure 750°C, 1000h

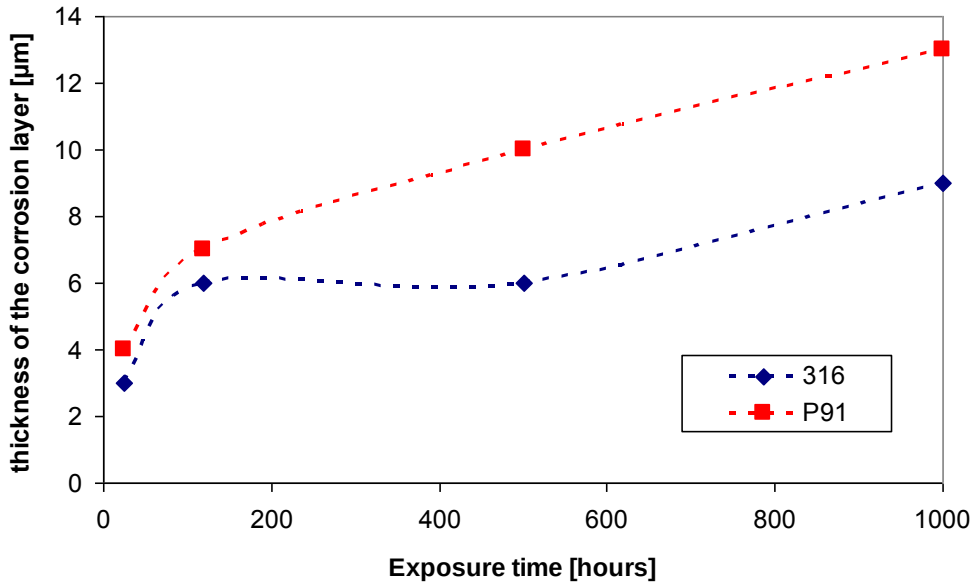

Figure 22: Thickness of oxide layer depending on time of exposure in gaseous atmosphere according to Table 7

Table 16: Thickness of corrosive layers, of chrome depleted, and of layers without carbide after exposure at 750°C

material/ sample surface	Expo-sure	Corro-sion layer (metallo-graphy)	corrosive layer (GD-OES or SEM/EDX)	region without carbide (metallo-graphy)	Cr depleted region (GD-OES, SEM/EDX)	Cr de-pletion [wt. %]

	[h]	[µm]	[µm]	[µm]	[µm]	
316/grounded	24	3,0	3	Not identified	4	10
	120	6,0	6		4	9
	500	0,64	6		16	23
	1000	1,96	9		12	19
316/machined	1000	1,43	-		18	8
P91/grounded	24	-	4	6	7	15
	120	-	7	11	9	10
	500	2,67	10	16	23	15
	1000	1,86	13	17	4	25
P91/machined	1000	1,88	-	22	33	11

Evaluation of exposure of sample PG15

This sample was exposed together with a sample from alloy 800H in gaseous mixture, see Table 9, at a temperature of 760°C for 1500h in HTF. The basic parameters, i.e. temperature characteristics in dependence of time of exposure and concentration of water in gas, are described in the next chapter. The samples before and after exposure are shown in Figure 23a) and b), respectively.

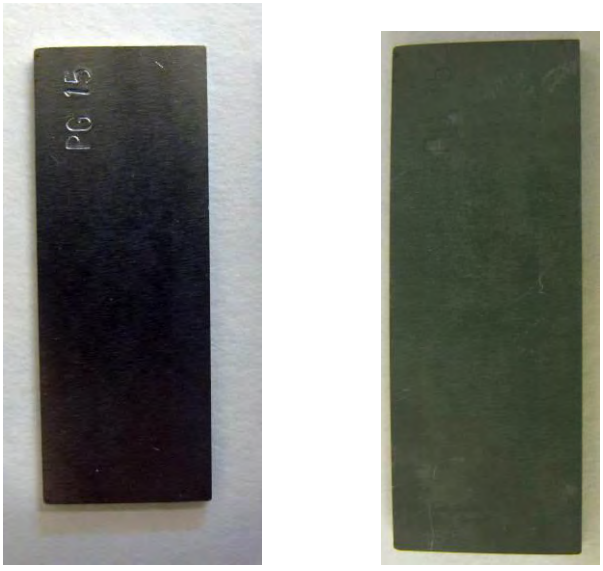

a) b)

Figure 23: Samples of steel P91 (PG 15): a) initial state, b) after exposure in gaseous blend (see Table 9) at 760°C for 1500h

After exposure a mass growth of 0.268mg/cm2 determined. This figure differs only marginally from mass growth on samples from steel P91 after exposure in gaseous atmosphere according to Table 7 at 750°C for 1000h. Figure 24 shows a picture of the surface of sample PG51 from steel P91 from electron microscope.

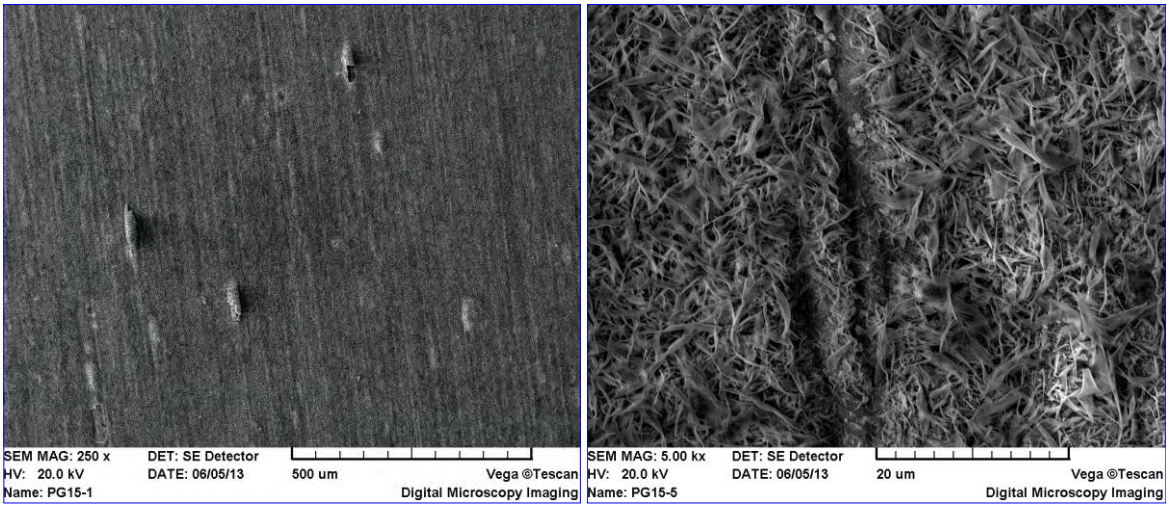

Figure 24: SEM picture of the sample surface from steel P91 (PG15) after exposure in gaseous atmosphere according to Table 7

The chemical composition of the sample surface was analysed at five positions. Average values are summarized in Table 17. It is possible to say that the surface is made up mainly of oxides from chrome and manganese.

Table 17: Chemical composition of sample surface PG15 after exposure at 760°C for 1000h, average value from 5 position

	O	Cr	Mn	Fe
% by weight	30.49	49.08	18.57	1.86
at. %	60.38	27.85	10.71	1.06

Microstructure on the cross section of the specimen consists of ferritic-carbidic structure, carbides (probably $M_{23}C_6$) are suspended on the boundaries of martensitic bars – see Figure 25. Also decarburization was observed on the cross section of the specimen – see Figure 26. The thickness of corrosive layer observed by microscope is approx. 3 µm (according to line scan approx. 6 µm).

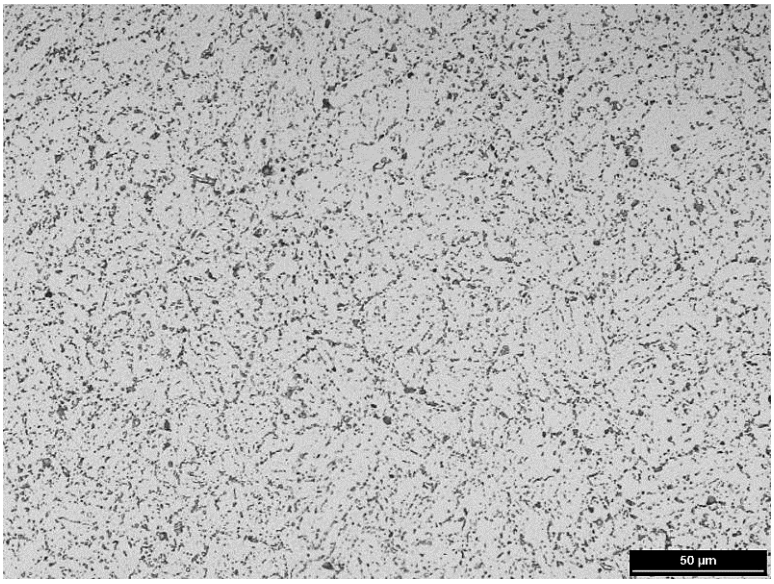

Figure 25: Microstructure of the cross section of the specimen P91 (PG15) after exposure of 1500 h at 760°C in impure helium

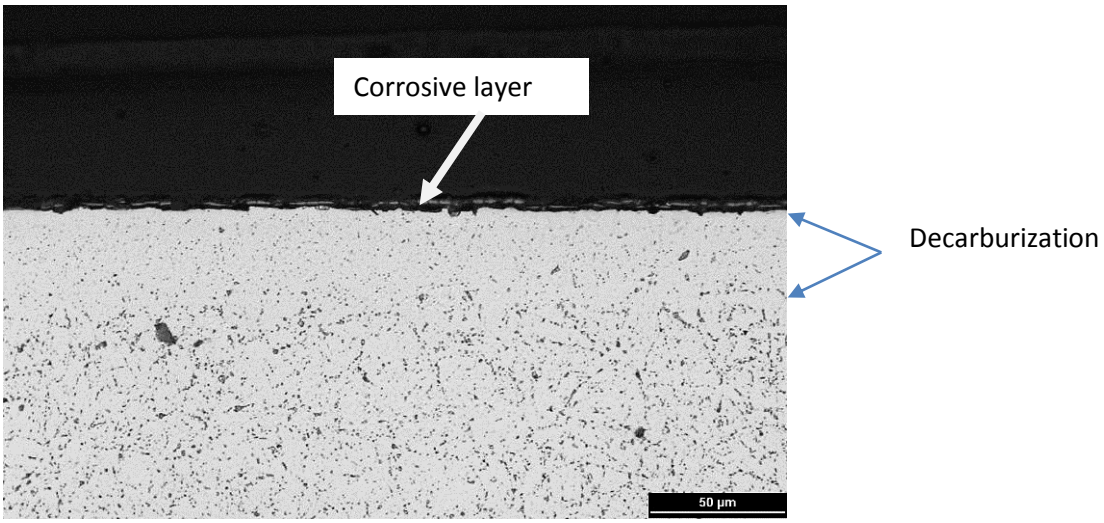

Figure 26: Undersurface decarburization zone on the cross section of the exposed specimen of P91 (PG15)

Summary of results of sample evaluation from steel P91 and 316 exposed in HTF

Test results from steel P91 and 316 exposed in HTF at temperatures between 750 and 760°C in gaseous atmosphere according to Table 7 and Table 9 are summarized as followed:

- For steel 316 a decrease in fracture toughness by 67% compared to the initial state was observed. The weakening of fracture toughness in case of steel P91 was moderate. Reduction in hardness after exposure of 100h was approx. uniform for steel P91, for steel 316 it was fluctuating. It can be assumed that the change in mechanical properties is influenced mainly by the temperature on its own than by the composition of the gaseous atmosphere. To confirm this thesis, further experiments would be necessary.

- The corrosion layer thickness was in the range of approx. 2 to 12µm, the thicker corrosion layer was determined for samples from steel P91. Also the weight growth after exposure was greater for steel P91.

- At samples from steel P91 a zone without carbides was observed. That was not the case for steel 316.

- The corrosion layer is apparently made up from chrome and manganese oxides, although the gaseous atmosphere was slightly reductive. It is supposed that during experiments there was little amount of air in the apparatus. As it is a flow through setup at ambient pressure it is not possible to remove air completely. In the gas was also residual humidity, approx. 10vppm, see figure in the next chapter.

Tests after exposure in HTHL

Test I.

Evaluation of specimens after 665 hours of test operation of HTHL are finished (PG11, PG12). Average mass gain of specimens after exposure is 0.13 mg.cm^{-2}.

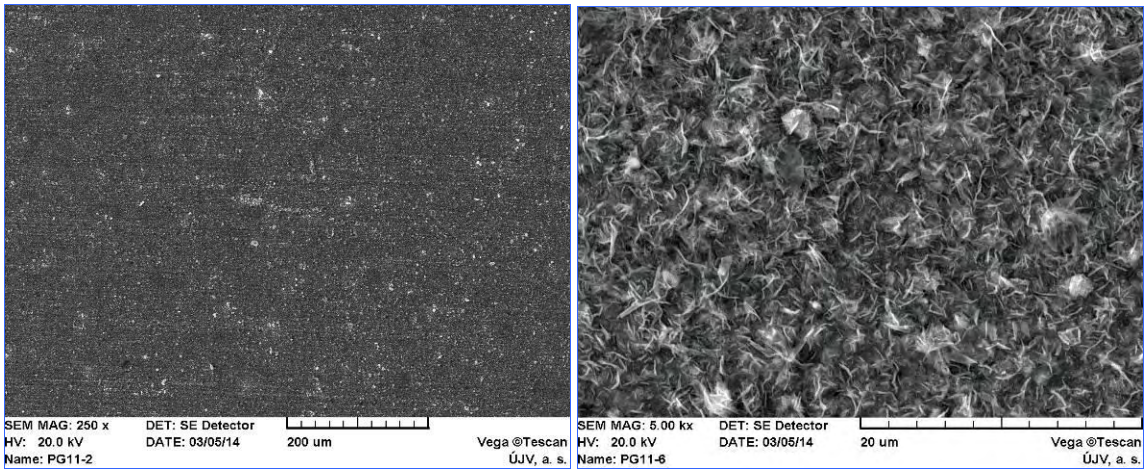

Figure 27: SEM picture of the sample surface of steel P91 (PG11) after exposure in HTHL during the Test operation of the device

Table 18: Average chemical composition of sample surface PG11 and PG12 after exposure in HTHL during the Test operation (665 hours)

	O	Al	Si	V	Cr	Mn	Fe
% by weight	27.0	0.4	0.9	0.7	38.2	15.3	17.4

Average values of chemical composition of the surface layer are listed in Table 18. Compared with chemical composition of the surface layer after exposure in HTF (see Table 17) the differences were found out, especially the content of Fe is higher and the content of Cr is lower in case of the specimen exposed in HTHL compared to that exposed in HTF. The cause could be the different

chemical composition of the environment (among others less content residual O_2 is expected in HTHL than in HTF) and also exposure time and physical parameters (temperature, pressure, flow rate) were different. The thickness of corrosive layer was estimated to be 5 µm (according to line scan). On the cross-section depleted Cr zone 20 µm under corrosive layer was observed.

Test II.

Test conditions, temperature and pressure in the loop were kept at 760-800°C, and 3,5MPa. During the exposure also gas impurities were added, 10 ppm H_2 + 10 ppm CH_4 + 50 ppm CO. Impurity levels in the flowing helium are controlled through a feedback mechanism based on gas chromatography with HID detector (GC-HID) measurements of the gas chemistry at the inlet from a HTHL-1 containing the test materials. The duration of the test was 100h.

The micro structure of steel P91 in the initial state is formed by carbide-ferritic mixture, whereat carbide (most likely M23C6) are separated mainly at borders of martensitic material.

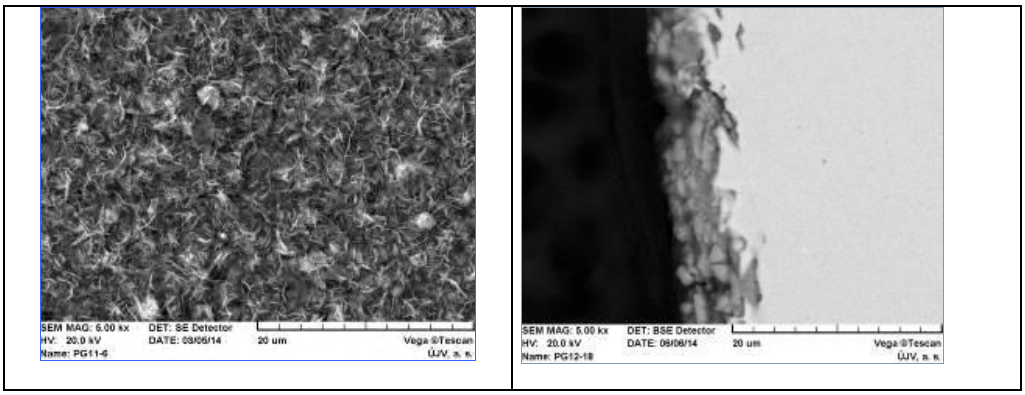

Fig. 28 SEM micrographs of specimen of P91 exposed to impure helium at 800°C for 100 h. a) surface; b) cross-section

It was found out that the corrosive layer after exposure is not uniform. It consists mainly of Fe oxides, on basis of Fe3O4. Beneath the outer oxidation layer, a layer depleted in chrome was observed. For steel P91 the sub-corrosive layer contained no carbides.

Sample evaluation from alloy 800H

Tests after exposure in HTF

In Figure 29 can be seen the temperature profile and the concentration of residual humidity in the gas mixture before entering the alembic in the oven. The residual humidity during operation at 760°C was approx. 10vppm, this corresponds to a partial pressure of 1Pa, after passing the molecular sieve. During heating-up a short-term rising of humidity occurred.

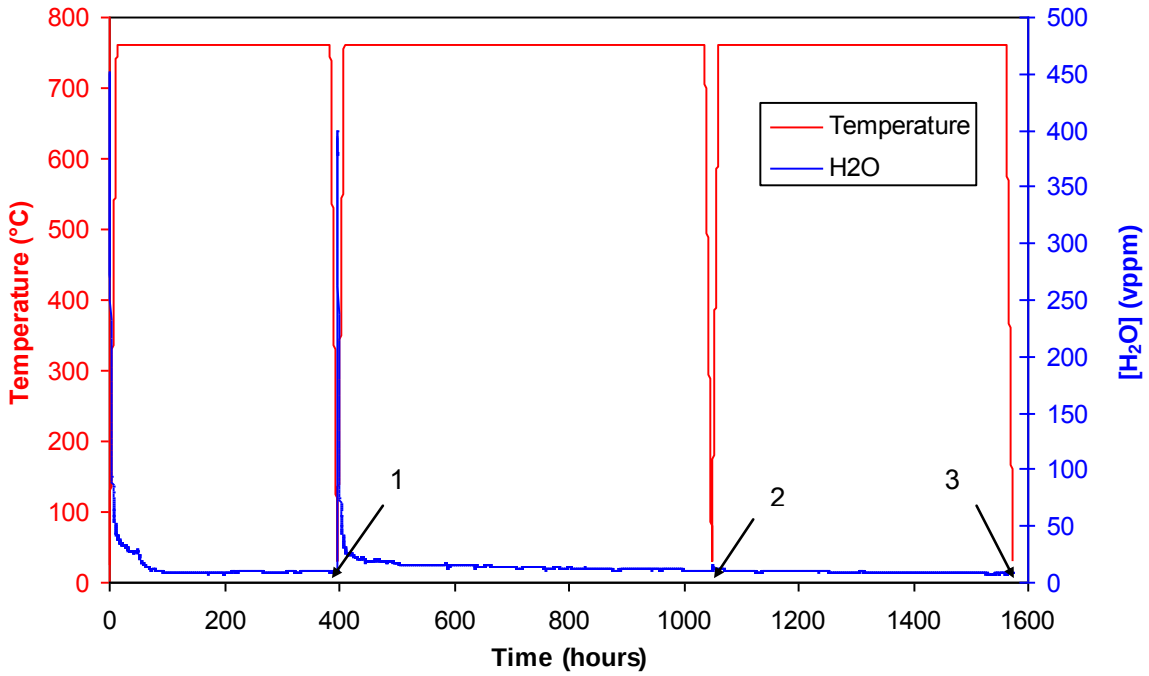

Figure 29: Temperature profile in the oven and humidity concentration in the gas before entering the oven: 1) removal of the 1st series of samples after 372h, 2)) removal of the 2nd series of samples after 1000h, 3)) removal of the 3rd series of samples after 1500h

Figure 30 shows the samples in original state, picture of samples after exposure shows Figure 31. On the surface of the samples a black-greenish corrosion layer is visible. For samples with weld metal (WM), with heat affected zone (HAZ), and basic metal (BM) the corrosive layer showed a different nature within these specified regions, see Figure 32. The mass changes depending on time of exposure are presented in Figure 33. The mass change for alloy 800H is greater than for steel P91 after exposure at 760°C for 1500h at an atmosphere as described in Table 9. Further information will be provided in the next section.

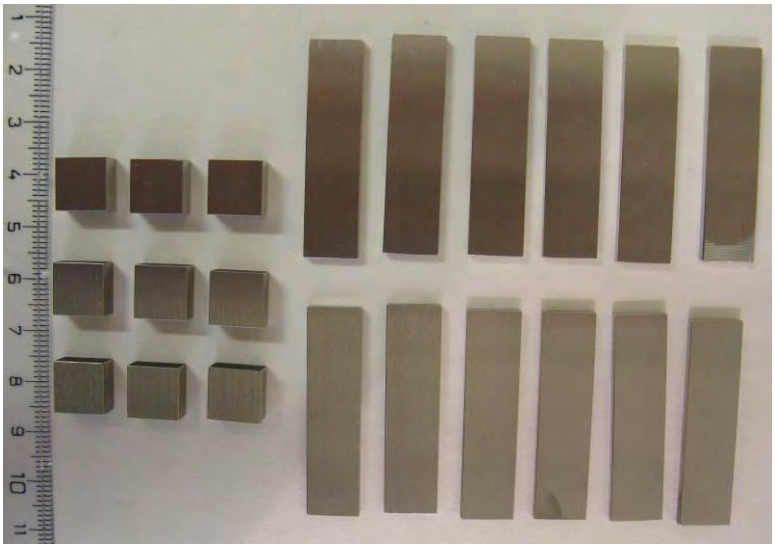

Figure 30: Samples from alloy 800 H for tests in HTF

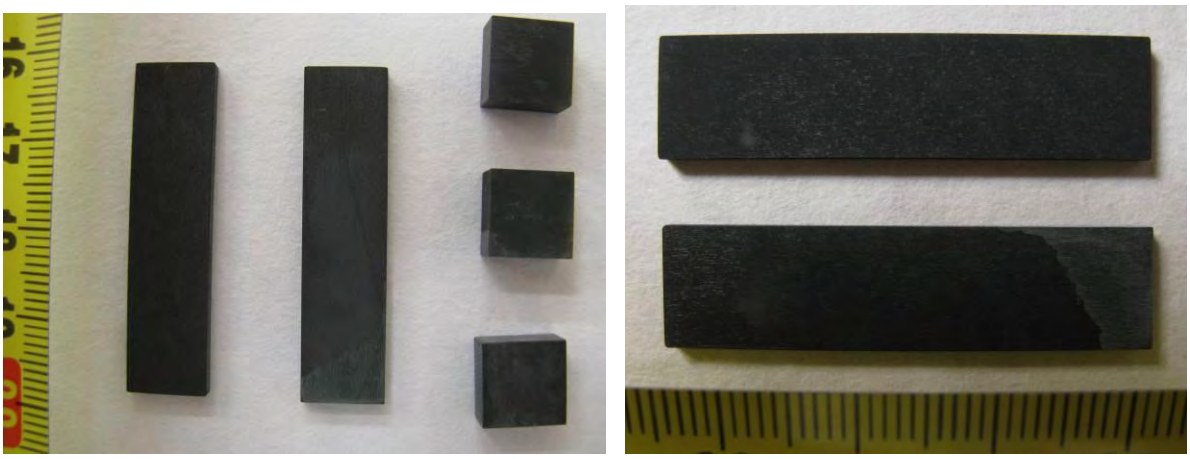

a) b)

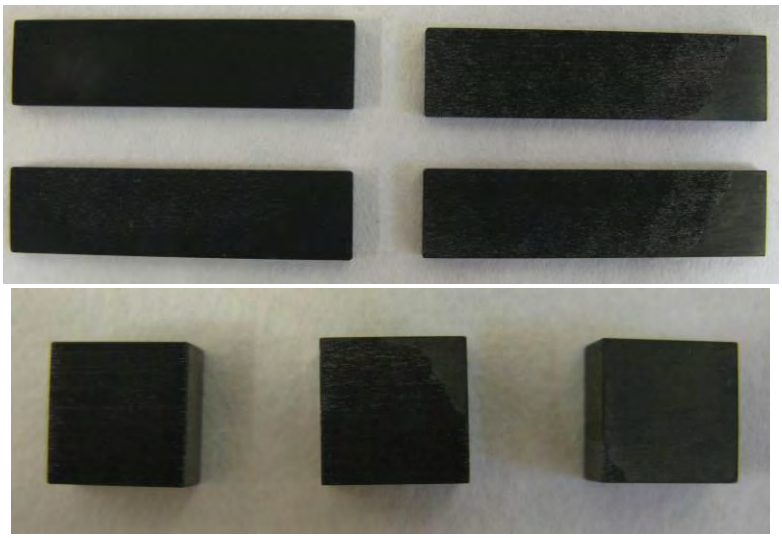

c)

Figure 31: Samples from alloy 800 H after exposure in HTF a) after 372h, b) after 1000h c) after 1500h

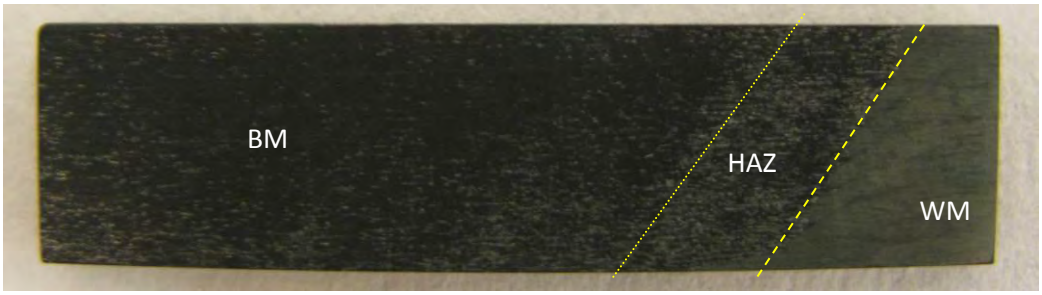

Figure 32: Sample after exposure for 1500h – characters of corrosion at BM, HAZ, and WM

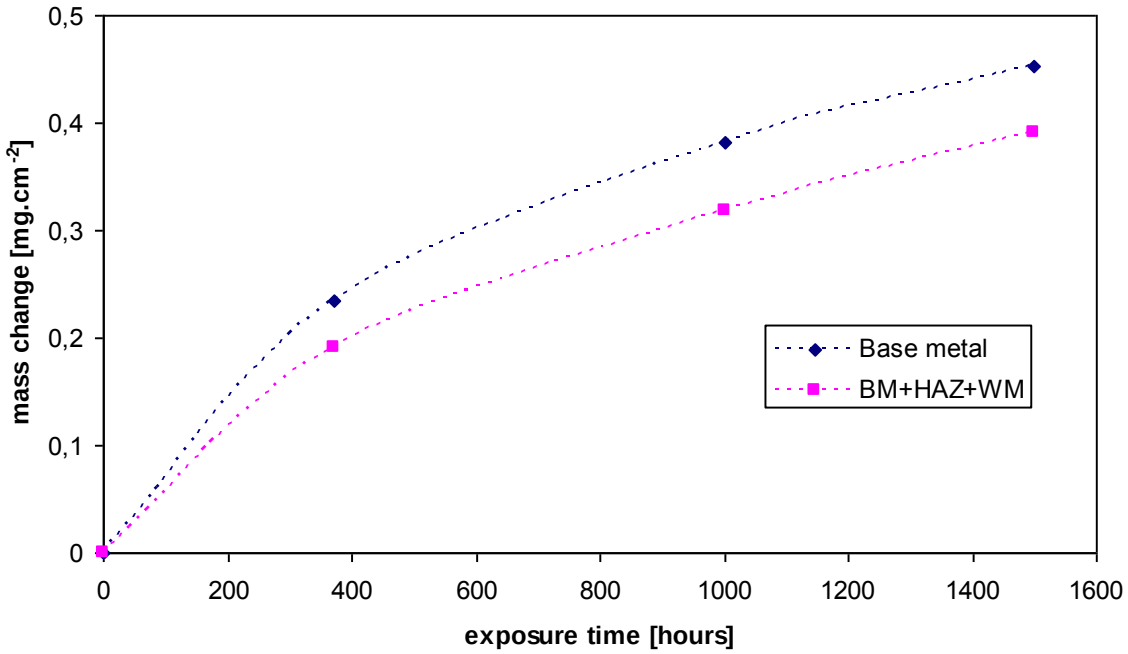

Figure 33: Mass changes for samples from alloy 800 H, exposed to gaseous mixture according to Table 9 at 760°C

Microscopical pictures of sample surfaces in initial state and after exposure show Figure 34 to Figure 37. The results of surface analysis in original state and after exposure are summarized in Table 19. The sample surfaces were investigated at five positions. In the table the average values are noted. With increasing time of exposure the iron concentration in the corrosion layer decreases, as can be learned from Table 19. The corrosion layer is formed for the most part from chrome compounds. The results from surface analysis of welded metal (MW) and heat affected zone (HAZ) are represented in Table 20 and Table 21. It can be observe that, e.g. on the surface from welded metal a low concentration of chrome and a enriched content of manganese was measured in contrast to the initial state of the material and in comparison with heat affected zone. This can be caused be the different appearance of the samples after exposure.

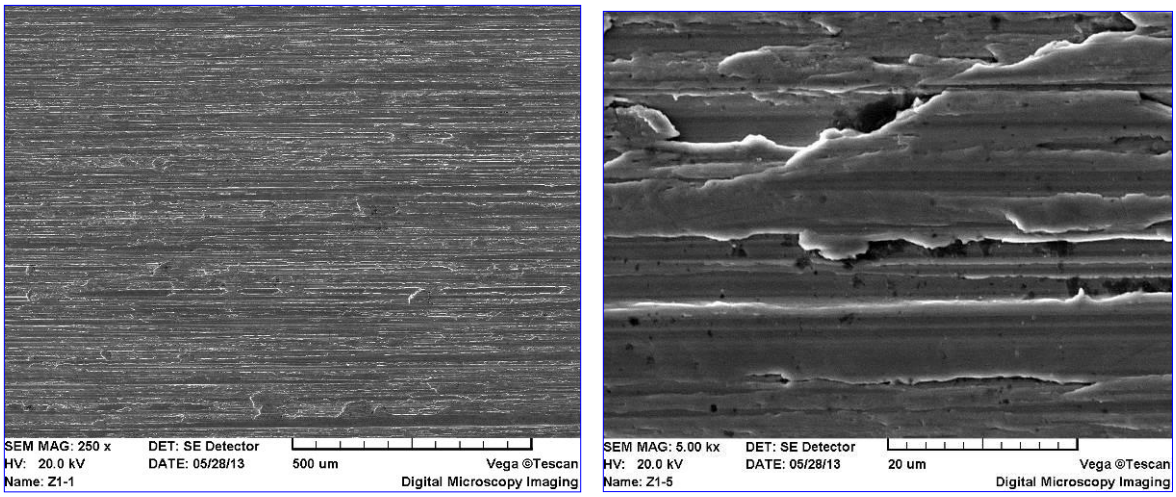

Figure 34: SEM picture of sample surface of alloy 800 H (Z1) in initial state

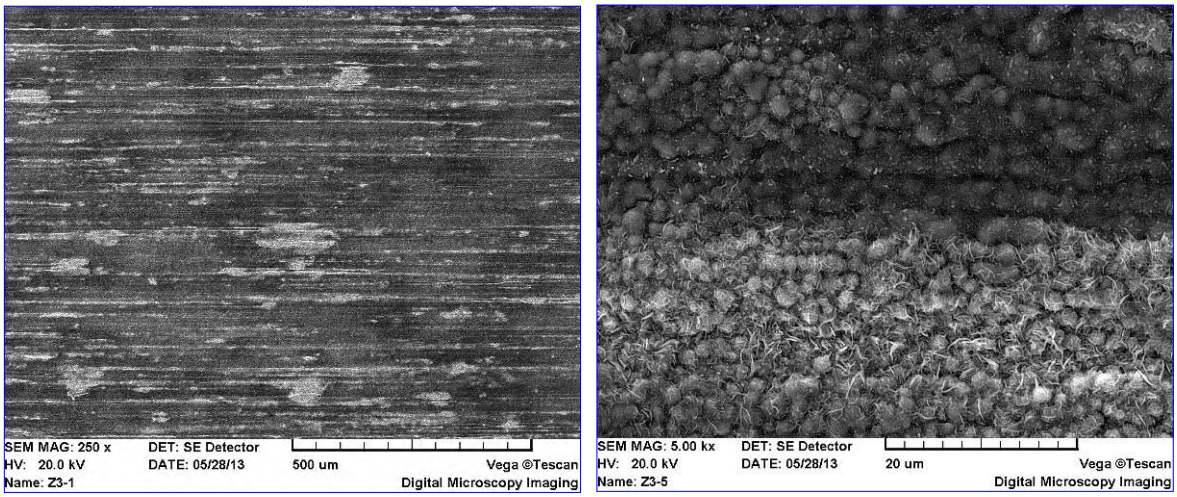

Figure 35: SEM picture of surface sample from alloy 800 H (Z3) after exposure at 760°C for 372h in gaseous atmosphere according to Table 9

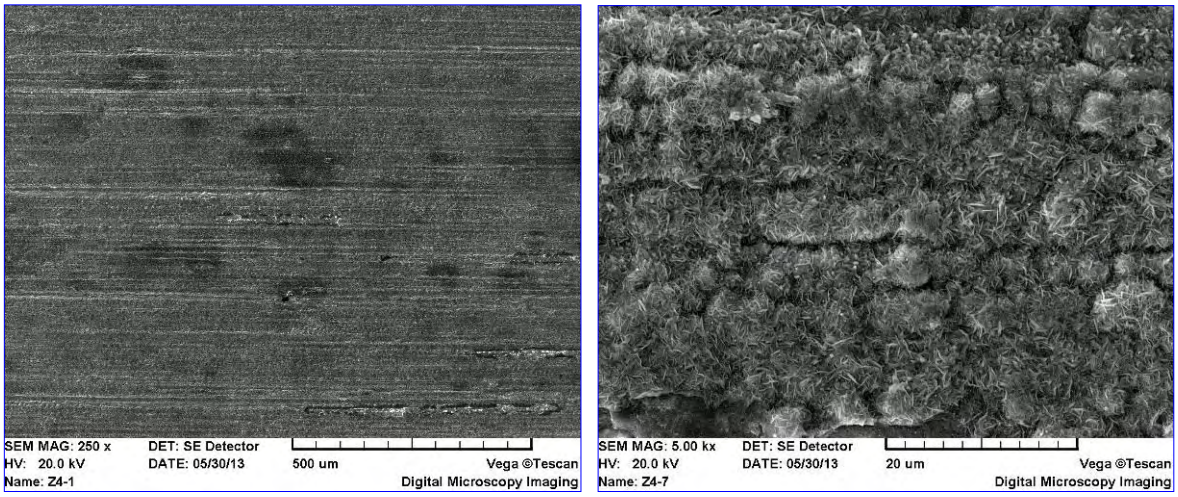

Figure 36: SEM picture of surface sample from alloy 800 H (Z4) after exposure at 760°C for 1000h in gas mixture according to Table 9

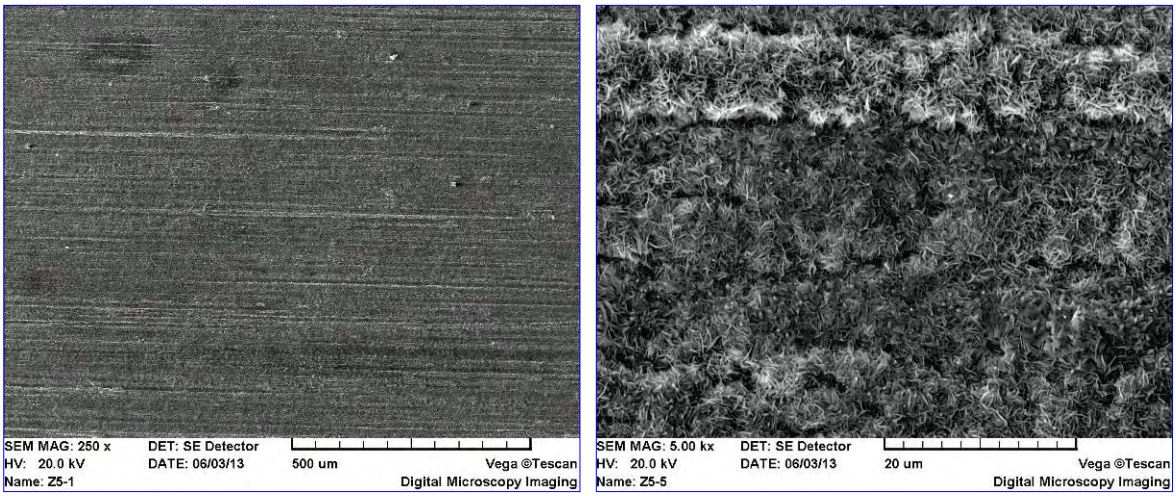

Figure 37: SEM picture of samples surface from alloy800 H (Z5) after exposure at 760°C for 1500h in atmosphere according to Table 9

Table 19: Analysis of sample surface from alloy 800H in initial state and after exposure (Z1, Z3 – Z5)

Sample	Element	O	Al	Si	Ti	Cr	Mn	Fe	Ni
Z1 Initial state	% by weight	1.60	0.51	0.59	0.39	21.30	0.94	45.29	29.38
	atomic %	5.30	1.00	1.11	0.43	21.72	0.91	42.99	26.54
Z3 Exposure 372h	% by weight	31.08	-	0.54	1.79	49.77	9.08	5.14	2.6
	at. %	59.62	-	0.59	1.15	29.38	5.07	2.83	1.36
Z4 Exposure 1000h	% by weight	29.49	0.05	0.21	2.09	48.71	13.32	4.06	2.06
	at. %	57.90	0.06	0.23	1.37	29.43	7.62	2.28	1.10
Z5 Exposure 1500h	% by weight	30.74	-	0.05	2.36	48.95	15.16	1.85	0.89
	at. %	59.33	-	0.05	1.52	29.07	8.52	1.02	0.47

Table 20: Analysis of sample surface with heat affected zone (HAZ) from alloy 800 H in initial state and after exposure (S1, S3 – S5)

Sample	Element	O	Al	Si	Ti	Cr	Mn	Fe	Ni	Nb
S1 Initial state	% by weight	1.87	0.40	0.45	0.38	20.83	1.17	38.39	36.09	0.42
	at. %	6.20	0.79	0.85	0.42	21.26	1.13	36.48	32.63	0.24
S3 Exposure 372h	% by weight	30.02	0.20	0.72	2.04	43.28	6.92	10.62	6.20	-
	at. %	58.52	0.23	0.80	1.33	25.96	3.93	5.93	3.29	-
S4 Exposure 1000h	% by weight	29.23	-	-	2.59	51.17	13.18	2.72	1.12	-
	at. %	57.58	-	-	1.71	31.02	7.56	1.54	0.60	-
S5 Exposure 1500h	% by weight	26.93	0.23	0.18	2.35	43.73	11.94	9.47	5.17	-
	at. %	54.95	0.28	0.21	1.60	27.46	7.10	5.54	2.88	-

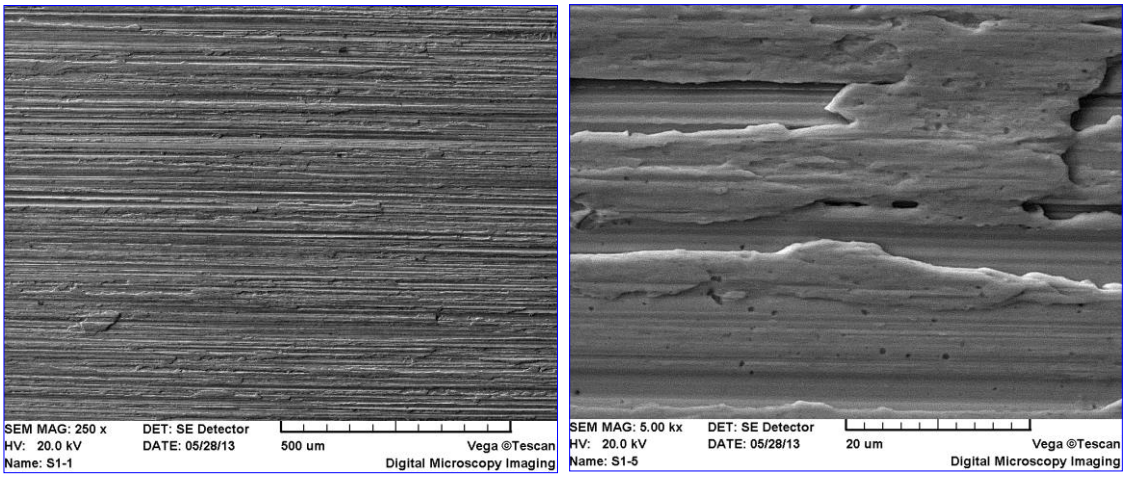

Figure 38: SEM picture of sample surface with heat affected zone (HAZ) and welded metal from alloy 800 H (S1) in initial state

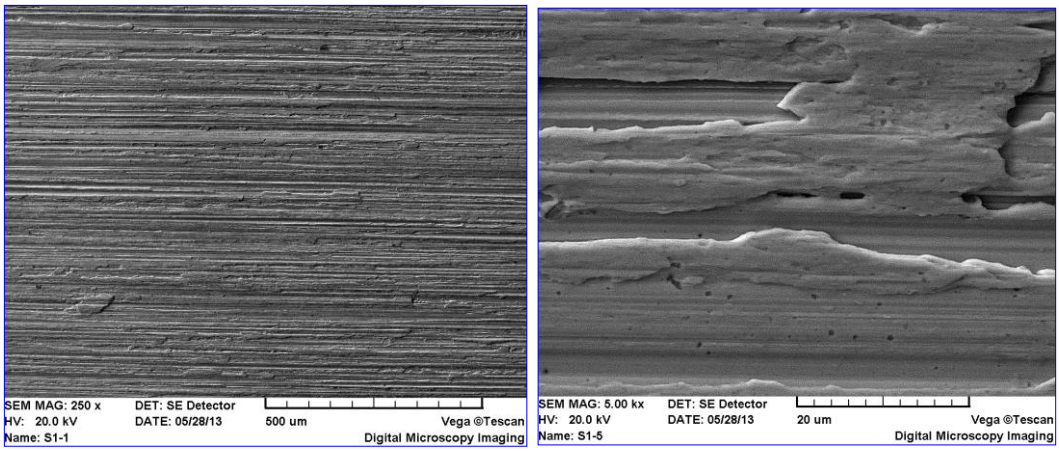

Figure 39: SEM picture of sample surface with heat affected zone (HAZ) and welded metal (WM) from alloy 800H (S1) in initial state

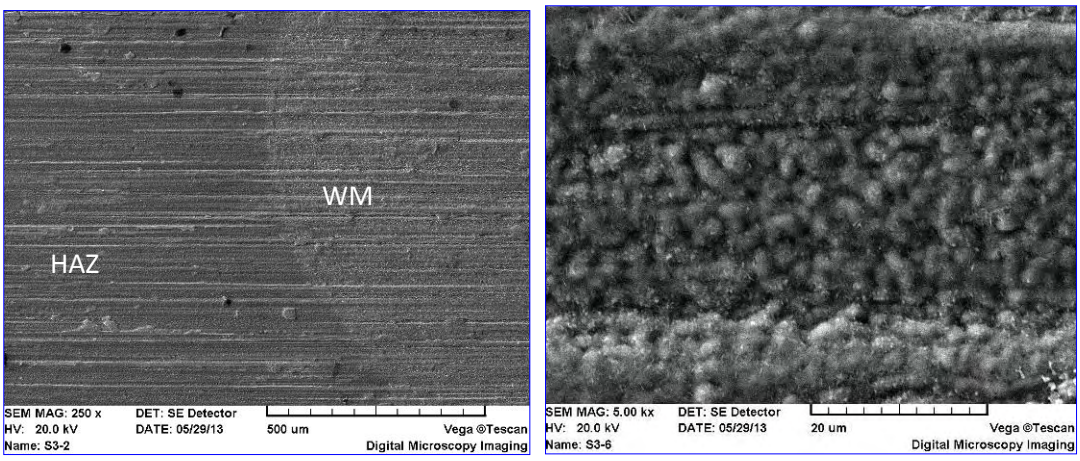

a) b)

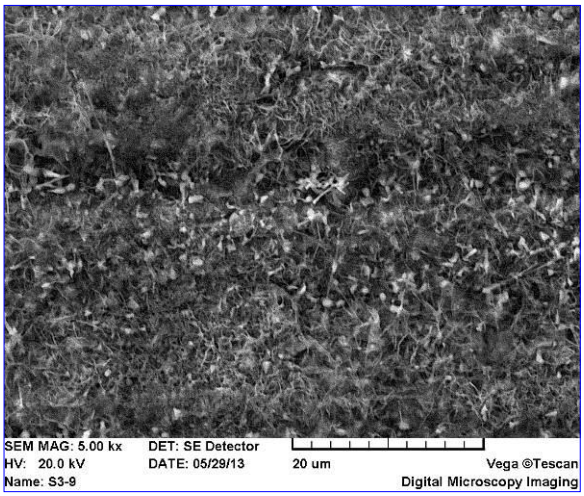

c)

Figure 40: SEM picture from sample surface with heat affected zone (HAZ) and welded metal (WM) from alloy 800H (S3) after exposure at 760°C for 372h in gas atmosphere according to Table 9: a) HAZ + WM, b) HAZ, c) WM

Table 21: Analysis of sample surface with welded metal from alloy 800H in initial state and after exposure (S1, S3 – S5)

Sample	Element	O	Al	Si	Ti	Cr	Mn	Fe	Ni	Nb
S1 Initial state	% by weight	2,09	0.52	0.33	0.29	20.78	2.81	10.06	61.03	2.10
	at. %	7.02	1.04	0.63	0.33	21.47	2.75	9.68	55.87	1.21
S3 Exposure 372h	% by weight	29.26	0.16	0.16	0.99	37.27	19.47	1.03	10.90	0.76
	at. %	58.16	0.19	0.18	0.66	22.79	11.27	0.59	5.91	0.26
S4 Exposure 1000h	% by weight	27.12	-	-	0.73	40.36	27.25	0.78	2.79	0.12
	at. %	55.66	-	-	0.50	25.49	16.29	0.46	1.56	0.04
S5 Exposure 1500h	% by weight	19.30	-	-	0.89	34.52	33.33	0.56	1.31	0.09
	at. %	47.70	0.00	0.00	0.74	26.25	23.99	0.40	0.88	0.04

The thickness of corrosive layer was measured on the cross-section of the specimen by optical microscopy and also calculated from line scan. The results are summarized in Table 22.

Microstructure on cross-section of base metal of Alloy 800 H in as-received state consists of grains with maximum size approx. 600 µm. Also smaller grains originated likely by recrystallization in thermal processing, unevenly extruded precipitates (MC, M_6C) and orange colored inclusions (probably Ti, C, and N) were observed. After exposure of 1000 hours significant precipitation of particles (probably $M_{23}C_6$ and γ´) was observed. On the surface thin, compact and sporadically non-uniform about 2.5 µm thick corrosive layer was observed. Under the corrosive layer ~20 µm undersurface layer without precipitates was observed, corrosive attack interfere with material 5 – 7 µm deep under the corrosive layer. After exposure of 1500 hours in impure helium at 760°C significant precipitation of carbides (probably $M_{23}C_6$ and γ) was observed. The undersurface layer without precipitates was about 20 µm and corrosive attack interfere with material 5 – 7 µm deep under the corrosive layer was also observed. The thickness of non-uniform surface corrosive layer was about 3µm. For comparison of microstructure of base metal of Alloy 800 H in as-received state and after exposure see Figure 43.

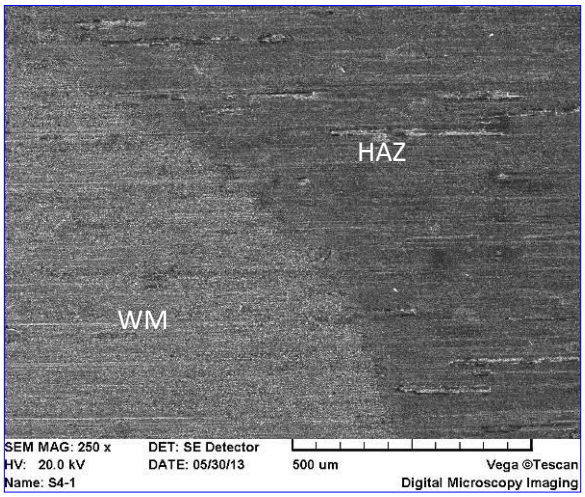

a)

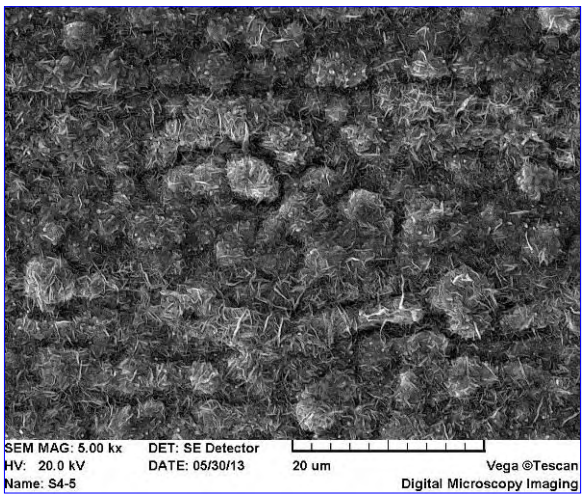

b)

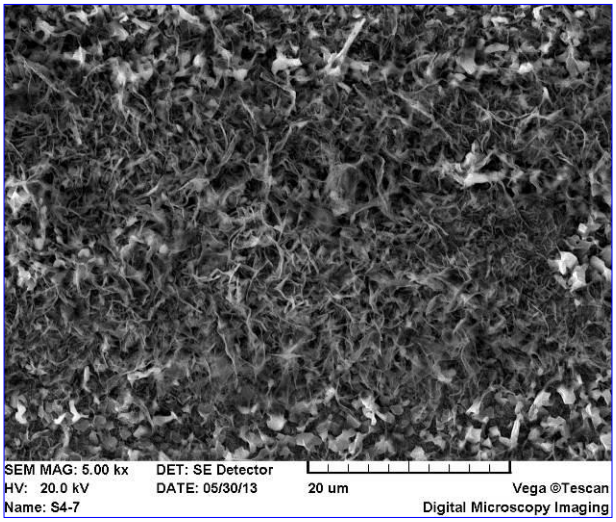

c)

Figure 41: SEM picture of sample surface with heat affected zone (HAZ) a welded metal (WM) from alloy 800H (S4) after exposure at 760°C for 1000h in gaseous blend (Table 9): a) HAZ + WM, b) HAZ, c) WM

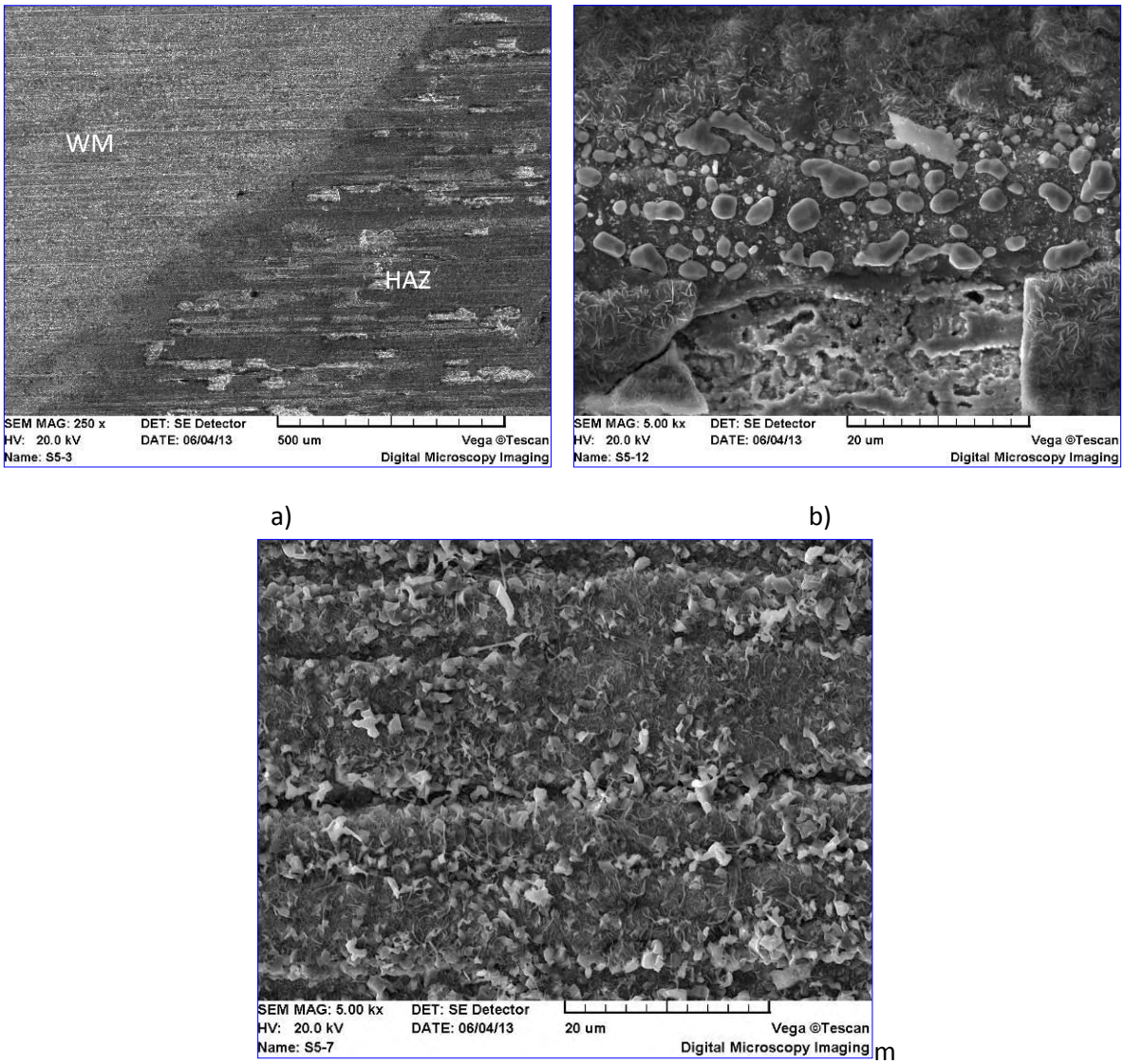

a) b)

m

c)

Figure 42: SEM picture of sample surface with heat affected zone (HAZ) a welded metal (WM) from alloy 800H (S5) after exposure at 760°C for 1000h in gaseous blend (Table 9): a) HAZ + WM, b) HAZ, c) WM

Table 22: Thickness of corrosive layer on the surface of Alloy 800 H specimens after exposure in impure helium at 760°C.

Time of exposure (hours)	Base metal		HAZ		Weld metal	
	By microscopy (µm)	From line scan (µm)	By microscopy (µm)	From line scan (µm)	By microscopy (µm)	From line scan (µm)
372	1-2	-	1-2	~2	1-2	~5
1000	2.5	9	~2.5	~5	~2.5	~6
1500	3	9	~3	-	~3	~11

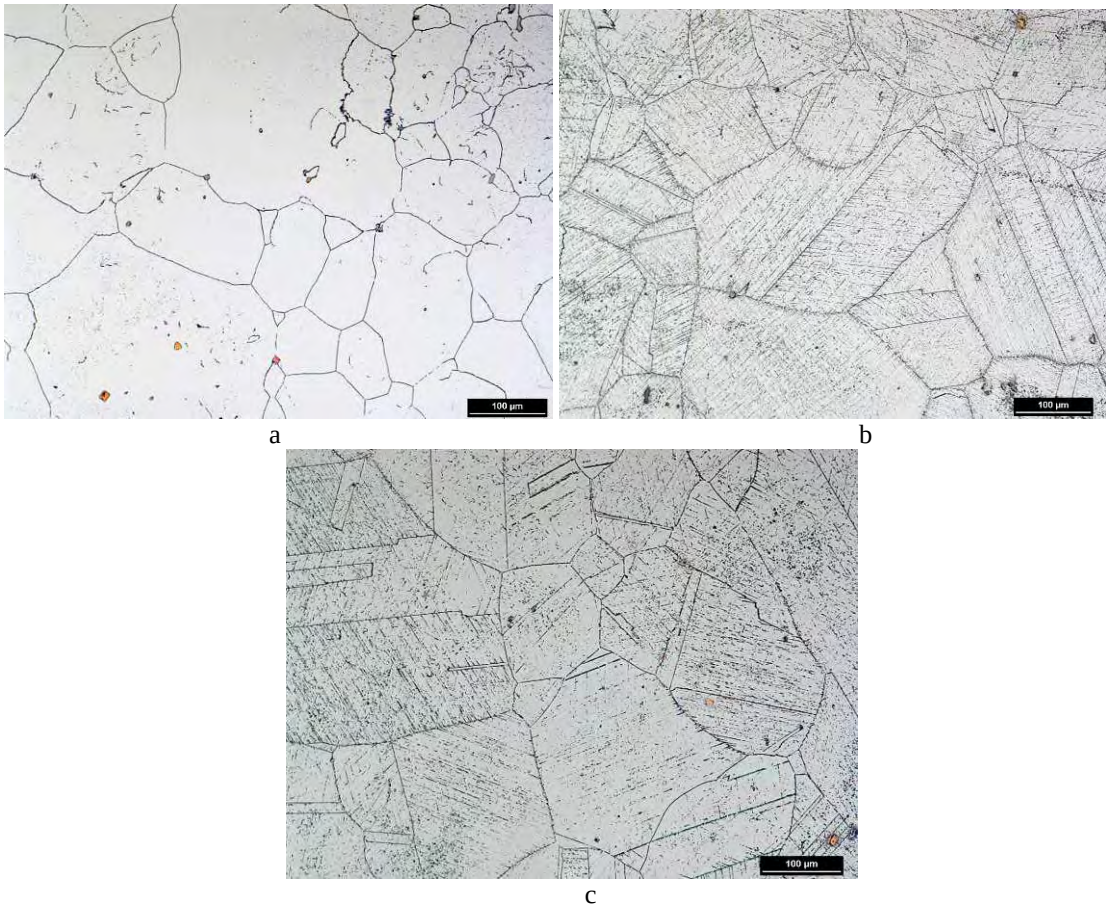

a b c

Figure 43: Microstructure of base metal of Alloy 800 H on the cross-section of specimens: a –in as-received state, b-after exposure of 1000 hours, c-after exposure of 1500 hours in impure helium at 760°C.

On the cross-section of specimens containing weld metal the partially-melted zone was observed. After exposure the precipitation of particles were observed and also the under surface layer without precipitates about 20 µm and corrosive attack interfere with material 5 – 7 µm deep under the corrosive layer was also observed as in case of base metal specimens. The microstructure of cross

section of the interface of weld metal and heat affected zone in as-received state and after exposure in impure helium at 760°C re compared on Figure 44.

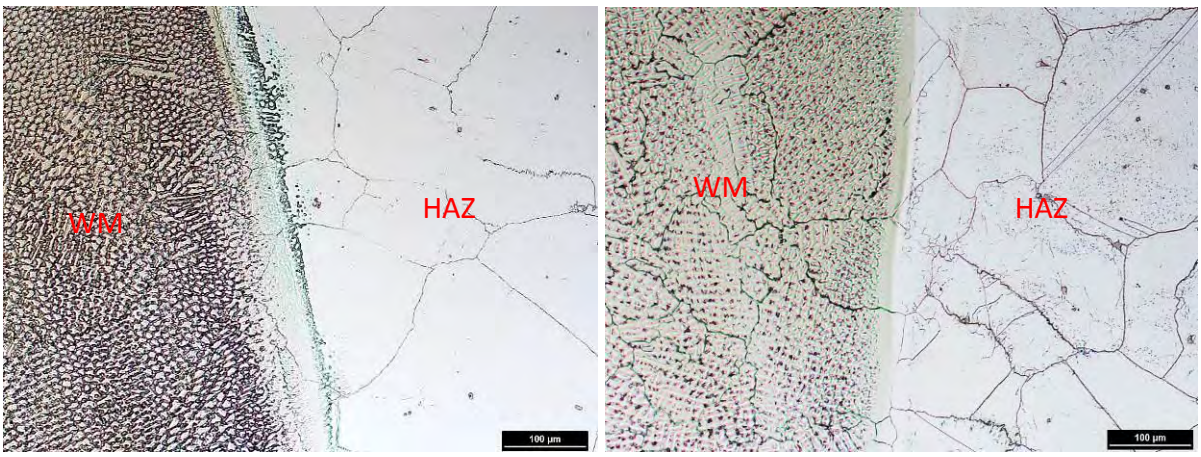

a b

Figure 44: Microstructure of interface of weld metal and heat affected zone of alloy 800 H: a-in as-received state, b-after exposure of 1500 hours in impure helium at 760°C

Results of tests of hardness and micro hardness

The results of tests of hardness and micro hardness on exposed specimens of BM, HAZ and WM of Alloy 800 H are summarized on Figure 45 and Figure 46. Hardness could be said to slightly increase with exposure in case of BM and HAZ and slightly decrease in case of WM. In original state hardness of weld metal is the highest and hardness of base metal is the lowest, after exposure the difference of hardness of tested materials decreased. Micro hardness of all tested materials after exposure decreased.

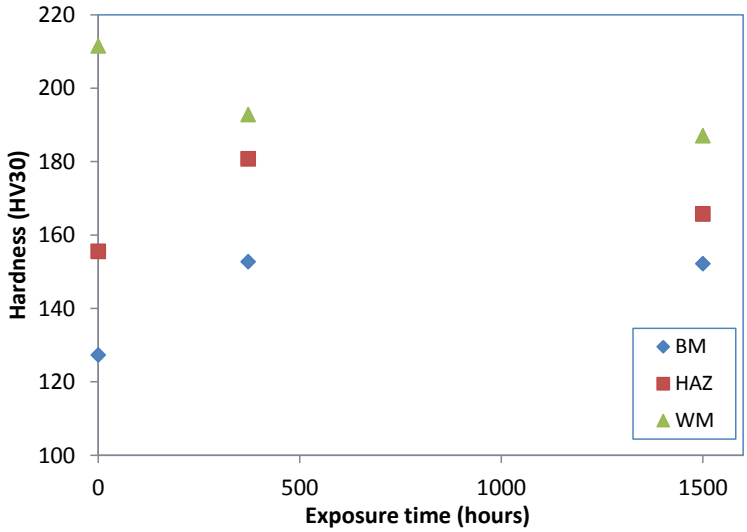

Figure 45: Hardness of welded 800 H specimens depending on exposure time

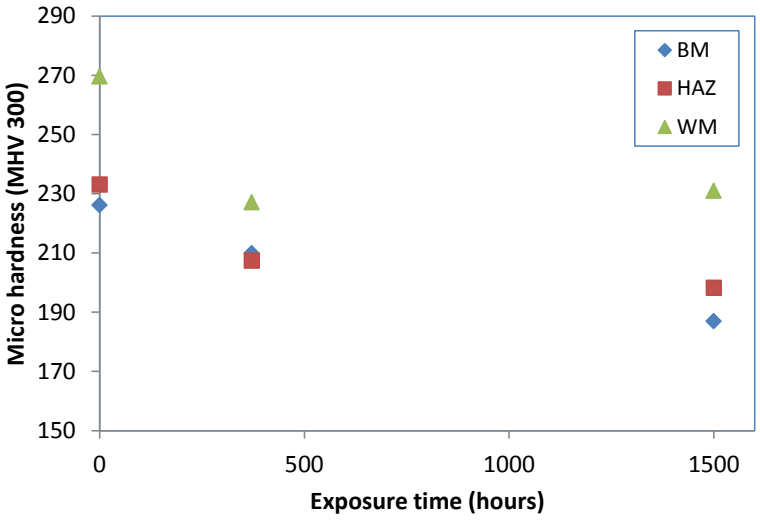

Figure 46: Micro hardness of welded 800 H specimens depending on exposure time

Tests after exposure in HTHL

Tests after exposure during the test operation of HTHL

Test I.

The specimens of Alloy 800H were exposed during 264 and 665 hours. The parameters of environment were not constant. The dependence of mass change of specimens after exposure is summarized in the chart on Figure 47. The mass gain after 264 hours during test operation of HTHL is much less than after exposure in HTF (760°C/372 hours), after 665 hours the mass gain is comparable to that after exposure in HTF (760°C/1000 hours). It could be caused by different parameters – different content of minor compounds in helium atmosphere, lower temperature during the first period and higher maximum temperature during the second period, higher gas flow and pressure etc.

The SEM surfaces if exposed specimens can be seen on Figure 49and Figure 52. The results of SEM analysis are summarized in Table 23. Certain differences compared to composition of surface layer after exposure in HTF were observed (compare with Table 19). During exposure content of Fe and Ni on the surface layer significantly decreased, content of Cr and Mn increased.

Microstructure of Alloy 800 H base metal after exposure of 665 hours during test operation of HTHL consists of mainly by large grains with occurrence of twinning. Smaller grains originated by recrystallization were also observed. Precipitates are suspended unevenly inside the grains and also on the grain boundaries. Also orange colour inclusions with grey edges– probably Ti (C, N) – and grey particles –probably TiC - were observed. See Figure 52. The surface non-uniform corrosive layer is 2-3 µm thick. 5 -10 µm under this layer corrosive attack on the grain boundaries was observed (red arrow – see Figure 51).

After 264 hours of exposure during test operation of HTHL (probably) spalling of surface corrosive layer on the surface of heat affected zone and weld metal was observed (see Figure 52). The darker and lighter areas on the surface were analysed by SEM – see Figure 53, Figure 54, Table 24 and Table 25 for results. The results of SEM analysis of sample surface of the heat affected zone and weld metal

after exposure in HTHL during the test operation is listed in Table 26 and Table 27. As could be seen, the content of chromium (oxide) increase with exposure time, content of Fe and Ni decrease.

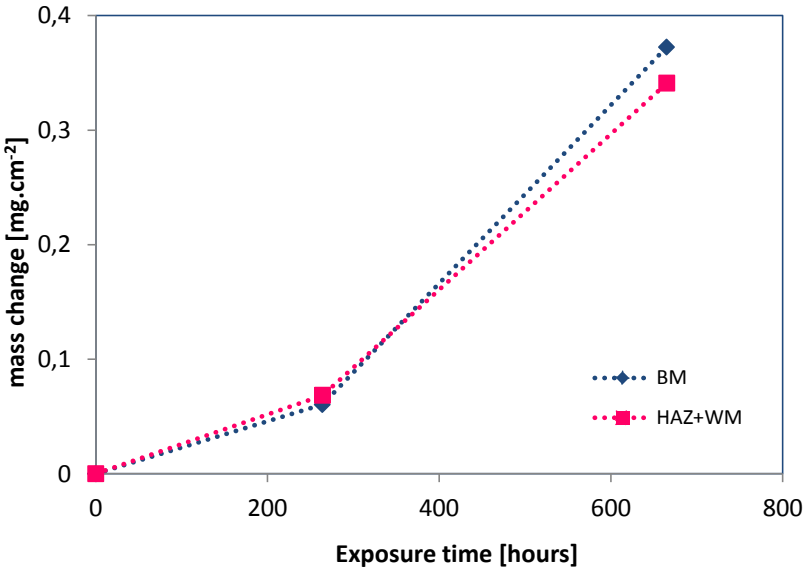

Figure 47: Mass changes of specimens after exposure during test operation in HTHL

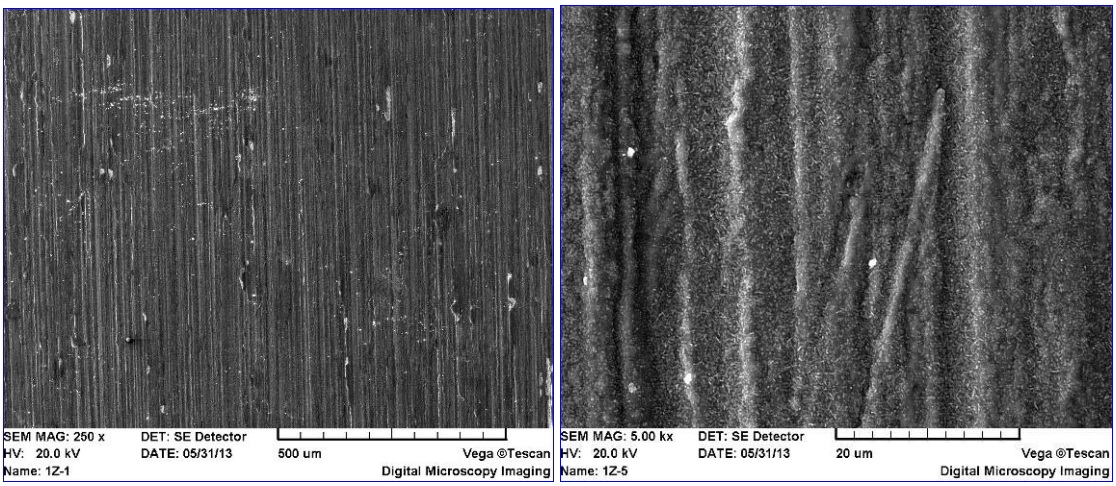

Figure 48: SEM picture of the Alloy 800H BM specimen surface after exposure of 264 hours in HTHL during the test operation

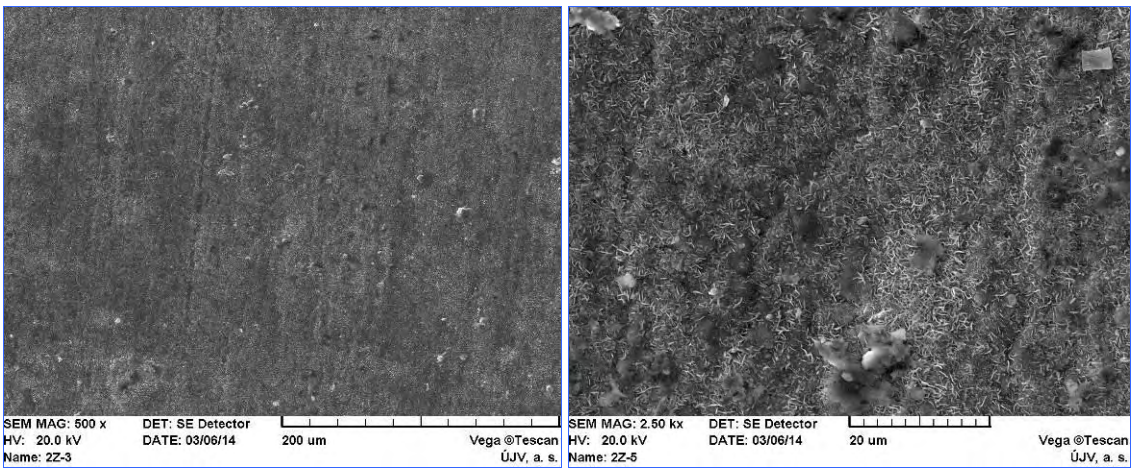

Figure 49: SEM picture of the Alloy 800H BM specimen surface after exposure of 665 hours in HTHL during the test operation

Table 23: Analysis of sample surface of Alloy 800 H base metal exposed in HTHL during the test operation

Sample	Element	O	Al	Si	Ti	Cr	Mn	Fe	Ni
1Z Exposure 264 hours	% by weight	25.71	0.60	0.76	0.75	30.30	2.36	24.47	15.06
2Z Exposure 665 hours		29.7	0.5	0.4	1.5	45.7	12.9	8.7	0.7

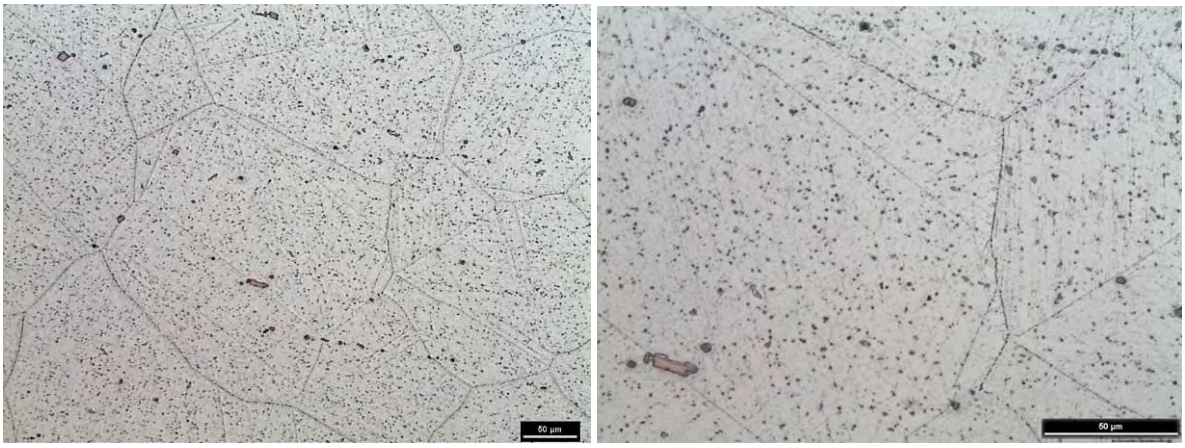

Figure 50: Microstructure of Alloy 800 H base metal on the cross-section of the specimen after exposure of 665 hours during test operation of HTHL

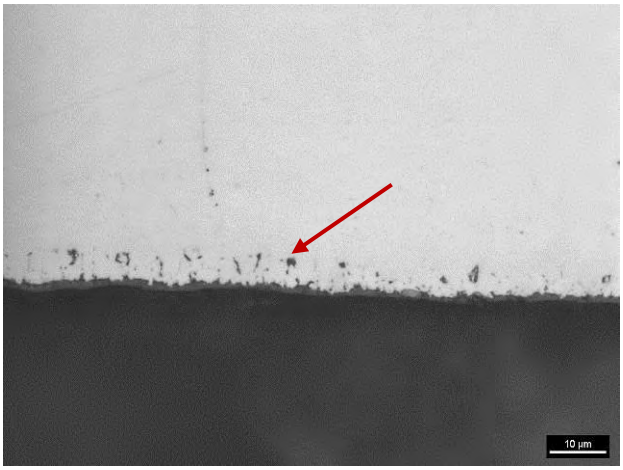

Figure 51: Undersurface corrosive attack of Alloy 800H base metal after exposure of 665 hours during test operation of HTHL

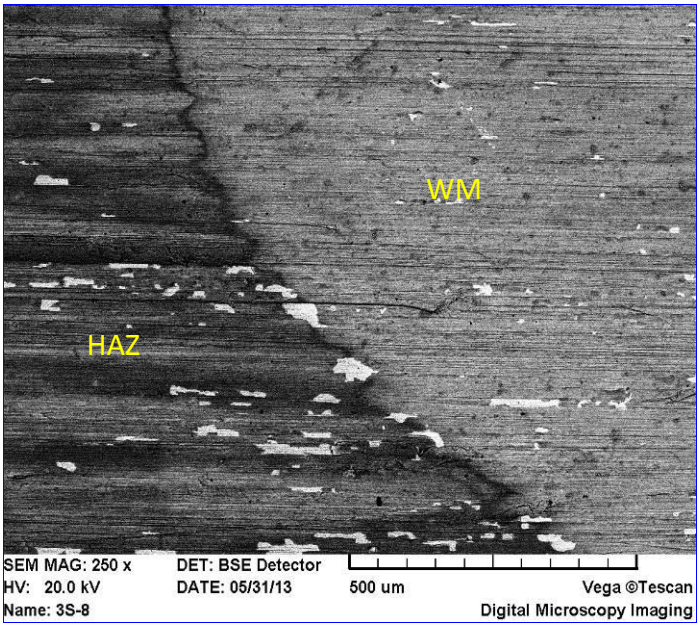

Figure 52: SEM picture of the Alloy 800 H HAZ-WM boundary after exposure of 264 hours in HTHL during the test operation

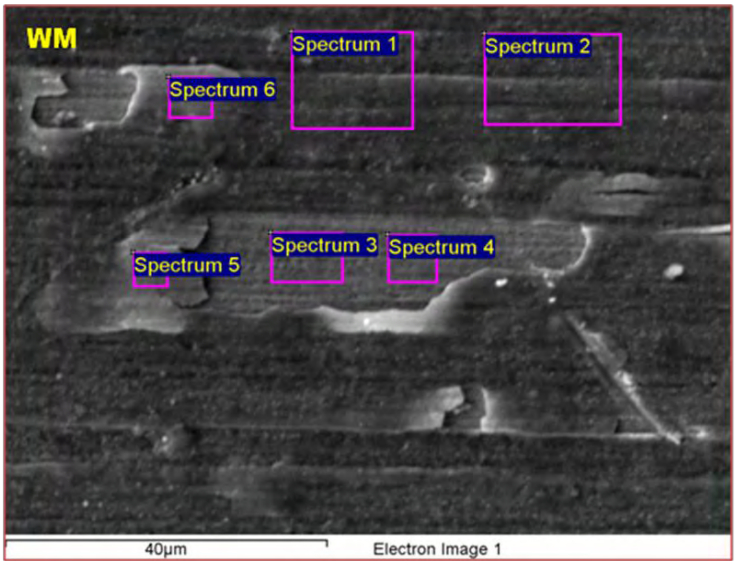

Figure 53: Analysis of darker and fighter areas on the surface of weld metal after exposure of 264 hours during test operation of HTHL

Table 24: Results of analysis from Figure 53

Spectrum	O	Al	Si	Ti	Cr	Mn	Fe	Ni	Nb
1	23.04	0.32	0.48	0.42	25.71	6.52	3.65	37.60	2.25
2	21.98	0.10	0.46	0.56	24.05	6.05	3.33	41.34	2.14
5	23.40	0.04	0.23	0.39	24.66	4.85	3.60	41.10	1.73
6	23.38	0.14	0.56	0.42	24.03	5.39	4.02	40.20	1.86
3	7.73	0.25	0.10	0.37	19.10	1.88	5.81	62.62	2.14
4	7.66	0.19	0.24	0.42	18.03	1.85	5.66	63.79	2.17

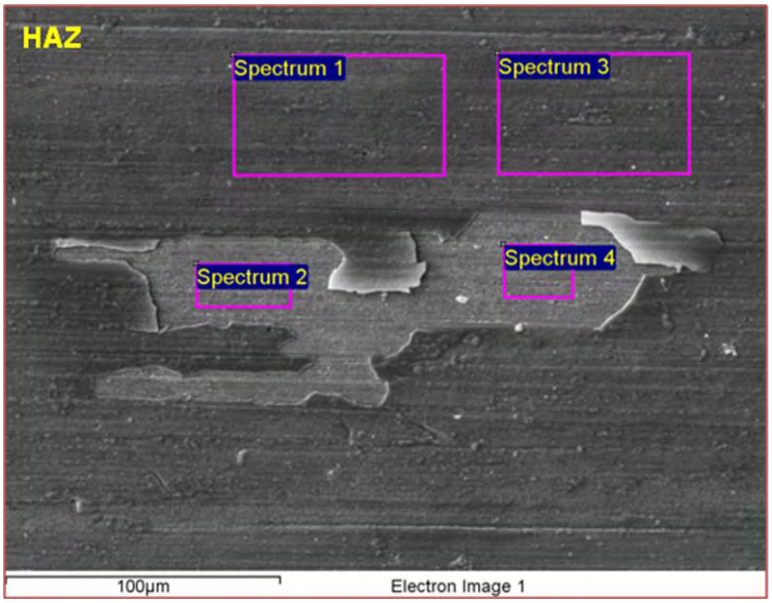

Figure 54: Analysis of darker and fighter areas on the surface of heat affected zone after exposure of 264 hours during test operation of HTHL

Table 25: Results of analysis from Figure 54

Spectrum	O	Al	Si	Ti	Cr	Mn	Fe	Ni
1	30.74	0.80	0.53	1.83	34.09	4.38	17.71	9.92
3	30.64	0.60	0.54	1.35	35.83	4.61	16.83	9.60
2	10.16	3.08	1.06	0.91	17.37	0.38	41.23	25.80
4	9.66	2.89	1.21	0.94	16.70	1.05	41.92	25.62

Table 26: Analysis of sample surface of Alloy 800 H heat affected zone exposed in HTHL during the test operation

Sample	Element	O	Al	Si	Ti	Cr	Mn	Fe	Ni
3S Exposure 264 hours	% by weight	26.66	0.95	0.62	1.23	31.49	3.46	22.23	13.37
5S Exposure 665 hours		31.3	0.8	0.3	1.5	49.8	9.5	5.9	1.0

The microstructure on the cross section of welded specimen exposed 665 hours (5s) is illustrated in Figure 55. Inclusions and precipitations were also observed. The corrosive layer on the heat affected zone and weld metal was 2 -3 µm thick, corrosion on the grain boundaries interfere in the depth of 10 – 15 µm under the surface layer (see Figure 56). The cross section of the root and the peak of the weld (weld metal and HAZ) of the specimen exposed during 665 hours were observed also by SEM (see Figure 57 - Figure 60). The damage of the sub-surfaces layers is more marked on the peak of the root. Chemical analysis of the cross section revealed e.g. chromium depleted zone under the corrosive surface layer of the root of the weld – about 4 µm in case of WM and about 9 µm in case of HAZ. On the peak of the weld the subsurface oxides in weld metal (Cr, Mn) were found.

Table 27: Analysis of sample surface of Alloy 800 H weld metal exposed in HTHL during the test operation

Sample	Element	O	Al	Si	Ti	Cr	Mn	Fe	Ni	Nb
3S Exposure 264 hours	% by weight	22.26	0.28	0.37	0.52	23.83	5.88	3.61	40.81	2.44
5S Exposure 665 hours		29.1	1.1		1.2	40.5	23.3	2.1	2.7	

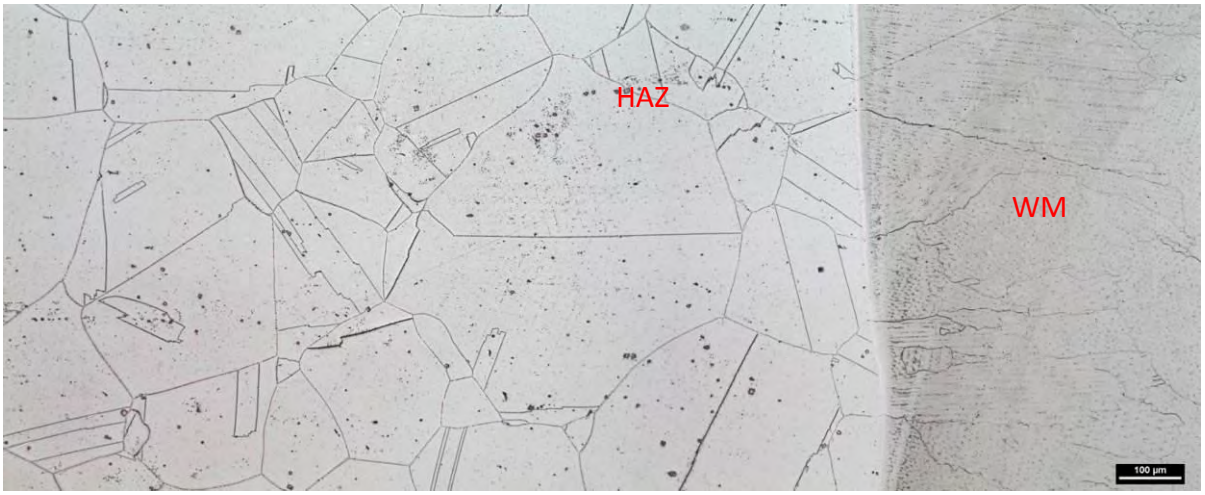

Figure 55: Microstructure of the cross section of the HAZ-WM boundary of the specimen 5S exposed in HTHL during test operation during 665 hours

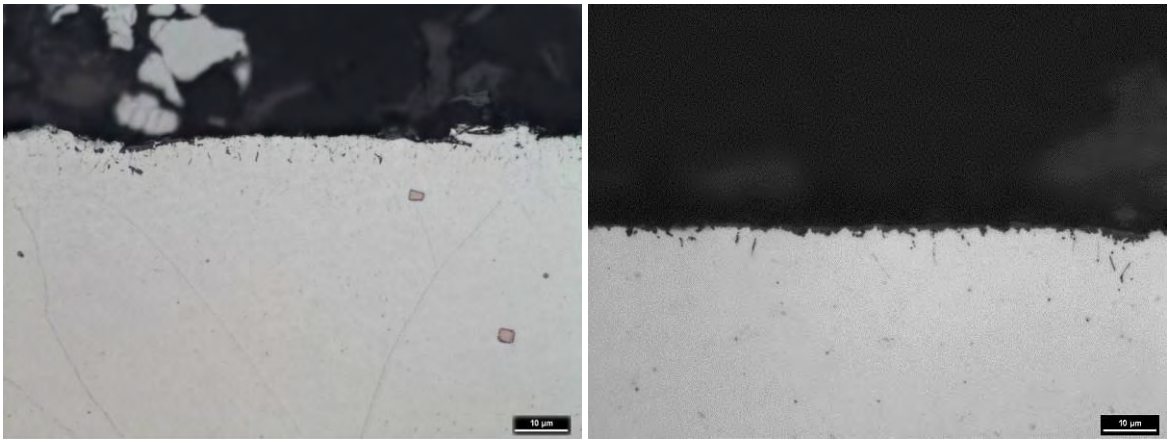

a b

Figure 56: Corrosive layer on the surface of the welded specimen of alloy 800 H exposed in HTHL during 665 hours

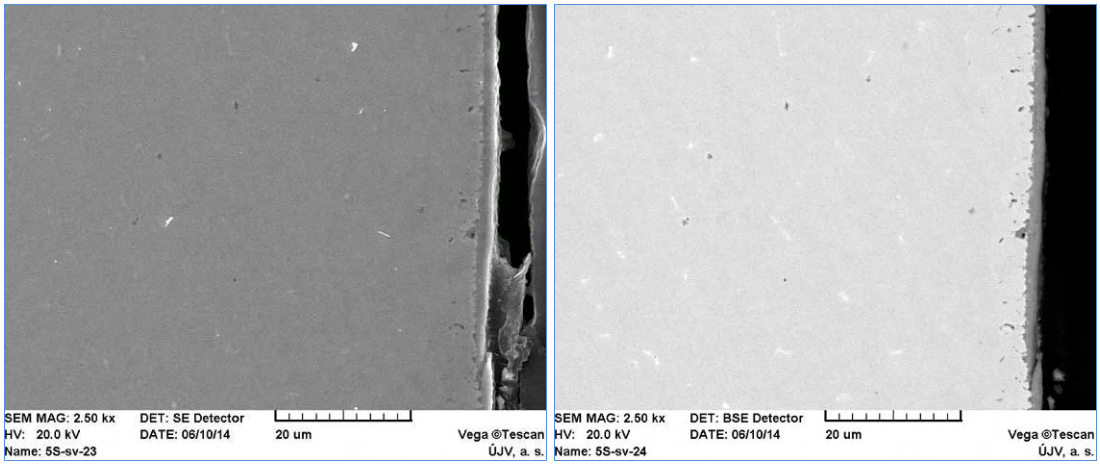

Figure 57: SEM picture of the cross section of the root of the weld – weld metal after exposure of 665 hours during the test operation of HTHL

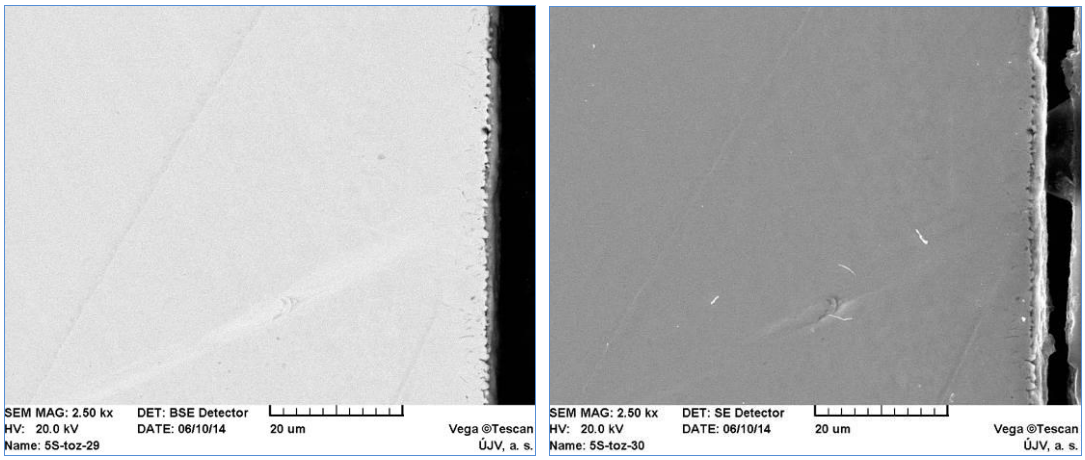

Figure 58: SEM picture of the cross section of the root of the weld – heat affect zone after exposure of 665 hours during the test operation of HTHL

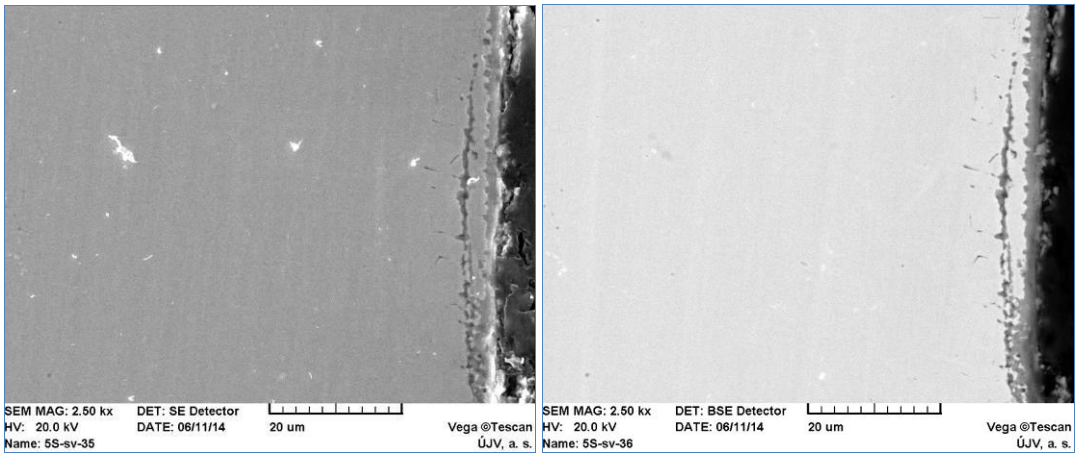

Figure 59: SEM picture of the cross section of the peak of the weld – weld metal after exposure of 665 hours during the test operation of HTHL

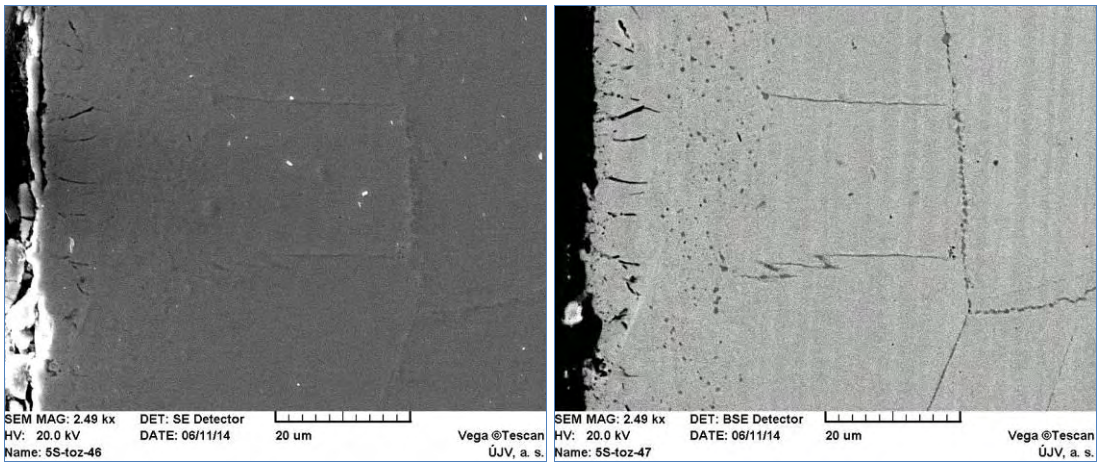

Figure 60: SEM picture of the cross section of the peak of the weld – heat affected zone after exposure of 665 hours during the test operation of HTHL

Tests after exposure during corrosion test in HTHL

Test II.

Until the finalization of this report only the specimens exposed during 160 hours of operation of HTHL (109 hour at 760°C) were tested. The exposure has continued with remaining specimens after repair of HTHL (marked by grey colour in Table 13). For SEM pictures of the surface of specimen exposed during the first period of corrosion test see Figure 61. On the surface of the root of the weld the spalling of the top layer is evident (Figure 61 a). The average chemical composition of WM, HAZ and base metal surface is listed I Table 28. The chemical composition of the surface corrosive layer of the root of the weld is different compared to the surface of the peak of the weld, HAZ and base metal. It could be caused, among others, by inhomogenities due to spalling of surface layer – see Figure 62). The composition of darker and lighter areas on the surface is in Table 29 – composition of lighter areas contains less Cr and O and more Fe and Ni. The SEM pictures of the cross section of the root and the peak of the weld (WM and HAZ) could be found in Figure 63 and Figure 64. The damage of the metal interferes with the depth of ca. 3 – 4 µm under the metal surface. Chemical analysis revealed Cr and Mn under surface depleted zones, there were little differences among WM and HAZ and also the root and the peak of the weld. The average mass gain if welded specimens after exposure were 0.26 $mg.cm^{-2}$, i.e. more than after 264 hours during the first period of the test operation in HTHL.

Table 28: Analysis of Alloy 800 H welded sample surface exposed in HTHL during the first period of the corrosion test

Sample	Element	O	Al	Si	Ti	Cr	Mn	Fe	Ni	Nb
The root of the weld	% by weight	11.3	0.7	0.7	1.4	20.8	3.9	16.4	42.6	2.5
The peak of the weld		28.5	0.3		1.7	43.5	23.0	0.9	2.3	
HAZ		30.9			2.2	52.3	11.6	2.0	1.1	
Base metal		30.7			2.0	52.2	12.8	1.6	0.7	

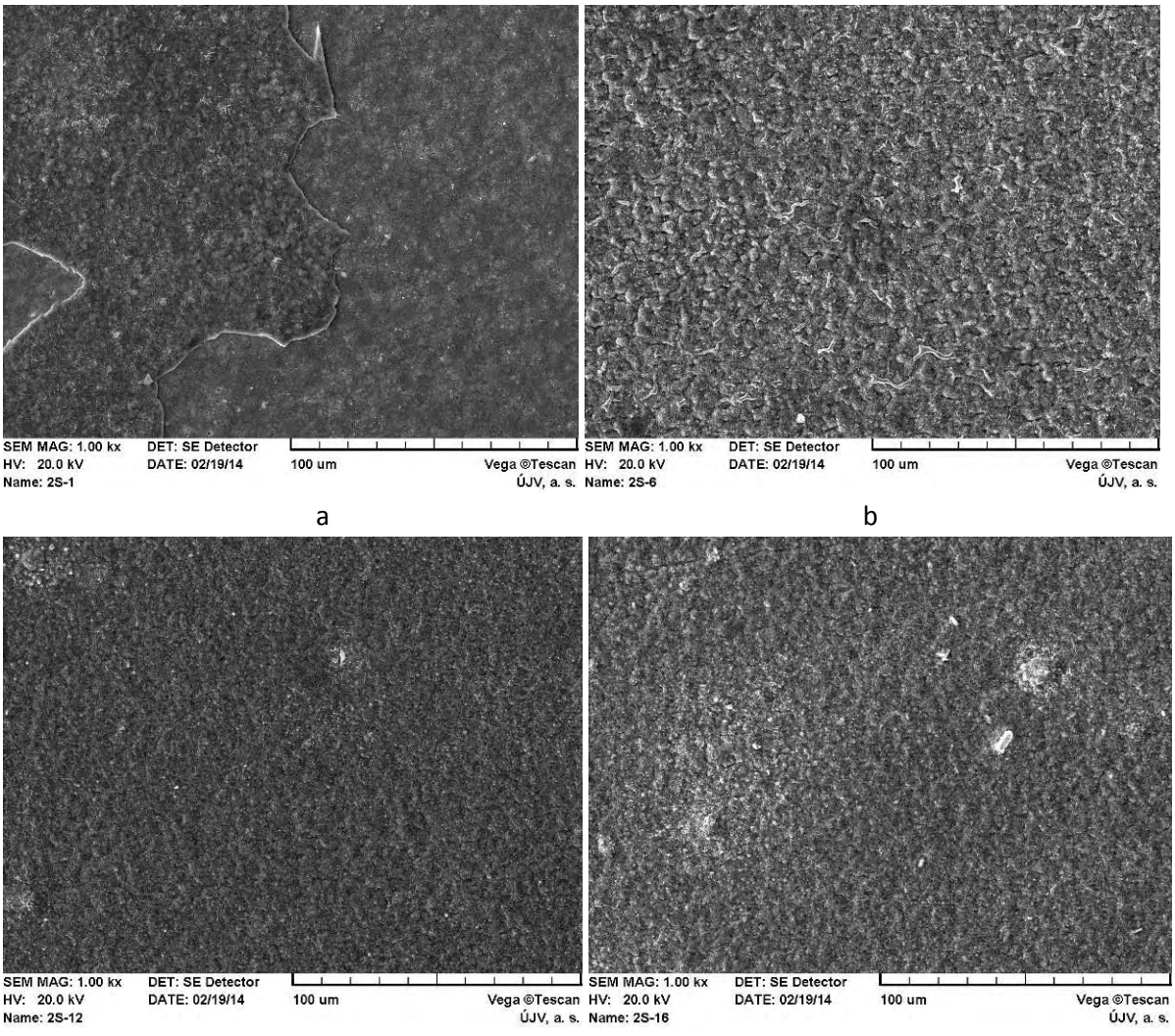

Figure 61: SEM picture of the sample surface of Alloy 800H weld metal after exposure in HTHL during the first period of the corrosion test a – the root of the weld, b-the peak of the weld, c – the heat affected zone, d – the base metal

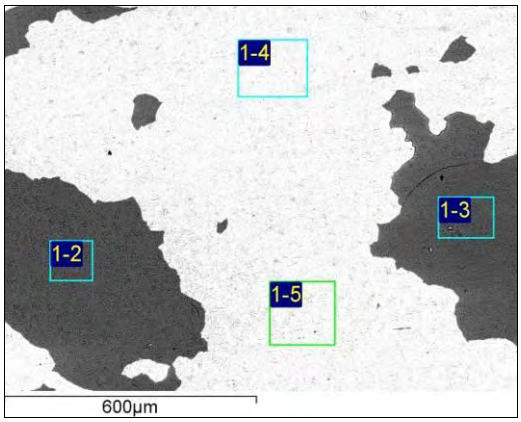

Figure 62: Inhomogenities of the surface of the root of the weld exposed during the first period of corrosion test in HTHL

Table 29: Analysis of the surface of the root of the weld after exposure in HTHL - according to Figure 62

Analysis	O	Al	Si	Ti	Cr	Mn	Fe	Ni	Nb
1-2	28.9			0.9	43.7	20.8	1.8	3.9	
1-3	29.0			0.7	44.9	21.1	1.8	2.5	
1-4	5.7	0.9	0.5	1.3	17.1	1.3	17.5	53.1	2.7
1-5	6.1	0.9	0.4	1.3	17.1	1.2	18.0	51.8	3.1

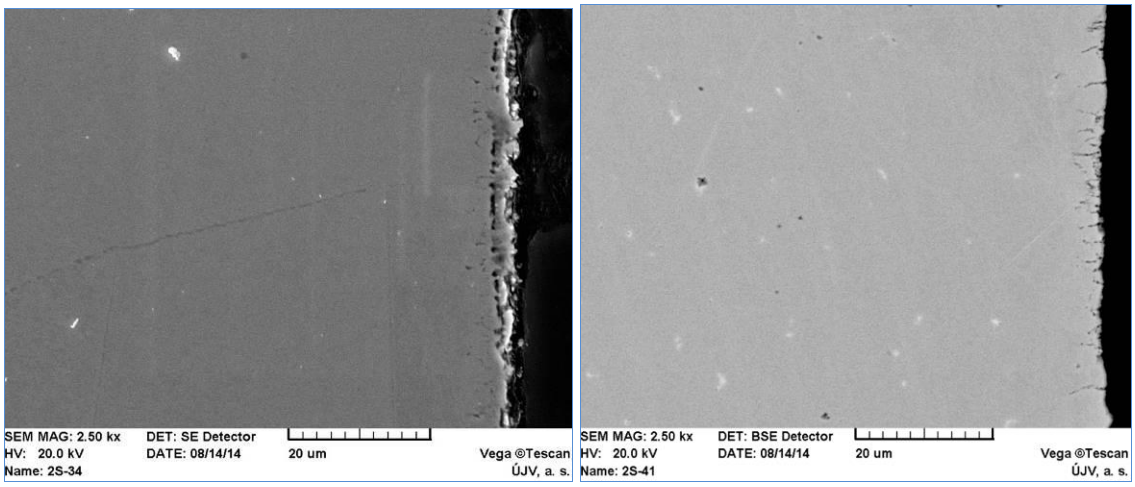

a b

Figure 63: The SEM picture of the cross section of the root of the weld after exposure in HTHL: a – the heat affected zone, b –weld metal

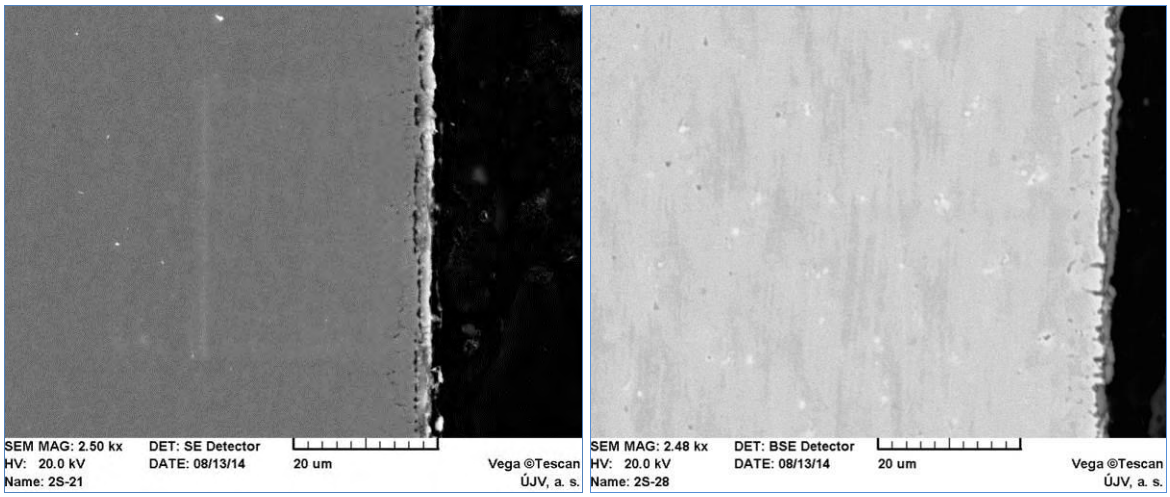

a **b**

Figure 64: The SEM picture of the cross section of the peak of the weld after exposure in HTHL: a – the heat affected zone, b –weld metal

Test III.

Test conditions, temperature and pressure in the loop were kept at 760-800°C, and 3,5MPa. During the exposure also gas impurities were added, 10 ppm H_2 + 10 ppm CH_4 + 50 ppm CO. Impurity levels in the flowing helium are controlled through a feedback mechanism based on gas chromatography with HID detector (GC-HID) measurements of the gas chemistry at the inlet from a HTHL-1 containing the test materials. The duration of the test was 100h.

Significant oxidation on the surface of specimens Alloy 800H (welded) was observed, see Fig. 65. Surface of each coupon and its chemical composition has been investigated by means of SEM coupled with the EDX analysis. The chemical composition of the surface of weld material (Nicrofer S7020) is relatively homogeneous. The main oxides formed on the surface are chromium oxides and manganese oxide, see Table 30 .

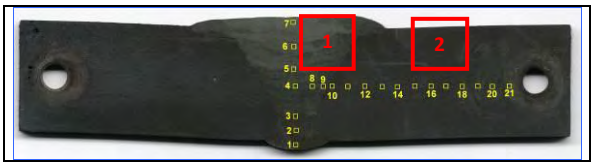

Fig. 65 Corrosion coupon after the exposure test in HTHL-1; 1-weld material; 2- Heat affected zone (HAZ)

Compare to the chemical composition of the surface oxide of the welding filler, the oxides formed on Alloy 800H contained more chromium and significantly less manganese. Manganese is an austenite stabiliser. An isothermal section of the Mn–Cr–O phase diagram at 818 °C was calculated [i]. Results from the phase diagram confirmed our findings after the exposure test in high temperature impure helium. Welding material Nicofer S7020, richer in manganese (3.2%), formed a scale layer (probably Mn_3O_4) that might have prevent the base material against carburization. The internal precipitation of the carbides in weld material is somewhat less than in welded Alloy 800H, see Fig. 66 a) and b).

Table 30 Chemical composition of the surface oxides formed on the welded material Alloy 800H (5S-10-21)/weld S7020 (5S-1-7) after exposure in impure He at 800°C for 100 h

wt.%	O	Al	Si	Ti	Cr	Mn	Fe	Ni
5S-1-7	29,1	1,1	0,0	1,2	40,7	23,0	2,2	2,7
5S-10-21	31,5	0,8	0,3	1,5	50,0	8,8	5,9	1,1

The microstructure - cross-section of welded sample is shown in Fig. 66 a) and b). Alloy 800H contains 0.40% titanium and 0.02% carbon and hence tends to form titanium carbide and titanium nitride or carbonitride during high-temperatures exposure. Precipitates - carbides were found in the austenitic matrix (40 microns from the gas-metal interface) and along the grain boundaries, see Fig. 66b).

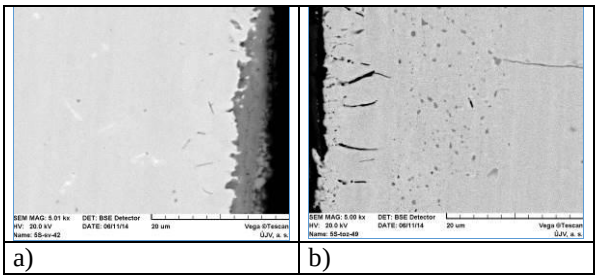

a) b)

Fig. 66 Cross-sectional SEM micrographs of the welded specimen exposed to impure helium at 800°C for 100 h. a) weld material Nicrofer S7020; b) Heat Affected Zone Alloy 800H.

Conclusion

During the Czech HTR experimental program these materials were tested: ferritic steel P91, austenitic steel 316 and welded Alloy 800 H. The specimens were exposed to simulated helium coolant environment (750 – 760°C, helium containing minor impurities – CO, CO_2, CH_4, H_2, H_2O) for up to 1000 – 1500 hours. For exposure two experimental devices were used: laboratory scale High Temperature Furnace (HTF) and semiindustrial scale High Temperature Helium Loop (HTHL). The specimens were exposed already during the test operation in HTHL, the parameters of environment were not constant during this test. Because of frequent problems with the new device HTHL only the results of 160 hours of the "correct" corrosion test are available for this report. After exposure the changes of specimens were evaluated. The accurate mass change of specimens was evaluated; the surface corrosive layer was observed and analyzed by SEM, the subsurface layers and changes of microstructure on cross section of selected specimens were also investigated by SEM and optical microscopy, further linescans on cross section or GD-OES analysis were done. The tests of hardness and micro hardness and fracture toughness (on P91 and SS 316 only) were carried out.

Selected results of the tests:

- Highest mass gain of tested materials after exposure showed Alloy 800 H

- The thickness of corrosive layer after exposure observed by optical microscopy on the cross section of the specimen was 1 – 4 µm. The thickness estimated from linescan or GD-OES analysis was higher.
- The corrosive layer on the surface was formed mainly by chromium and manganese oxides.
- Some differences between the corrosive layer formed during exposure in HTF and HTHL on the same tested material were observed
- On the heat affected zone and weld metal of Alloy 800 H the spallinig of corrosive layer after exposure was observed
- After exposure the undersurface chromium depleted zone was observed – mainly in case of 316 and P91. The undersurface decarburization zone was observed on P91.
- Fracture toughness of 316 after exposure decreased significantly (by 67 %). Fracture toughness of P91 after exposure decreased slightly (almost no change of the value of $J_{0.2}$ integral).
- The hardness of base metal and heat affected zone of Alloy 800 H increased after exposure, the hardness of P91, 316 and Alloy 800 H weld metal decreased. The highest change of hardness was observed in case of Alloy 800 H base metal (increase by ca. 19%).
- The micro hardness of all tested materials decreased after exposure. He highest decrease was recorded on Alloy 800 H base metal (ca. 17 %).
- Also other changes in microstructure of the materials after exposure were observed.

References

[1] Jan Berka: D42.21: Survey of the data generated in previous HTR and related programmes, report of Archer project, 2011

[2] Natesan K., Purohit A., Tam S. W.: report NUREG/CR-6824: Materials Behaviour in HTGR Environments, Office of Nuclear Regulatory Research, Washington, 2003.

[3] Dr. Kloewer: Deliverable D42.11: Procurement of test material, report of ARCHER project, 2011

[4] J. Berka, J. Matěcha, M. Černý, I. Víden, F. Sus, P. Hájek: Nuclear Engineering and Design 251 (2012) 203– 207

[5] A. Kříž, M. Šmíd: Application of GD-OES; http://www.ateam.zcu.cz/Pouziti_metody_GD-OES.pdf

Appendixes

SEM/EDX linescan of cross-cut of specimen L01 (steel 316, machined surface, exposure 750°C/1000 hours in He (composition listed in Table 5))

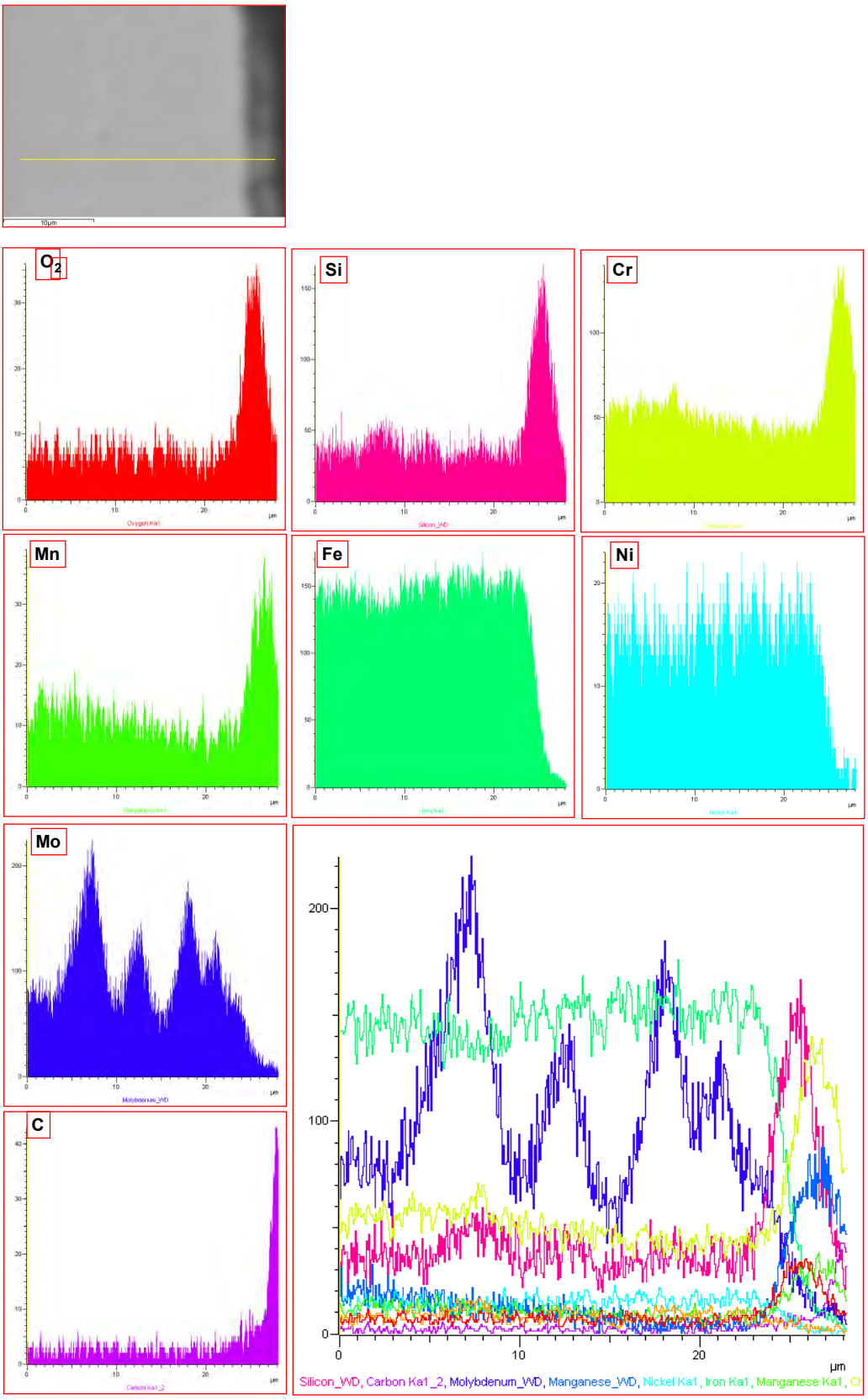

SEM/EDX linescan of cross-cut of specimen L28 (steel 316, grounded surface, exposure 750°C/500 hours in He (Table 5))

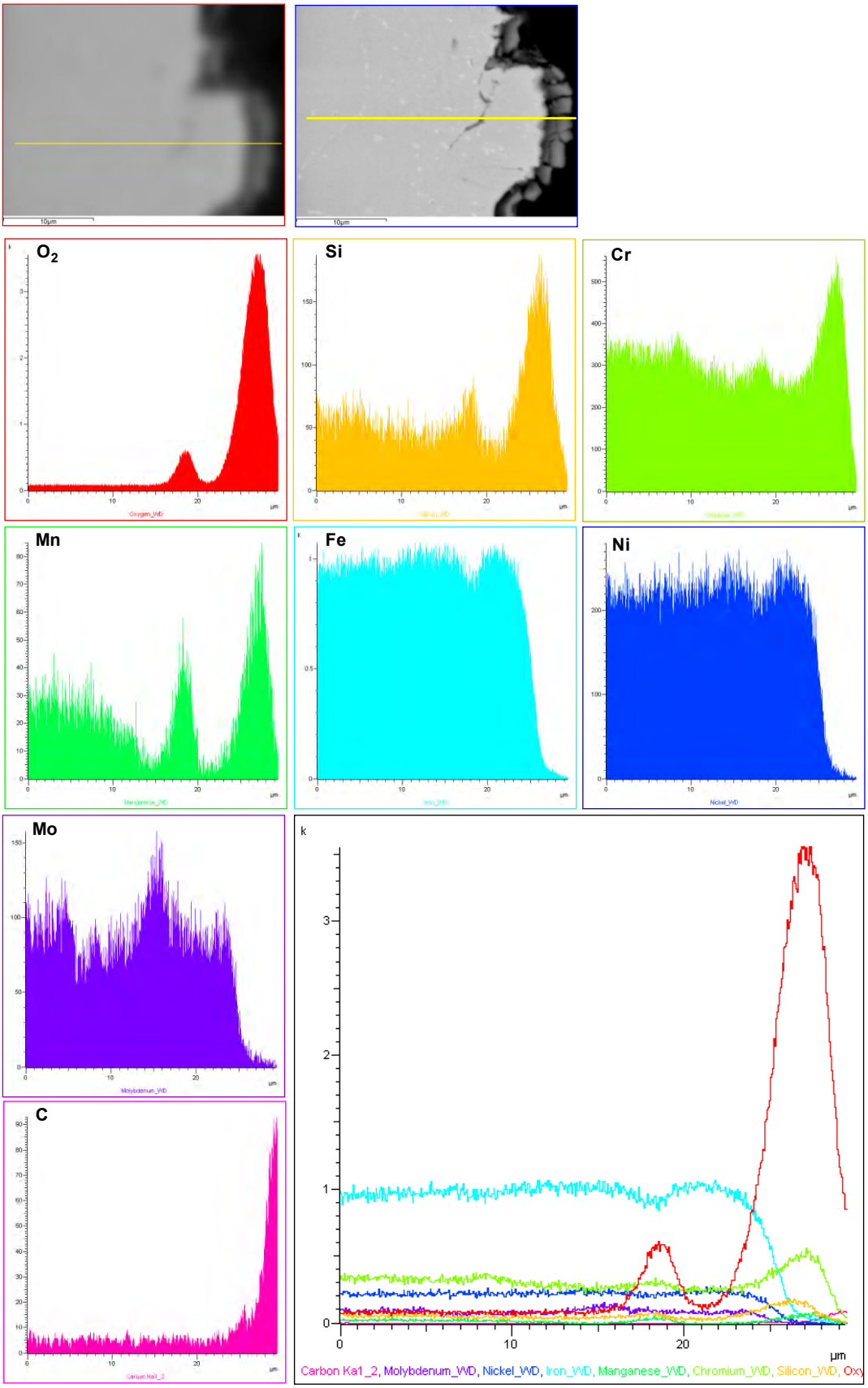

SEM/EDX linescan cross-cut of specimen L29 (steel 316, grounded surface, 750°C/1000 hours in He mixture(Table 5))

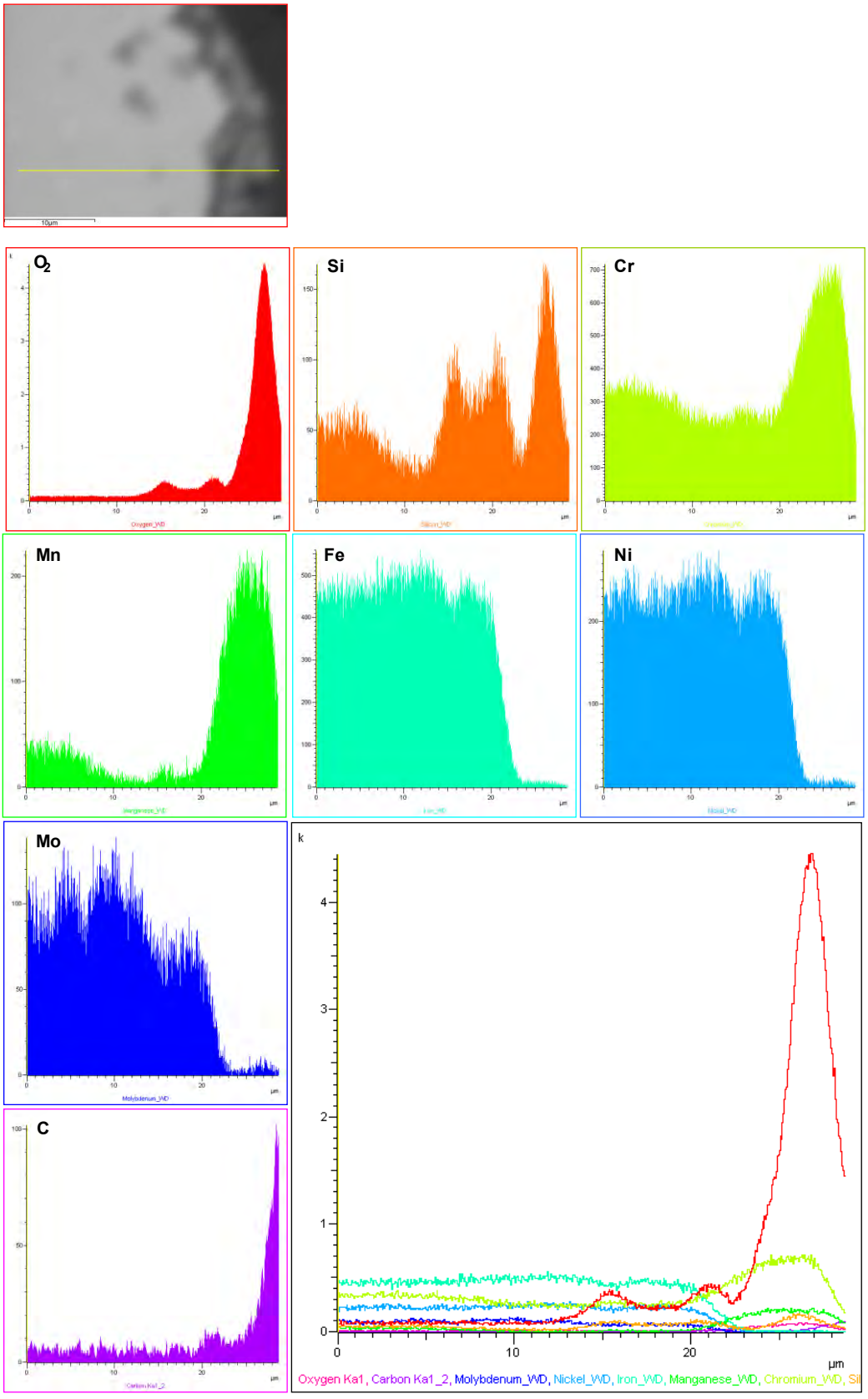

SEM/EDX linescan of cross-cut of specimen P01 (steel P91, machined surface, 750°/1000 hours in He mixture (Table 5))

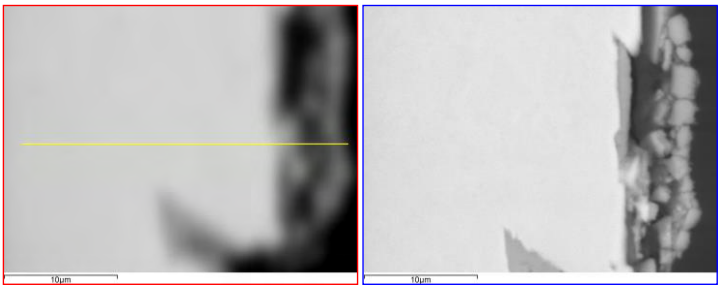

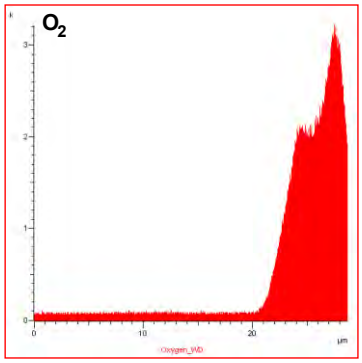

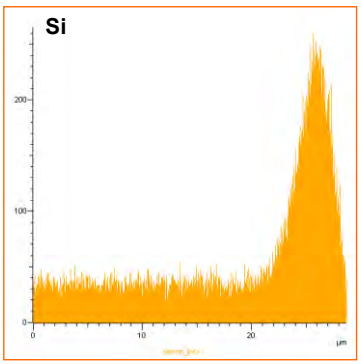

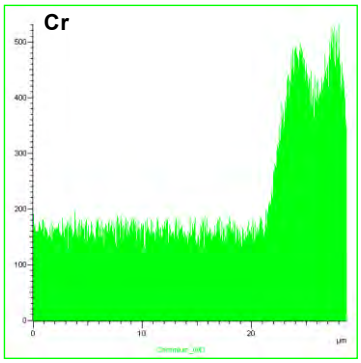

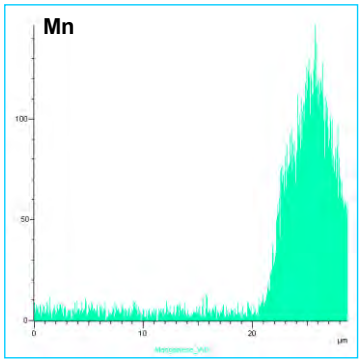

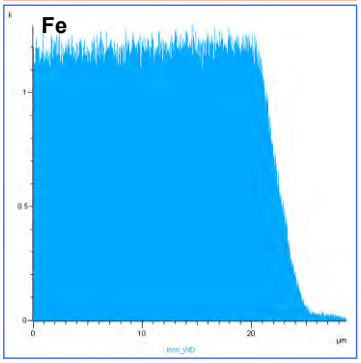

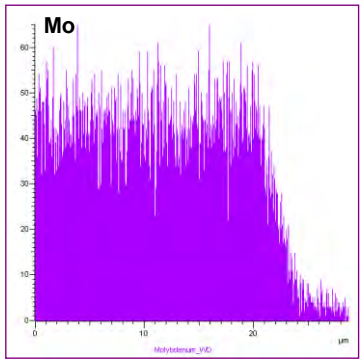

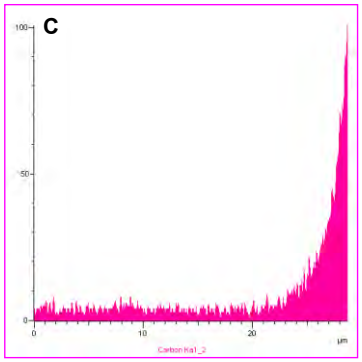

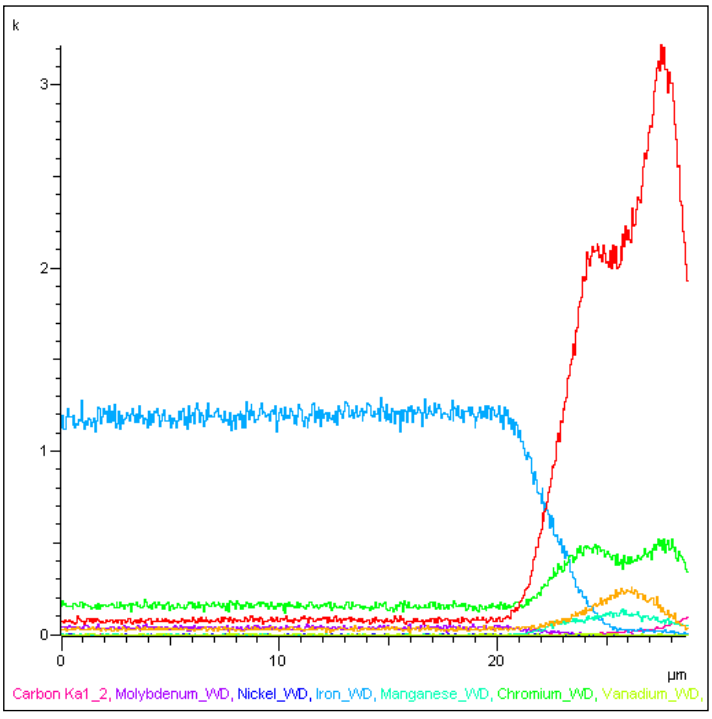

SEM/EDX linescan cross-cut of specimen P31 (steel P91, grounded surface, 750°C/500 hours in He mixture (Table 5))

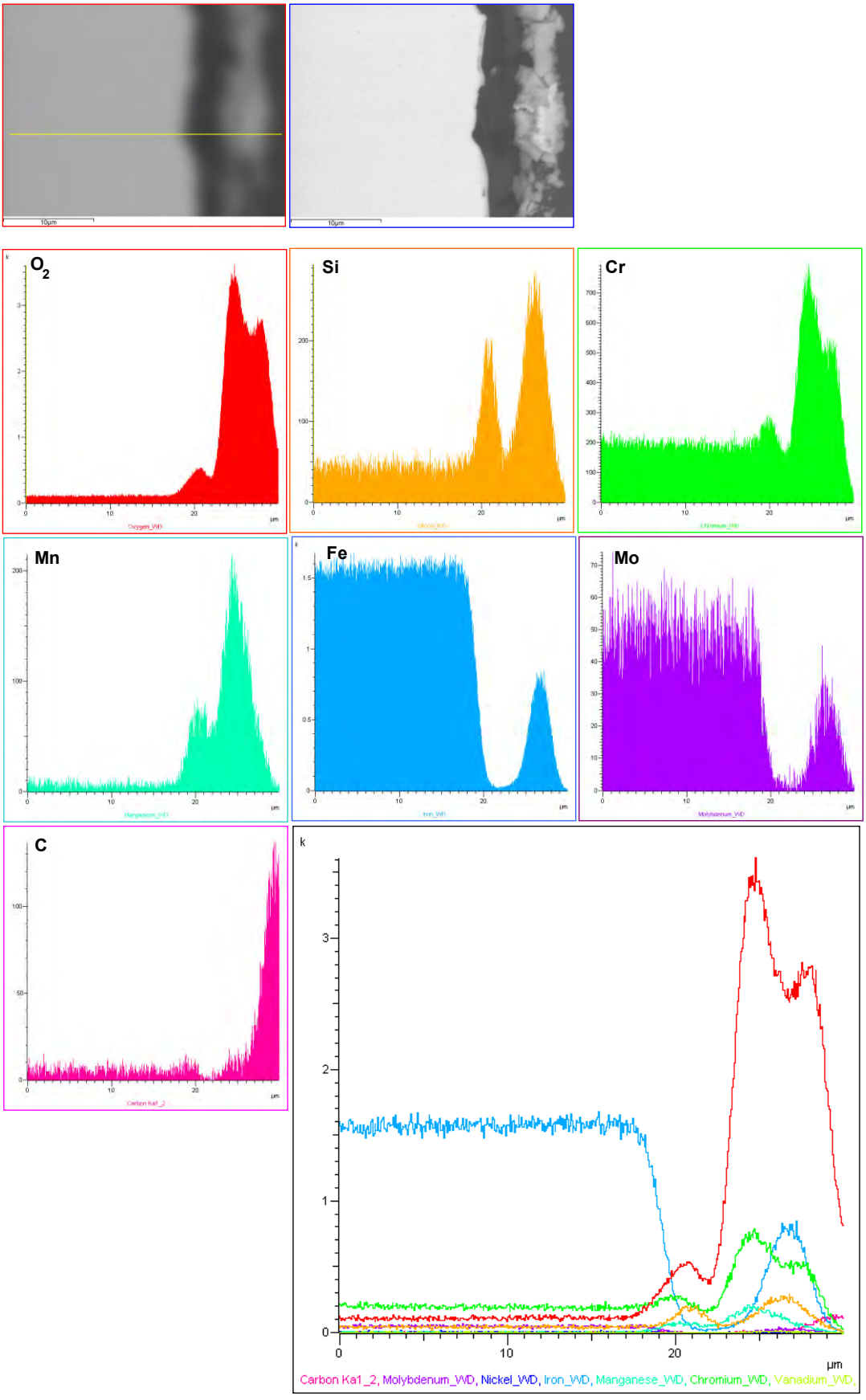

SEM/EDX linescan cross-cut of specimen P32 (steel P91, grounded surface, 750°C/1000 hours. In He mixture (Table 5))

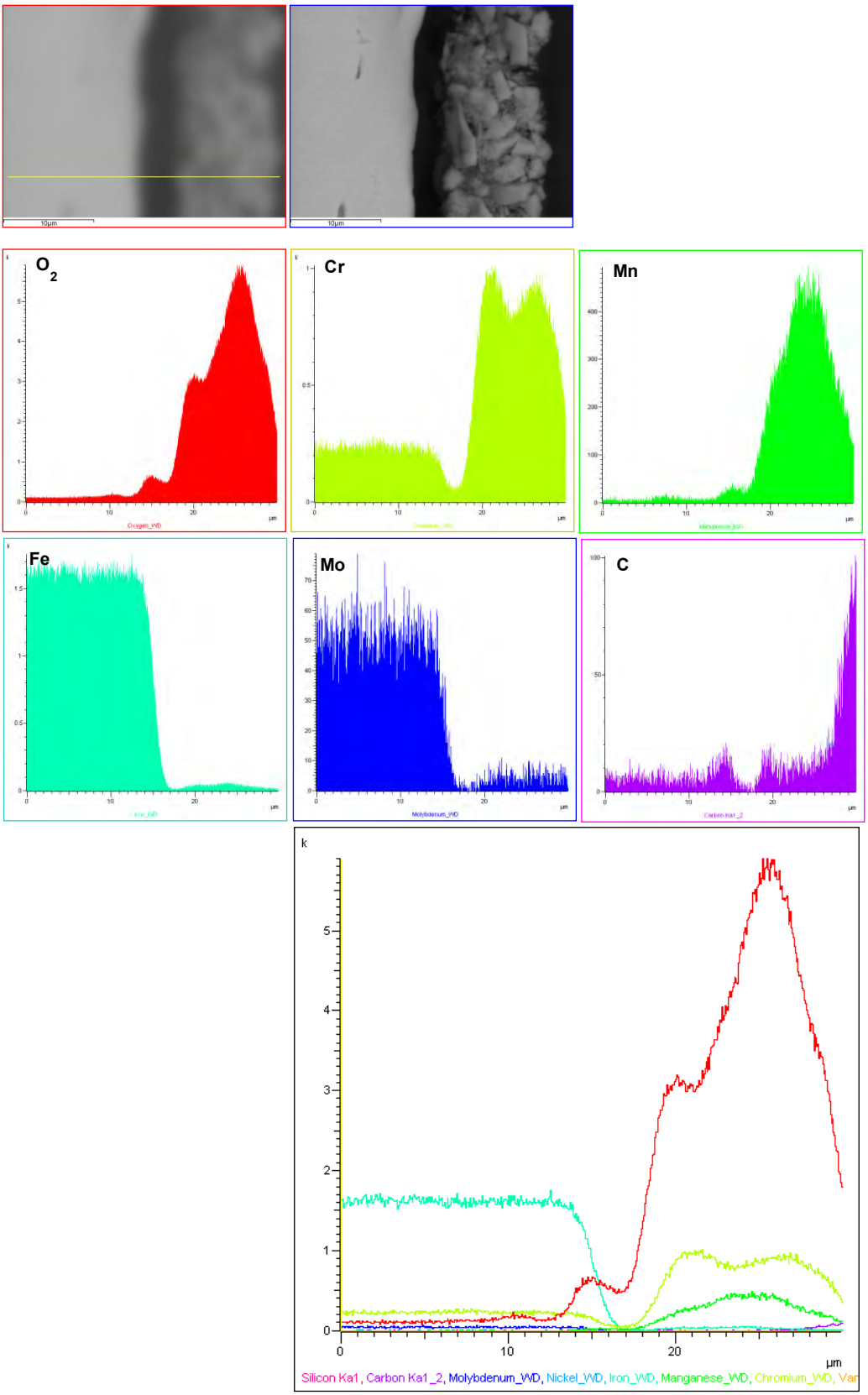

GD-OES graph of specimen of steel 316 L38 (He (Table 5)/750°C/24 hours.)

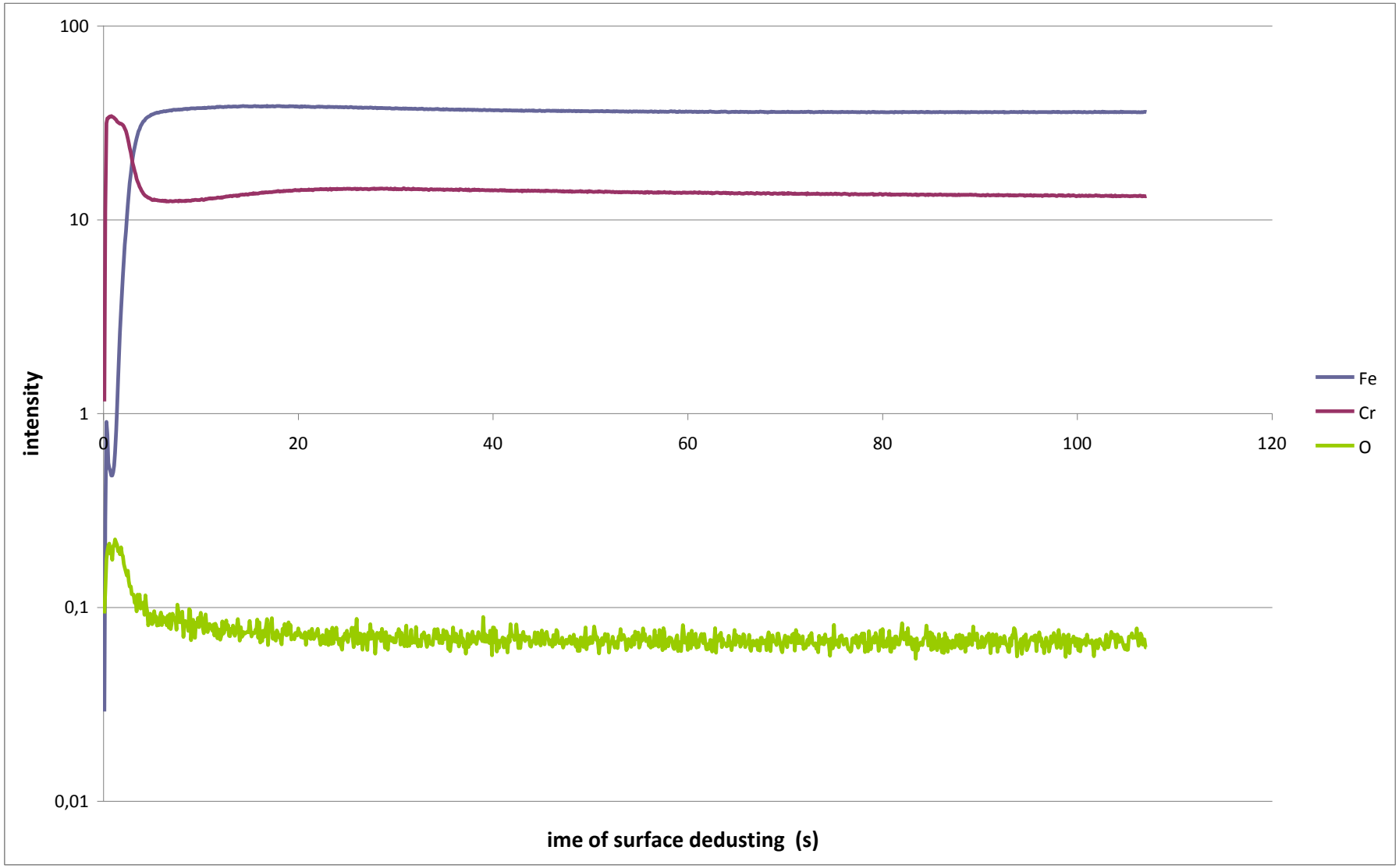

GD-OES graph of specimen of steel 316 L40 (He (Table 5)/750°C/120 hours.)

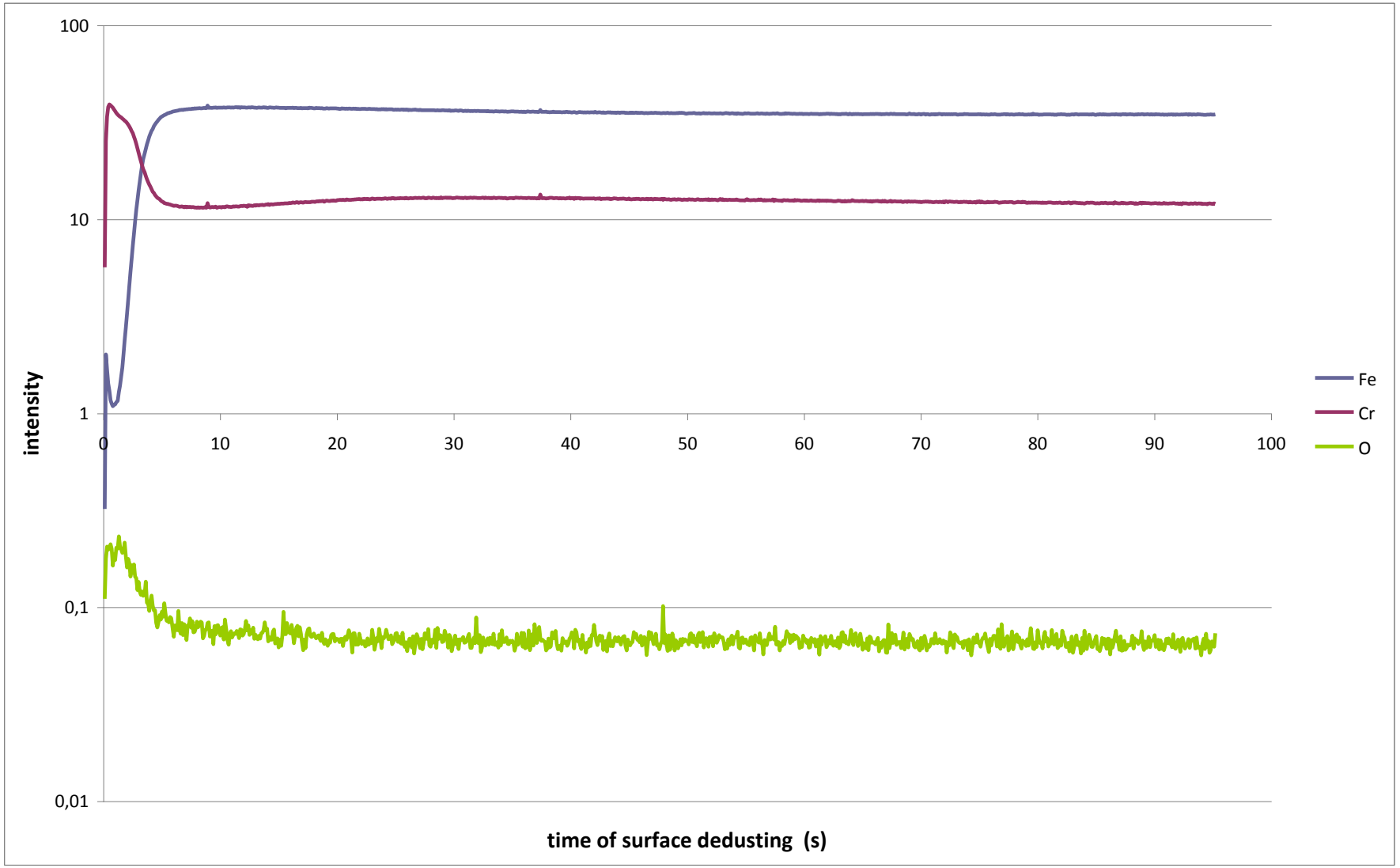

GD-OES graph of specimen of steel P91 P38 (He (Table 5)/750°C/24 hours.)

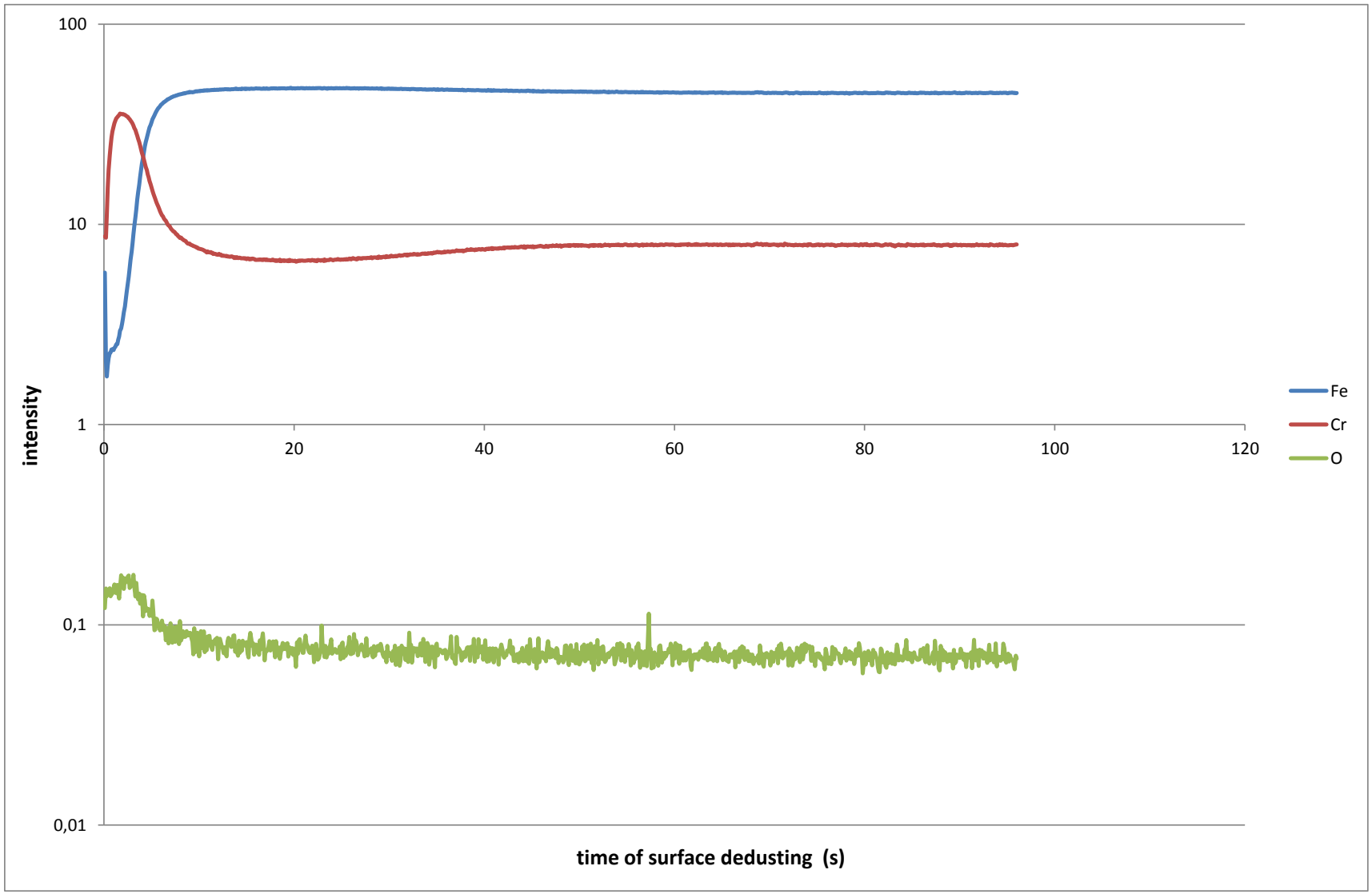

GD-OES graph of specimen of steel P91 P40 (He (Table 5)/750°C/120 hours.)

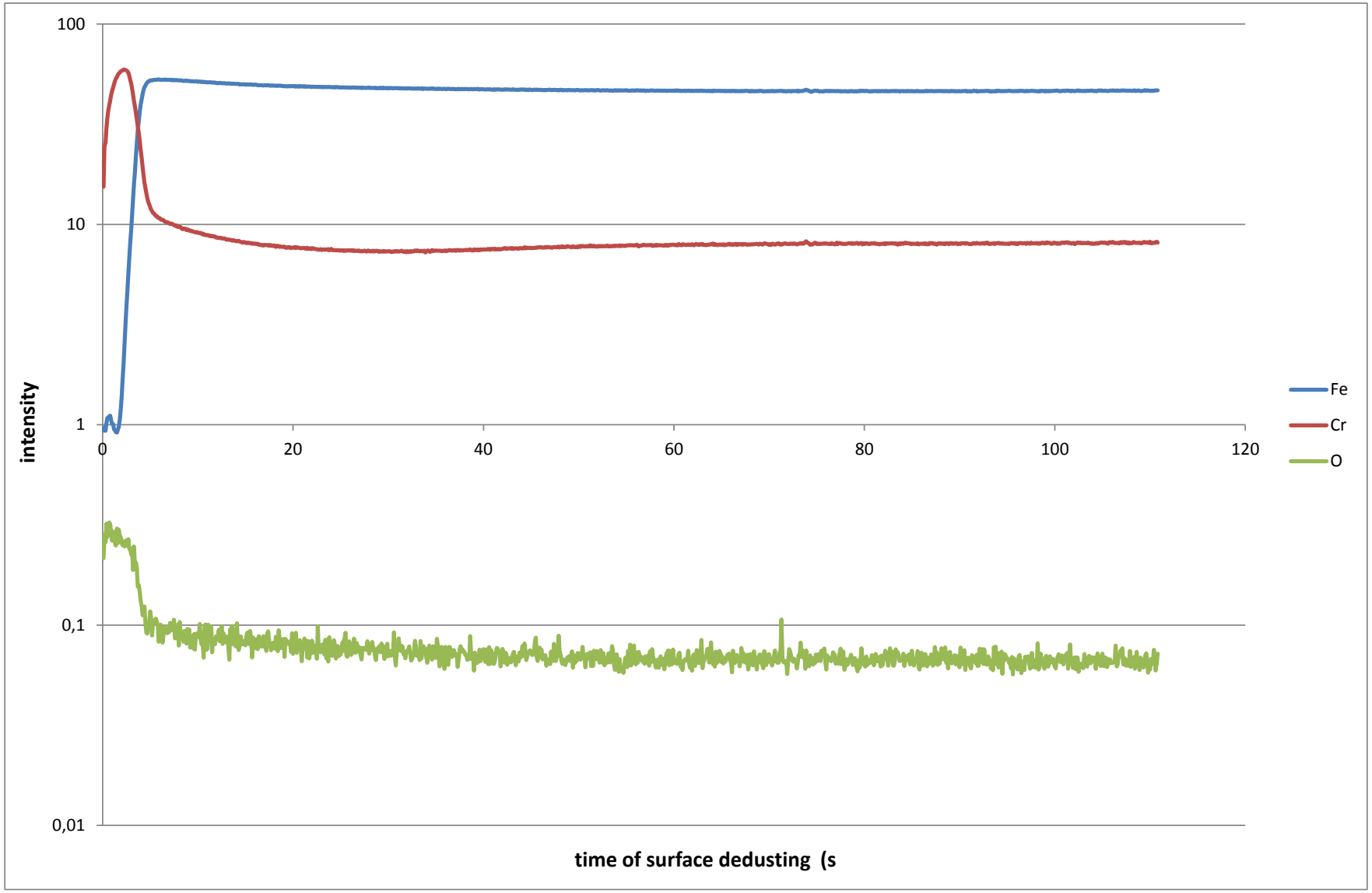

[i] Thuan Dinh Nguyen, Jianqiang Zhang, David J. Young, Water vapour effects on corrosion of Fe–Cr and Fe–Cr–Ni alloys containing cerium and manganese in CO2 gas at 818°C, Corrosion Science, 2014, ISSN 0010-938X